Development of Brain Machine Interface Systems and its Applications to Prosthetic Hand Control

By

Trongmun Jiralerspong

(錢智定)

Supervised by

Professor Jun Ishikawa

Department of Advanced Multidisciplinary Engineering

Tokyo Denki University

This dissertation is submitted for the degree of

Doctor of Philosophy

March 2018

Abstract

This dissertation presents a study on hybrid brain machine interface system (HBMI) that combines electroencephalographic (EEG) and electromyographic (EMG) signals to extend the controllability and usability of existing standalone BMI system. In developing HBMI system, the emphasis will be placed on the practicability and usability of the system. For this purpose, a consumer-grade EEG/EMG acquisition device will be used. To develop a HBMI system, first, several types of BMI system (steady state visual evoked potential-based (SSVEP) BMI, motor imagery-based BMI, electromyography-based BMI) are developed to evaluate the feasibility of the consumer-grade acquisition device as well as grasp the strengths and weaknesses of each system. In the next step, a control paradigm for HBMI system is proposed with consideration to the strength and weaknesses of each standalone system. In this study, HBMI will be applied to prosthetic control as an example. Experiments are conducted to evaluate the feasibility of the proposed HBMI system.

In the design of a 3-class self-paced SSVEP-based BMI, two low-cost EEG sensors are used to capture the SSVEP responses. Multiple second order bandpass filters are employed to extract SSVEP features and the type of response is classified using artificial neural network (ANN). Experimental results showed that the proposed design is capable of achieving an average accuracy of up to 93% and a mean information transfer rate of up to 4.2 bits/min. Furthermore, tradeoff between the number of commands and accuracy is also presented. This tradeoff allows the user to adjust the responsiveness and the accuracy to suit their preference or target application. Overall, the results of this study have demonstrated that a consumer-grade EEG device can serve as a modality in SSVEP-based BMI for device control applications.

In the design of a 3-class motor imagery based BMI, 8 low-cost EEG sensors are used to capture the EEG signals. Power spectrum densities are extracted from EEG signals during mental tasks and fed to the ANN in order to detect the user intention. Experiment results showed that the proposed method is capable of achieving an overall true positive rate of up to 67% with 15 minutes of training time by a first time BMI user. Furthermore, a tradeoff between true positive rate and false positive rate is also presented. Again, based on this tradeoff, the user can adjust the responsiveness and the accuracy to suit their preference or target application.

In the design of an EMG-based BMI, 6 consumer-grade EMG electrodes are used to capture muscle activity during arm/hand movements. Power spectrum densities are extracted from EMG signals and fed to the ANN in order to detect the hand motions. Experimental results showed that the proposed algorithm achieves an overall correct classification rate of up to 83%; thus, demonstrating the potential to classify 17 movements from 6 EMG sensors. Furthermore; classifying 9 motions using this method could achieve an accuracy of up to 92%. These results show that if the prosthetic hand is intended for a specific task; limiting the number of motions can significantly increase the

performance and usability. Compared to EEG, EMG is easier to analyze and more reliable as an input source. Despite these advantages, more improvements in responsiveness and accuracy is still needed to raise the level of usability.

In the design of a hybrid BMI (HBMI) system, EMG and EEG are fused together in an attempt to raise the controllability of the system. EMG is used to control the prosthetic hand while EEG is used to reduce misclassifications. Results showed that using EEG in parallel with EMG helps reduce erroneous classifications. The results also show that EEG can be used to modify the motion trajectories of the prosthetic hand. Based on these results, HBMI is effective for raising the controllability and usability of BMI systems.

Overall, this work has provided a foundation for further research that aims to develop a practical BMI system with consumer-grade acquisition device. Our results are supportive that consumer-grade acquisition device can serve as a modality in device control, and their usability can be further enhanced by combining multiple BMI systems together.

Keywords: Artificial neural network; Brain machine interface (BMI); electroencephalography (EEG); electromyography (EMG); motor imagery; steady state visual evoked potential (SSVEP); prosthetic hand.

Contents

List of Figures

List of Tables

Dedication

This dissertation is gratefully dedicated to

my parents:
Trong Jiralerspong and Wimon Sae-Heng,
who have always been a source of inspiration, encouragement and stamina to undertake my higher studies and to face the eventualities of life with zeal and enthusiasm,

my sister
Trivoramai Jiralerspong
who have always been a source of support in times of hardships,

Ms. Chao Liu,
Professor Jun Ishikawa,
and all professors at Tokyo Denki University
who instilled in me the virtues of perseverance and commitment and relentlessly encouraged me to strive for excellence.

1 Introduction

Chapter 1 offers an introduction to the topic and the extent of this study through three different sections. Section 1.1 describes the motivation of this research. Section 1.2 states the aim and describes the approach to the research question. Section 1.3 gives an overview of the layout of the dissertation.

1.1 Motivation

The realization of robotic systems that understand human intentions and produce accordingly complex behaviors is needed particularly for disabled persons and would consequently benefit the aged. For this purpose, a novel control technique that uses brain signals to control external devices called brain machine interface (BMI) have been suggested [1]-[3]. Through the detection of specific brain patterns, BMIs can provide a communication channel without the involvement of muscular activity and therefore possess the potential to be utilized as assistive technology. At Brown University, a research conducted by Hochberg and their team has demonstrated that it is possible to use neural responses from the brain to control robotic arms in 3D space and grab objects. In their research, they implanted an electrode into a patient's head whose suffering from amyotrophic lateral sclerosis (ALS) and analyzed the electrical impulses obtained from the electrodes [4]. The result of their work suggests that ALS patients who are unable to move their body, or in some cases unable to speak at all, would greatly benefit from using BMI systems. Other related works in [5]-[7] also show promising results. The disadvantage of this invasive BMI system is that there are risks from surgery when implanting the electrode and are hence unsuitable for healthy people. For this reason, noninvasive BMI systems have been preferably adopted and extensively studied over the past several years.

In a noninvasive BMI system, electroencephalograph (EEG) signals recorded from the scalp are often used to identify the user intent. Chae and their research team at Korea Advanced Institute of Science and Technology have successfully demonstrated the ability of the user to control a humanoid robot and navigate it to reach a target in an indoor maze. By using the combination of 3 basic motor imagery (MI) states i.e. left hand, right hand and foot imagery, the subjects were able to control the

humanoid through five complex instructions i.e. stop, turn head to the left, turn head to the right, turn body and walk forward. In this system, the EEG signals are recorded using a 32-channel EEG recording system. To identify the user intent, amplitude features of the EEG signal are extracted using power spectrum analysis and the informative feature components are selected based on fisher ratio. Two classifiers are constructed using linear discriminant analysis (LDA) and quadratic discriminant analysis (QDA) [8].

Other uses of BMI system include controlling wheelchairs [9]-[11]. A joint research organized by Riken and Toyota demonstrates a user controlling the wheelchair forward, turn right and turn left using EEG signals. In order to move forward, the subjects imagine themselves walking. To turn left or right, they imagine gripping their left or right hand [12]. Recently, BMI systems intended for quadcopters [13], smart home controls [14]-[17] and video games [18]-[21] have also been suggested.

Although large amounts of research have demonstrated the bright future perspectives of BMI technology, these existing BMI systems have yet been successfully deployed in homes. There are several challenges inherent in employing BMI control for real-world tasks. These challenges can be generalized into several categories.

- Low information transfer rate (ITR) and high error rate [22]
- Existing system are expensive and rely on convention acquisition equipment [23], [24]
- Require expert assistance to mount the electrode or EEG cap on the user's scalp [24]
- Most system do not incorporate an idle signal for when the user is in an idle state [25]
- Classification of continuous data are not fully explored (most study focus on classification of single-trials) [26], [27]

First of all, even one of the best average ITR for experienced subjects and well-tuned BMI systems are relatively low, in the vicinity of 24 bit (roughly three characters) / min [1]. This is too slow for natural interactive conversation and many research groups are finding ways to overcome this challenge. Also, the ITR achievable through EEG, is approximately one order of magnitude lower than the one observed by invasive methods in monkey studies [31]-[33]. That said, the potential benefits of brain-implanted based BMI have so far not been demonstrated to be worth the associated cost and risk in the most disabled of patients, let alone in healthy users. EEG seems for now the only practical brain-machine interaction choice (cost and ITR limitations hamper other non-invasive methods). Furthermore, a significant complicating factor in the slow ITR of BMI users is the high probability of errors Brain signals are highly variable, and this problem is exacerbated in severely disabled user by fatigue, medications, and medical conditions such as seizures or spasms.

Self-reporting errors is also extremely difficult, particularly if the subject has little or no communication channel outside of the BMI system itself. Devising methods of quickly resolving or preventing errors is critical to successful BMI interaction [22].

Secondly, implementing and effective BMI system requires multielectrode research/clinical-grade EEG device to accurately capture brain signals, and such equipment are very expensive. In addition, standard EEG practice involves the tedious application of conductive gel on EEG electrodes in order to provide for accurate measurements of the micro-volt level scalp potentials that constitute EEG signals. Unfortunately, most of the existing BMI systems still require extensive assistance from caretakers to properly set up the electrodes or signal receiving devices in BMI sessions, which makes it impractical to deploy this technology in a home environment.

So far, most BCI systems are capable of performing asynchronously (self-paced). However, this can become tiring since the user is required to continuously imagine one of the two classes. Often the user does not intend to control anything but rather leave the BMI inactive, thus BMI usability would benefit from an “idle” or “rest” class where the cursor does not respond when no active class (from a set of two or more) is activated, on top the BMI being self-paced. The “idle” state may take one of two forms: a “relax” state where the subject stays still and tries to “think of nothing”, or can do almost any other mental task than those which belong to the active classes, but the latter may not be intuitive. Remaining challenges are to find a classifier that can induce rest state without a “relax” cue and to optimize the relationship between classifier output and BMI command. Due to physiological variations in background EEG activity, where a main factor is fatigue, introduction of a controller layer is necessary for maximal performance [25].

Lastly, most study only focus on the classification of single-trials. A characteristic feature of all of these systems is that the onset of mental activity is known in advance and associated with a specific cue or trigger stimulus. In the case of an ideal asynchronous BMI system, no cue stimulus is used, and the subject can intend whenever she/he wishes, a specific mental activity. The ongoing brain signals have to be analyzed and classified continuously. Mental events have to be detected and discriminated from noise and nonevents and transformed into a control signal as quickly and accurately as possible [26], [27].

Due to all of the above challenges, the current BMI technology have very little to offer healthy users and thus have limited the target user range to only ALS and tetraplegic patients. To solve these problems, researchers have come up with numerous solutions and they can be generalized into four areas.

- Improvement of ITR and the error rate
- Improvement of the usability and practicability
- Improvement of equipment hardware
- Development of novel applications

To raise the ITR, new preprocessing techniques, feature selection method [28], and classification algorithms [29] have been suggested. In addition, methods to reduce erroneous commands (error rate) such as the use of error-related potentials have been introduced [30]. To improve the usability and practicability of BMI systems, hybrid BMIs that concurrently utilizes two or more types of brain signals (e.g. SSVEP and motor imagery) have been developed. The benefits of using these systems includes expansion in the number of commands (tasks) and improvements in ITR (see section 6 for more details). In recent years, developments of more and more inexpensive EEG device by specialized companies such as Emotiv or Neurosky have started to appear in the market and these companies have already started to develop some initial applications towards the general public. However, despite these efforts, the current BMI technology is still far from being used in real life scenarios, mainly due to the ITR and the number of commands still being far too low.

For the purpose of increasing the ITR and the number of commands, the use of electromyographic (EMG) activities to control external devices are shown to be very effective. EMG signal is a biomedical signal that measures electrical currents generated in muscles during its contraction representing neuromuscular activities. Since movement and muscle activities are generated based on the neural signal, in a broader sense, the definition of BMI can be extended to include EMG signals. Applications of EMG signal are mostly found in the field of myoelectric prostheses control, robotic exoskeleton, and wheelchair navigation. Since the signal level of EMG signals is higher compared to EEG signals, it is easier to analyze and discriminate different signal patterns from EMG signal. Usually, if the target user is able to generate EMG signal, adopting is type of signal as the control signal would greatly enhanced the practicability and usability of the system. However, there are also some challenges in developing EMG-based control system. Changes in muscle condition or the occurrence of unintended subtle muscle activities can cause the system to perform erroneous actions. Considering the case that the target application is aimed at assistive technologies for people with disabilities or the aged, erroneous actions can be potentially dangerous. From the viewpoint of safety, the reduction of erroneous actions is strongly preferred.

1.2 Research Aims and Approach

This study aims to develop a practical BMI system using a consumer-grade acquisition device. In this work, the feasibility of consumer grade device in BMI-based control as well as concurrent use of EEG and EMG for the purpose of enhancing the usability of BMI systems will be explored. To realize this aim, first, two types of EEG-based BMI systems (steady state visual evoked potential (SSVEP) based BMI and motor imagery-based BMI systems) are developed to evaluate the feasibility of the consumer-grade EEG device.

Next, we will shift our attention to focus on the development of EMG-based gesture recognition for prosthetic hand control. The feasibility of low-cost EMG sensors will be evaluated.

Finally, taking into account the strengths and weaknesses of EEG and EMG, a hybrid BMI (HBMI) system that uses both EEG and EMG will be developed to enhanced to controllability and usability of the existing BMI system. Experiments will be conducted to evaluate the feasibility of the prosed HBMI system.

Based on the results obtained, this study also aims to answer the following questions.

(1) Is it possible to develop a BMI system using a consumer-grade EEG acquisition device? If so, to what extent can the system perform with limited hardware?
(2) Can a consumer grade EMG sensor serve as a modality in myoelectric prosthetic control?
(3) Does the concurrent use of EEG and EMG signals help improve the practicability and usability of the existing system?

1.3 Organization of Dissertation

The rest of the dissertation are organized as follows:

Chapter 2 presents the fundamental background knowledge on the human brain anatomy, BMI systems, brain activity measurement modalities, types of control signal used in BMI systems, electromyography and the anatomy of forearm and hand muscles.

Chapter 3 proposes the design of a self-paced steady state visually evoked potential (SSVEP) based BMI. The proposed system is to classify SSVEP responses which is elicited by presenting the user with flashing LED stimuli. Multiple bandpass filters are used to extract features and artificial neural network (ANN) is employed to for classification. Online experiments are conducted to evaluate the accuracy, response speed, and the information transfer capability of the proposed system. The feasibility of the system is shown and the limitations of this study are

discussed. In addition, future research is outlined.

Chapter 4 presents a design of motor imagery based BMI which alleviates the restriction of having to continuously gaze at the stimulus during device control. The system is designed to classify user intentions of moving an object up or down as well as rest state. Power spectrum densities (PSD) is used to represent the features of each intent and classified using ANN. Online experiments are conducted to evaluate the accuracy of the proposed system. Tradeoffs between true positive value and false positive value are also presented. The feasibility of a consumer-grade EEG device as a modality in device control is shown and the limitations of this study are discussed. In addition, future research is outlined.

Chapter 5 presents a signal processing technique for electromyography (EMG) based control of prosthetic hands. The aim of this study is to classify a reasonable large number of arm/hand motions using a small set of low-cost EMG sensors. FFT will be applied to the EMG signals in order to extract PSD features. ANN is employed to classify the arm/hand motions. Online experiments are conducted to evaluate the accuracy of the system. Comparisons with existing studies are given to confirm the feasibility of the proposed method. The limitations and future research are also discussed.

Chapter 6 starts by talking about the strength and weaknesses of EEG and EMG-based control and proposes a concept EEG-EMG-based hybrid BMI (HBMI) system which uses both EEG and EMG signals to improve the operability of the system. This study considers applying the HBMI to prosthetic hand control as an example to show that combination of multiple BMI protocols can provide extended controllability even with consumer-grade devices. Experiments are conducted to evaluate the validity of the proposed system.

Chapter 7 concludes the dissertation. The obtained results are summarized and discussed in this chapter. The contributions of this study and future research will also be highlighted.

2 Background and Overview

This chapter provides background information about the human brain anatomy. This is followed by an overview of the BMI system as well as brain activity measurement methods. Emphasis will be put on electroencephalography (EEG) since this is the most widely used method for noninvasive BMI applications and it is the method used in the work presented in this thesis. Lastly, different control signal types employed in current BMI system will be briefly explained.

2.1 Human Brain Anatomy

The central nervous system (CNS) consists of two main components, the spinal cord and the brain, where the latter is defined as the part that is located inside the skull. The cerebrum is the largest portion of the brain, and contains tools which are responsible for most of the brain's function. It is divided into four sections: the temporal lobe, the occipital lobe, parietal lobe and frontal lobe as shown in Fig. 2.1. Since the frontal lobe is responsible for motor planning and thinking, we will mainly focus on EEG signals on this part of the brain.

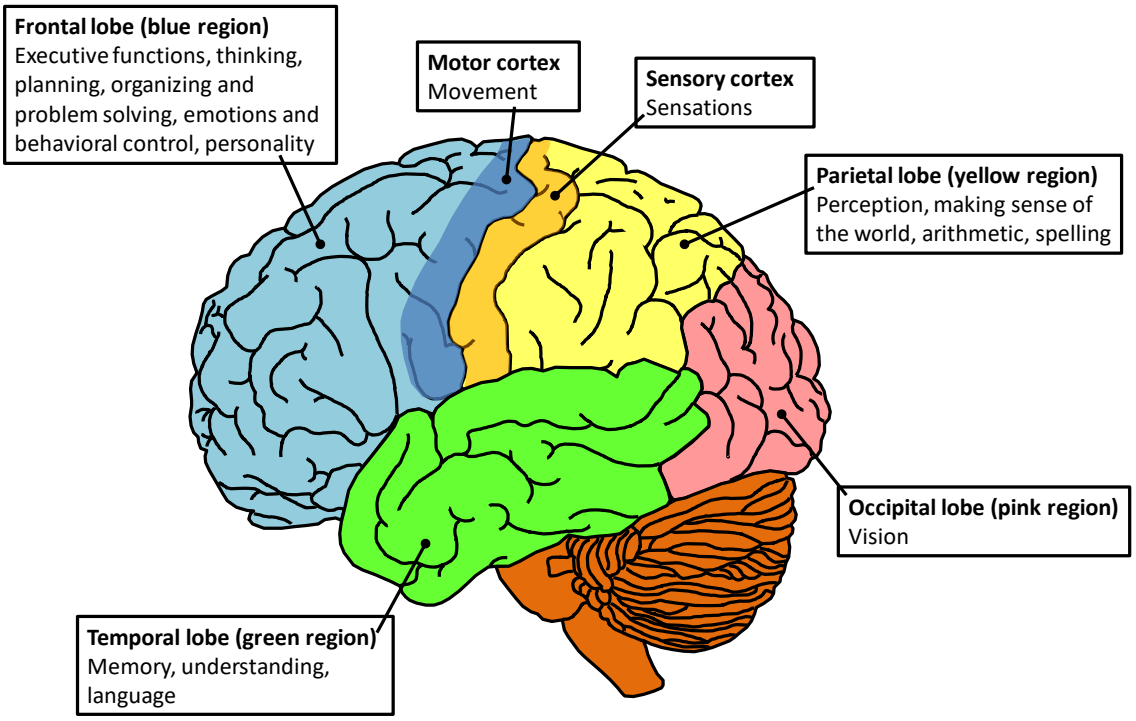

Fig. 2.1 The functionality of different areas of the brain

2.2 Brain Machine Interface Systems

Brain machine interface (BMI), or brain computer interface (BCI) represents a direct interface between the brain and a computer or any other system. BMI is a broad concept and comprehends any communication between the brain and a machine in both directions: effectively opening a completely new communication channel without the use of any peripheral nervous system or muscles activity. In principle this communication is thought to be two-way. But at present, BMI is mainly focusing on communication from the brain to the computer. This study will mainly focus on this type of BMI system.

In a BMI system, signals from the brain are being analyzed to determine the user's state of mind or intentions, which in turn can be translated into actions [34]. In order to achieve this, first of all, the subject performs a specific mental task in order to produce a signal of interest in his brain; then this signal is acquired and generally pre-processed in order to get rid of different artifacts. Afterwards, some discriminating features are extracted and classified (pattern recognition) to determine which specific signal was produced. Finally, the identified signal is associated to a specific action to be performed by a computer or any electronic device [35]. A diagram of a classic BMI system is shown in Fig. 2.2. BMIs can be categorized according to several criteria: i) exogenous or endogenous and ii) synchronous (cue-paced) or asynchronous (self-paced). Types of BMI are listed in Table 2.1 and Table 2.2 along with information related to brain signals that can be modulated to convey information as well as advantages and disadvantages.

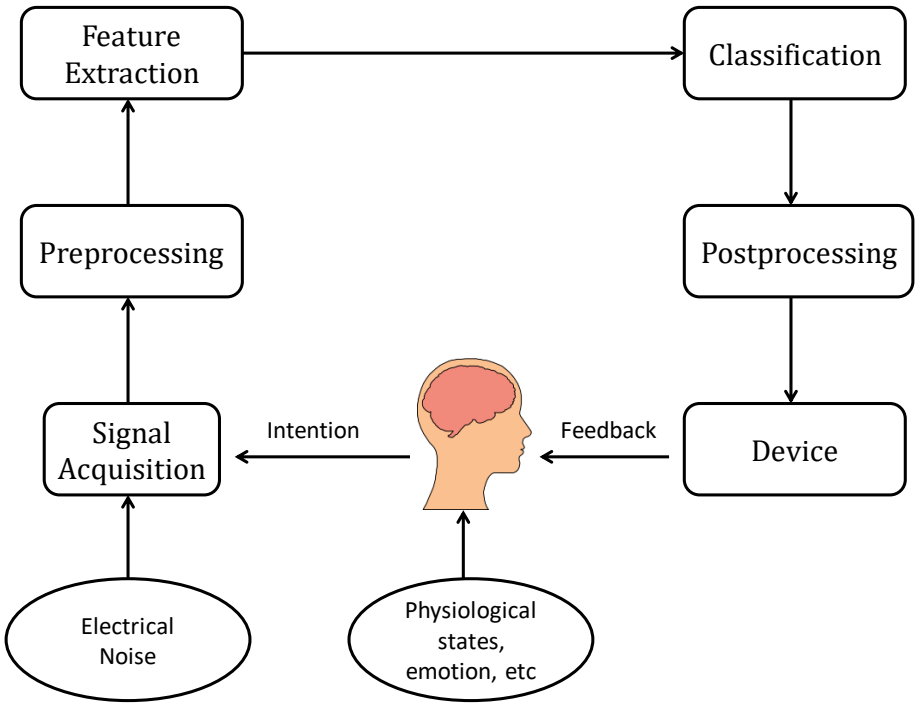

Fig. 2.2 General Scheme of a Classical Brain Machine Interface (BMI)

According to the nature of the signals used as input, BMI systems can be classified as either exogenous or endogenous. Exogenous BMI uses the neuron activity elicited in the brain by an external stimulus such as visual evoked potentials (VEP) or auditory evoked potentials. On the other hand, endogenous BMI is based on self-regulation of brain rhythms and potentials without external stimuli [36], [37]. Through neurofeedback training, the users learn to generate specific brain patterns which may be decoded by the BMI such as modulations in the sensorimotor rhythms [38] or the slow cortical potentials (SCP) [39].

According to the input data processing modality, BMI systems can be classified as synchronous or asynchronous. Synchronous BMIs analyze brain signals during predefined time windows. Any brain signal outside the predefined window is ignored. Therefore, the user is only allowed to send commands during specific periods determined by the BMI system. For example, the standard Graz BMI [40] represents a synchronous BMI system. On the other hand, asynchronous BMIs continuously analyze brain signals no matter when the user acts. Although they offer a more natural mode of human-machine interaction than synchronous BMI, this kind of interfaces requires a more complex and demanding signal processing pipeline: the detection of the non-control (non-action) state is essential.

Table 2.1 Main Differences Between Exogenous and Endogenous BMI Systems (adopted from [36])

Approach	**Brain Signals**	**Advantages**	**Disadvantages**
Exogenous BMI	-SSVEP -P300	-Minimal training -Control signal set-up easily and quickly -High bit rate (60 bit/min) -Only one EEG channel required	-Permanent attention to external stimuli -May cause tiredness in some users
Endogenous BMI	-SCP -Sensorimotor Rhythms	-Independent of any stimulation -Can be operated at free will -Useful for users with sensory organs affected	-Lots of training are needed (months or weeks) -Multichannel EEG recordings required for good performance -Lower bit rate (20-30 bit/min)

Table 2.2 Main Differences Between Synchronous and Asynchronous BMI Systems (adopted from [36])

Approach	Advantages	Disadvantages
Synchronous BMI	-Simpler design and performance evaluation -The user can avoid generating artifacts since they can perform eye blinks and other eye movements when brain signals are not analyze	-Does not offer a more natural mode of interaction
Asynchronous BMI	-No requirements to wait for external cues -Offers a more natural mode of interaction	-Much more complicated design -More difficult evaluation

2.3 Measuring Neural Activity

BMI uses brain signals to gather information on user intentions. There are several different approaches to measure activity in the brain. These approaches allow us to monitor two types of brain activities: first, the electrophysiological activity and, second, the hemodynamic response of the brain.

Electrophysiological activity is produced by the electro-chemical transmitters exchanging information between the neurons. The neurons generate ionic currents which flow within and across neuronal assemblies. The large variety of current pathways can be simplified as a dipole conducting current from a source to a sink through the dendritic trunk. These intracellular currents are known as primary currents. Conservation of electric charges means that the primary currents are enclosed by extracellular current flows, which are known as secondary currents [36], [41]. Electrophysiological activity can be measured by electroencephalography (EEG), electrocorticography (ECoG), magnetoencephalography (MEG), and invasive electrical signal measurement operated at the single neurons level.

The hemodynamic response is a process in which the blood releases glucose to active neurons at a greater rate than in the area of inactive neurons, thus, they allow us to distinguish active from less activated neurons. The presence of glucose and oxygen delivered through the blood stream results in a surplus of oxyhemoglobin in the veins of the active area. Hence, the local ratio of oxyhemoglobin to deoxyhemoglobin changes [36], [42]. These changes can be quantified by neuroimaging methods such as functional magnetic resonance (fMRI) and near infrared spectroscopy (NIRS), from which it is possible to build 3D maps of the brain activity. These kinds of methods are categorized as indirect, because they measure the hemodynamic response, which, in contrast to electrophysiological activity, is not directly related to neuronal activity.

In most current BMI systems, EEG is by far the most widely used neuroimaging modality. The prime reason for this is due to its high temporal resolution which is a necessity for real-time application. And although the spatial data resulting from EEG is often distorted and far from perfect, EEG offers direct functional correlation of brain activity. Another major advantage is the ease of applying this method. With a cap containing only a few electrodes, brain activity measurements can start. For practical uses and applications, it is small and relatively portable, which improves prospects of future applications. Aside from the ease of appliance, this is also a relatively low-cost method, certainly compared to methods like positron emission tomography (PET), MEG or MRI, which require expensive equipment and skilled professionals to operate. BMI systems based on EEG consist of a set of sensors that acquire electroencephalography signals from different brain areas. However, the quality of EEG signals is affected by scalp, skull, and many other layers as well as background noise. Noise is the key to EEG and to other neuroimaging methods, insofar as it reduces the signal to noise ratio (SNR) and therefore the ability to extract meaningful information from the recorded signals [36]. From the above reasons, EEG is used as the main method to measure brain activities in this study. Table 2.3 summarizes the different imaging techniques by listing in each case the type of brain activity measured, the temporal and spatial resolutions, safety and portability (adapted from [36]).

Table 2.3 Summary of Neuroimaging Methods (adapted from [36])

Neuroimaging Method	**Activity Measured**	**Direct/Indirect Measurement**	**Temporal Resolution**	**Spatial Resolution**	**Risk**	**Portability**
EEG	Electrical	Direct	~0.001 s	~10 mm	Non-invasive	Portable
MEG	Magnetic	Direct	~0.05 s	~5 mm	Non-invasive	Non-portable
ECoG	Electrical	Direct	~0.003 s	~1 mm	Slightly invasive	Portable
Intracortical Neuron Recording	Electrical	Direct	~0.003 s	~0.5 mm (LPF) ~0.1 mm (MUA) ~0.05 mm (SUA)	Strongly invasive	Portable
fMRI	Metabolic	Indirect	~1-10 s	~1 mm	Non-invasive	Non-portable
SPECT	Metabolic	Indirect	~10 s-30 min	~1 cm	Non-invasive	Non-portable
PET	Metabolic	Indirect	~0.2 s	~1 mm	Non-invasive	Non-portable
NIRS	Metabolic	Indirect	~1-10 s	~5 mm	Non-invasive	Portable

2.4 Control Signal Types in BMI Systems

Numerous studies have described a vast group of brain signals that might serve as control signals in BMI systems. Nevertheless, only those control signals employed in current BMI systems will be discussed below: visual evoked potentials, slow cortical potentials, P300 evoked potentials, and sensorimotor rhythms. All the signal controls are listed in Table 2.4, along with some of their main features (adapted from [36]).

Table 2.4 Summary of Control Signals (adopted from [36])

Signal	**Physiological Phenomena**	**Number of Choices**	**Training**	**Information Transfer Rate**
VEP	Brain signal modulations in the visual cortex	High	No	60-100 bits/min
SCP	Slow voltages shift in the brain signals	Low (2 or 4, very difficult)	Yes	5-12 bits/min
P300	Positive peaks due to infrequent stimulus	High	No	20-25 bits/min
Sensorimotor Rhythms	Modulations in sensorimotor rhythms synchronized to motor activities	Low (2, 3, 4, 5)	Yes	3-35 bits/mins

2.4.1 Visual Evoked Potential (VEP)

VEPs are brain activity modulations that occur in the visual cortex after receiving a visual stimulus [36], [43]. These modulations are relatively easy to detect since the amplitude of VEPs increases enormously as the stimulus is moved closer to the central visual field [44]. VEPs can be classified according to three different criteria which are the morphology of the optical stimuli, the stimulated frequency (it is possible to get a visual VEP response in the range 1-100 Hz [45]) and the field of stimulation [46], the focus here is on steady state visual evoked potential (SSVEP).

SSVEP is a strong steady state potential that mainly arises in the occipital area when a subject is looking at a visual stimulus which changes at a frequency higher than 6 Hz. If the stimulus is a flash, SSVEP shows a sinusoidal-like waveform, the fundamental frequency of which is the same as the blinking frequency of the stimulus. If the stimulus is a pattern, the SSVEP occurs at the reversal rate and at their harmonics [36], [47]. Fig. 2.3 shows an example of a SSVEP waveform and its frequency spectrum (adopted from [47]).

The typical VEP-based BMI application displays flashing stimuli, such as digits or letters, on a screen to induce SSVEPs while the user stares at one of the symbols. The user can move their gaze to the flashing digits or letters, in order to communicate with the computer [36], [48]. The main

advantage of this type of BMI is the relatively high SNR with a clear peak in the FFT occurring at the frequency of interest and some of its harmonics. Moreover, as discussed in [44], the SNR SSVEP response has three main frequency bands with peaks around 15 Hz, 31 Hz and 41 Hz. Logically, this leads to a high potential bit rate that can even reach around 100 bits/min [49]. Another big advantage of this type of control signal is that very little training is required. Its drawback is that the user has to watch the screen and keep his eyes fixed on one point. This type of control signal can only be used for exogenous BMIs. Therefore, VEPs are not suitable for patients in advanced stages of Amyotrophic Lateral Sclerosis (ALS) or with uncontrollable eye or neck movements. Some independent SSVEP-based BMIs that are controlled by the attention of the user have been introduced to overcome this drawback [36], [50], [51].

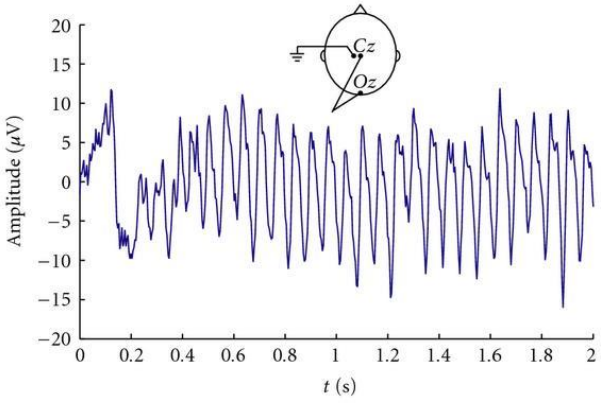

(a)

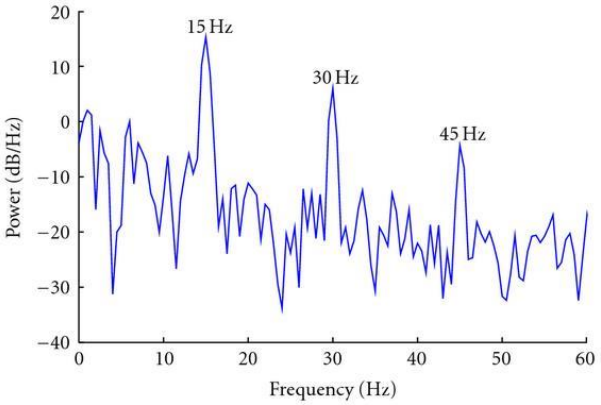

(b)

Fig. 2.3 Typical waveform of an EEG signal (Oz-Cz) acquired during visual light stimulation with a frequency of 15 Hz and its frequency spectrum. (a) SSVEP waveform resulting from the time-locked average of 10 realizations. A transient VEP can be observed at the moment where the stimulation began and a clear oscillation (the steady state VEP) can be seen afterwards; (b) Frequency content of the signal in (a). The SSVEP manifests itself in oscillations at 15 Hz and higher harmonics (adopted from [47]).

2.4.2 Slow Cortical Potential (SCP)

SCPs are gradual variations of the cortical activity, which can last from a second to several seconds. SCPs belong to the part of the EEG signals below 1 Hz, thus, they have the lowest frequency range of all EEG electrophysiological signals suitable for BMI systems [52].

SCPs are associated with changes in the level of cortical activity. Negative SCPs correlate with increased neuronal activity, whereas positive SCPs coincide with decreased activity in individual cells [36], [52]. These brain signals can be self-regulated by both healthy users and paralyzed patients to control external devices, e.g. to move a cursor and select the targets presented on a computer screen. People can be trained to generate voluntary SCP changes using a thought-translation device [39]. The thought-translation device typically comprises a cursor on a screen in such a way that the vertical position of the cursor constantly reflects the amplitude of SCP shifts.

Success in SCP self-regulation training depends on numerous factors, such as the patient's psychological and physical state, motivation, social context, or the trainer-patient relationship. It is known that the learning capability of the user drastically affects SCP modulation training. Other factors, such as sleep quality, pain, and mood also have an influence on self-regulation performance [36], [39]. Self-regulation of SCPs has been tested extensively with patients suffering from ALS [53]-[55]. Typical accuracy rates achieved for SCP classification are acceptable and vary between 70% and 80%, but the rates of information provided by SCP-based BMI are relatively low. Besides, longer training is required to use SCP-based BMI and it is likely that users will need continuous practice for several months.

2.4.3 P300 Evoked Potentials

P300 evoked potentials are positive peaks in the EEG due to infrequent auditory, visual, or somatosensory stimuli. The P300 responses are elicited about 300 ms after attending to an oddball stimulus among several frequent stimuli [36], [56], [57]. In an oddball paradigm, the user is requested to attend to a random sequence composed of two kinds of stimuli with one stimulus much less frequent than the other one. In case the infrequent stimulus is relevant to the user and, assuming that the subject was focusing on it by, for example, silently counting it, its actual appearance activates a P300 waveform in the user's EEG, which is mainly located in the parietal areas. Some studies have proven that the less probable the stimulus, the larger the amplitude of the response peak [58]. The use of P300 based BMIs does not require training. However, the performance may be reduced because the user gets used to the infrequent stimulus and consequently P300 amplitude is decreased [36], [59].

The most widely known P300 based BMI is the P300 speller [60]. As depicted in Fig. 2.4, it is basically composed of a 6×6 matrix of letters, symbols, numbers or commands [56], [9], [61]. The rows or columns of this matrix are flashed at random while the EEG is monitored. The user gazes at the desired symbol and counts how many times the row or column containing the desired choice flashes. P300 is elicited only when the desired row or column flashes. Thus, the BMI uses this effect to determine the target symbol. Due to the low SNR in EEG signals, the detection of target symbols from a single trial is very difficult. The rows or columns must be flashed several times for each choice. The epochs corresponding to each row or column are averaged over the trials, in order to improve their accuracy. However, these repetitions decrease the number of choices per minute, e.g., with 15 repetitions, only two characters are spelled per minute and therefore decreases the reactivity of the device [36], [56]. Although most of the applications based on P300 evoked potentials employ visual stimuli, auditory stimuli have been used for people with visual impairment [62].

P300 based BMIs provide a very low rate of information transmission because the classifier based on an average is too simple, and the accuracy of P300 potential detection is too low [63]. Consequently, too many trials are required to select a single symbol in the matrix. Accuracy of P300 based BMIs can be improved, while using a more complicated classifier than a simple average to ensure that the number of repetitions remain unaffected [63], [64].

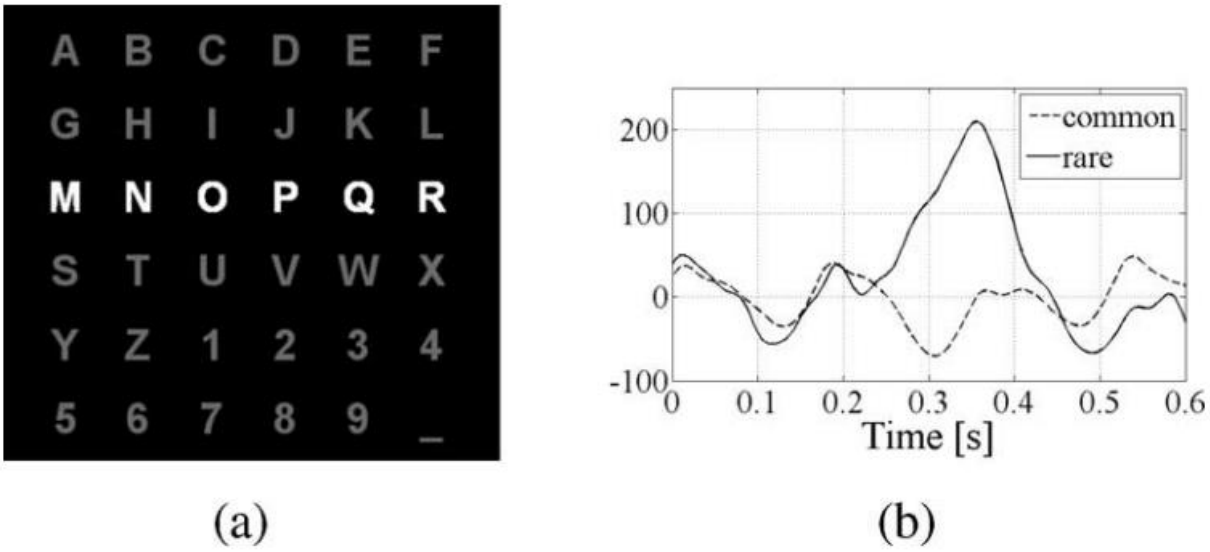

Fig. 2.4 BMI "*P300 speller*". (a) Screen display as shown to the subjects with the third highlighted row. (b) Time course of the actual signal waveforms at Cz. The continuous line represents the average over rare (*i.e*., target) stimuli and the dashed line corresponds to the average over common (*i.e*., nontarget) stimuli (adopted from [63]).

2.4.4 Sensorimotor Rhythms (mu and beta)

Sensorimotor rhythms comprise mu and beta rhythms, which are oscillations in the brain activity localized in the mu band (7-13 Hz), also known as the Rolandic band, and beta band (13-30 Hz), respectively. Both rhythms are associated in such a way that some beta rhythms are harmonic mu rhythms, although some beta rhythms may also be independent [36], [65]. The amplitude of the sensorimotor rhythms varies when cerebral activity is related to any motor task although actual movement is not required to modulate the amplitude of sensorimotor rhythms [66], [67]. Similar modulation patterns in the motor rhythms are produced as a result of mental rehearsal of a motor act without any overt motor output [66]. Sensorimotor rhythms have been used to control BMIs, because people can learn to generate these modulations voluntarily in the sensorimotor rhythms [68], [69].

Sensorimotor rhythms can endure two kinds of amplitude modulations known as event-related desynchronization (ERD) and event-related synchronization (ERS) that are generated sensory stimulation, motor behavior, and mental imagery [36], [68]. ERD involves an amplitude suppression of the rhythm and ERS implies amplitude enhancement. Fig. 2.5 (left panel) shows the temporal behavior of ERD and ERS during a voluntary movement experiment which involves brisk finger lifting [68]. The mu band ERD starts 2.5 s before movement on-set, reaches the maximal ERD shortly after movement-onset, and recovers its original level within a few seconds. In contrast, the beta rhythm shows a short ERD during the movement initiation of movement, followed by ERS that

reaches the maximum after movement execution. This ERS occurs while the mu rhythm is still attenuated. Fig. 2.5 also shows the gamma oscillation (36–40 Hz), which is another rhythm related to motor tasks as well [68]. Gamma rhythms reveal an ERS shortly before movement-onset. Finally, the right panel of Fig. 2.5 illustrates that simultaneous ERD and ERS are possible at different scalp locations [68].

Sensorimotor rhythms are related to motor imagery without any actual movement [36], [67]. This makes it possible to use sensorimotor rhythms for the design of endogenous BMIs, which are more useful than exogenous BMIs. Nevertheless, self-control of sensorimotor rhythms is not easy, and most people have difficulties with motor imagery.

Sensorimotor rhythms have been investigated extensively in BMI research. Well known BMI systems such as Wadsworth [70], Berlin [71], or Graz [40] BMIs employ sensorimotor rhythms as control signals. The BMIs based on sensorimotor rhythms can operate in either synchronous or asynchronous mode. The latest advances in the field of BMIs based on sensorimotor rhythms have shown that it is possible to predict human voluntary movements before they occur based on the modulations in sensorimotor rhythms [72]. Furthermore, this prediction could be provided without the user making any movements at all.

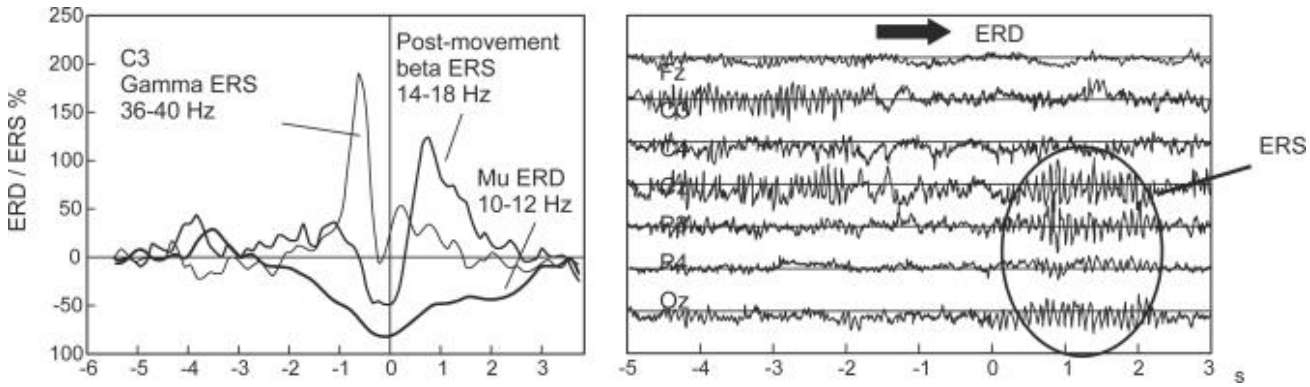

Fig. 2.5 Superimposed band power time courses computed for three different frequency bands (10-12 Hz, 14-18 Hz, and 36-40 Hz) from EEG trials recorded from electrode position C3 during right index finger lifting. EEG data triggered with respect to movement-offset (vertical line at t = 0 s). The right panel shows an examples of ongoing EEG recorded during right finger movement (adapted from [68]).

2.5 The Anatomy of the Forearm

There are thirty-nine hand muscles located either in the forearm or the hand itself [73]. These muscles are divided into two groups: the extrinsic and intrinsic muscles. The extrinsic muscles are responsible for crude movements of the hand, while the intrinsic muscles are responsible for the fine movements of the hand. These group of muscles must work together to fulfill the functionality of the hand [74]. In this section, the details of the intrinsic muscles will be omitted since it is not used in this study.

The extrinsic muscles are subdivided into the anterior compartments, and the posterior compartments, depending on the location of the muscles within the forearm.

The muscles in the anterior compartment of the forearm generally perform flexion at the wrist and fingers, and pronation. Within this compartment, muscles are divided into three categories: superficial, intermediate and deep. The superficial muscles include: the flexor carpi ulnaris, palmaris longus, flexor carpi radialis and pronator teres, which originate from a common tendon (see Fig. 2.6 (a)). The deep layer consists of three muscles: flexor digitorum profundus, flexor pollicis longus, and pronator quadratus (see Fig. 2.6 (b)). Sandwiched between the superficial and the deep layers lies the intermediate layer, which has only one muscle, the flexor digitorum superficialis (see Fig. 2.6 (a)). The median nerves innervate these muscles, as well as those in the superficial layer.

The muscles in the posterior compartment of the forearm generally produce the extension at the wrist and fingers, also known as the extensor muscles. The muscles are innervated by the radial nerve. The muscles in this layer are split into two layers: superficial and deep layers, which are separated by a layer of fascia. The superficial layer contains seven muscles: brachioradialis, extensor carpi radialis longus, extensor carpi radialis brevis, extensor digitorum, extensor digiti minimi, extensor carpi ulnaris and anoconeus (see Fig. 2.7 (a)). Within the deep layer, there are five muscles: supinator, abductor pollicis longus, extensor pollicis brevis, extensor pollicis longus and extensor indicis (see Fig. 2.7 (b)). These muscles act on the thumb and the index finger, except the supinator [75], [76].

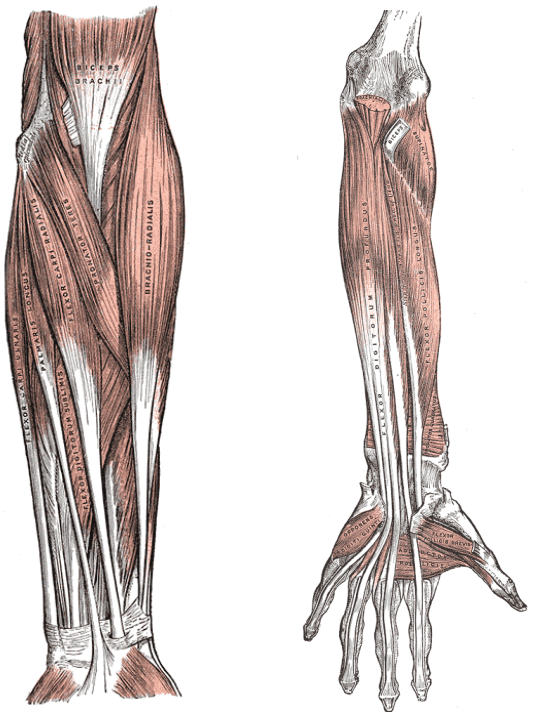

(a) (b)

Fig. 2.6 Anterior compartment of the forearm: (a) Superficial and intermediate muscles, (b) Deep muscles (adopted from [76]).

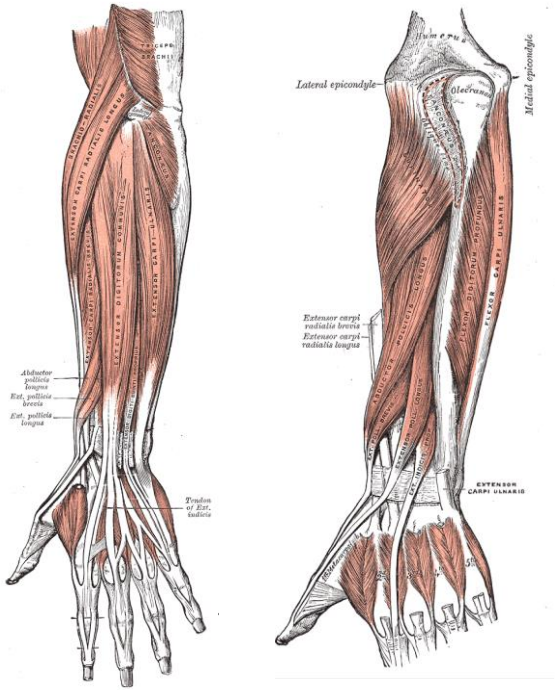

(a) (b)

Fig. 2.7 Posterior compartment of the forearm: (a) Superficial muscles (b) Deep muscles (adopted from [76]).

2.6 Measuring Muscle Activity

Electromyography (EMG) is an experimental technique that records and evaluates the electrical signals the body muscles emanate. The myoelectric signals are formed by physiological variations in the state of muscle fiber membranes.

The excitability of muscle fibers through neural control represents a major factor in muscle physiology. This phenomenon can be explained by a model of a semi-permeable membrane describing the electrical properties of the sarcolemma, the cell membrane of muscle cells, as shown in Fig. 2.8 [77]. The ionic difference between the inner and outer spaces of a muscle cell forms a resting potential at the muscle fiber membrane, at approximately -80 to -90 mV when not contracted. Similarly, a study done by Daud et al. showed that the amplitude of the EMG signal depends on the muscle types and conditions during the observation process, which ranges from microvolts, μV, to millivolts, mV [78]. This difference in potential which is maintained by physiological processes (ion pump) results in a negative intracellular charge compared to the external surface. The activation of an alpha-motor anterior horn cell (induced by the central nervous system or reflex) results in the conduction of the excitation along the motor nerve. After the release of transmitter substances at the motor endplates, an endplate potential is formed at the muscle fiber innervated by this motor unit. The diffusion characteristics of the muscle fiber membrane are briefly modified and Na+ ions flow in. This causes a membrane depolarization, which is immediately restored by backward exchange of ions within the active ion pump mechanism, i.e. repolarization [77].

There are two techniques used to acquire EMG signals: the invasive and non-invasive techniques. Invasive techniques involve inserting a needle or wire electrode directly into the muscle detect to detect and record EMG signals [79]. A more preferred technique is the non-invasive technique, since signals are acquired from the electrodes place on the surface of the skin, as it is free of discomfort and provides minimal risk of infection to amputees [80]-[83]. The signals obtained by both techniques is a composite of all the muscle fiber action potentials occurring in the muscles underlying the skin. They can be either positive of negative voltage, due to action potentials that occur at random intervals. In a single motor unit, the combination of the muscle fiber action potentials from all the muscle fibers is the motor unit action potential (MUAP) which can be detected by both invasive and non-invasive methods [3]. For surface EMG signals, the amplitude is in a range between 0 to 10 mV, with a frequency range restricted to 10 to 500 Hz [8].

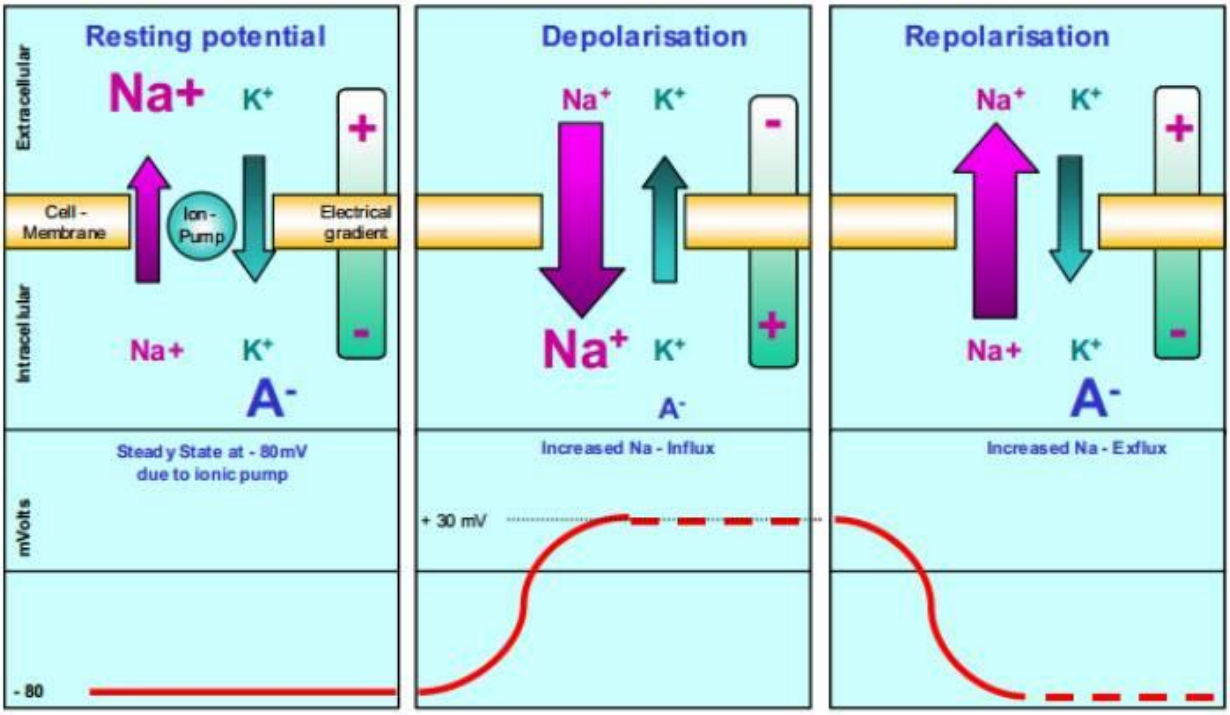

Fig. 2.8 Schematic illustration of repolarization/depolarization cycle within excitable membranes (adopted from [77]).

3 Development of Steady State Visually Evoked Potential Based Brain Machine Interface

Abstract: This chapter presents a signal processing technique to recognize human mental states from steady state visual evoked potentials (SSVEP). In this method, multiple bandpass filters are applied to the electroencephalographic (EEG) signals in order to extract the features of SSVEP. An artificial neural network classifier is used to recognize the type of SSVEP response. The main highlight will be the use of only two low-cost sensors for EEG recording. Experimental results showed that the proposed algorithm is capable of achieving an average accuracy of up to 93% and an information transfer rate of 4.2 bits/min. Furthermore, tradeoff between the number of commands and accuracy is also presented. Overall, the results of this study have demonstrated that a consumer-grade EEG device can serve as a modality in device control applications.

3.1 Introduction

According to the reports by the Japan Intractable Diseases Information Center, there are 9,950 people diagnosed with amyotrophic lateral sclerosis (ALS) in Japan [85], and it is estimated that over 400,000 people have ALS worldwide [86]. Depending on the stages of ALS, patients experience partial or complete paralysis which hinders the execution of daily activities. Brain machine interface (BMI) is an emerging technology developed to help these people by al-lowing them to manipulate devices with thought alone. BMI systems recognizes user intentions by decoding the brain signals and maps the outcome to several commands for control-ling the device [70].

BMI can be either invasive [87] or noninvasive [88], [89]. Noninvasive BMIs are often preferred over invasive ones because brain activities can be recorded without the need to implant any electrodes. Not only that it is safer, noninvasive BMIs also extends the target user range to include healthy people. In noninvasive BMIs, electroencephalography (EEG) is commonly employed because of its high time resolution, ease of acquisition, and cost effectiveness as compared to other measurement modalities [47].

EEG-based BMIs can be categorized into several different types depending on the brain activity patterns being used as control signal. For example, the use of event-related desynchronization/synchronization (ERD/ERS) [65], steady state visual evoked potentials (SSVEP) [90], P300 evoked potentials [56], and slow cortical potentials [91] have been studied by research groups across the globe. Compared to other types of BMI, SSVEP-based BMI has attracted increasing attention due to its high accuracy, high information transfer rate and little user training [51].

Current studies have demonstrated the potential of using SSVEP-based BMI as a mean to allow people to control external devices [92]-[95]. However, despite recent developments, many of these existing BMI systems are still difficult to be deployed at homes because they are very expensive in terms of cost and processing speed. Most BMI studies found in literature generally adopt high-end EEG equipment such as the g.USBamp (made by Guger Technologies in Austria) to get satisfactory performances [96]. Apart from the high financial costs, other drawbacks of using high-end devices are the need for longer preparation time and expert assistance. Usually, BMI users have to wash their hair before an experiment in order to remove oil or dirt on the scalp. In addition, it is required for the users to wear an electrode cap filled with conductive gel to ensure good conductivity. However, this procedure is generally time consuming, requires expert assistance to properly mount the electrode cap on the scalp and are usually uncomfortable [97]. Due to the above limitations, no BMI system has become commercially successful to this date. One way to counter this problem is by using a consumer-grade acquisition device to lower the cost. However, obtaining a high classification rate is very challenging due to lower accuracies of the acquisition device.

So far, only few studies have attempted to implement a SSVEP-based BMI with a consumer-grade EEG device such as the Emotiv EPOC (made by Emotiv Systems Inc. in USA) [98]-[101]. Güneysu and Akin [98] designed a four-class SSVEP-based BMI to control humanoid robots. They reported having achieved an average accuracy of 81.7% but no evaluation on recognition speed or the number of commands per minute were given. As such, it is hard to decide whether a low-cost device can serve as a modality in external device control. In comparison, a study done by Holewa and Nawrocka [99] reported having achieved an average accuracy of 73.75% and an average information transfer rate (ITR) of 11.36 bit/mins. How-ever, their evaluations are not based on classification of consecutive trials therefore it is un-certain to conclude whether the system will function satisfactorily under continuous input by the user. Very recently, a study done by Martišius and Damaševičius [100] addressed this issue by conducting real-time classification experiments where participants played a computer game using SSVEP-based BMI system. In their experiments, participants had to continuously command the spaceship to rotate left or right so that the cannon

points towards the target. Once the user is able to do so, they can issue another command to fire the cannon at the target. Their results have demonstrated that a consumer-grade EEG equipment has the potential to provide real-time gameplay. However, there are also has some limitations. The features of SSVEP are extracted using wave atom transform which is rather expensive in terms of computational costs, making the algorithm unsuitable for implementation on low-cost microcontrollers such as the Arduino. Similarly, works in [98] and [99] uses fast Fourier transform (FFT) in feature extraction and therefore also faces the same limitations. Overall, the accuracy, recognition speed, computational cost and ease of use of SSVEP-based BMI system still re-quire further improvements in order to raise the level of usability.

For the purpose of developing a user-friendly, low-cost SSVEP-based BMI system, this study presents a signal classification technique for a 3-class self-paced SSVEP-based BMI system with a rest state. There are two main features to this study. One is that this study uses only two electrodes from the Emotiv EPOC+ to acquire EEG signals. Another feature is the use of multiple bandpass filters to extract SSVEP features which requires very low computational cost and can be easily implemented on inexpensive microcontrollers like the Arduino. Artificial neural networks will be used to classify user intentions. The aim of this study is to explore and determine the extent of the recognition capabilities and the usability of a consumer-grade EEG acquisition device. The feasibility of the proposed method is evaluated based on the classification accuracy, recognition speed, and information transfer capability.

The rest of the chapter are organized as follows. Section 3.2 gives a brief introduction to SSVEP. Section 3.3 describes the system architecture, experimental methods as well as the necessary preprocessing procedures. Section 3.4 explains in detail, the feature extraction method using multiple bandpass filters and classification algorithm using artificial neural network. Section 3.5 presents an evaluation of the proposed algorithm. Discussions on accuracy, recognition speed, and information transfer capability will also be given in this section. Lastly, section 3.6 concludes the study.

3.2 Steady State Visual Evoked Potentials (SSVEP)

SSVEP are brainwave signals which occur naturally in response to visual stimulation. When the retina is stimulated by a visual stimulator (e.g. a flashing light) with a certain frequency, the brain generates response with the same spectrum as the stimulus. This response can be recorded in the form of electrical signal by placing electrodes on the occipital region of the brain [102]. Through numerous studies, researchers had concluded that SSVEP evoking frequencies had a wide range from 1 to at least 90 Hz, and the steady-state potentials exhibited clear resonance phenomena around 10,

20, 40, and 80 Hz [45]. The most commonly used frequencies range from 4 to 60 Hz. To elicit a SSVEP, repetitive visual stimulus (RVS) [47] has to be presented to the user. The RVS can be rendered on a computer screen by alternating graphical patterns or with external light sources able to emit modulated light. Alternating graphical patterns mainly include simple square flicker, checkerboard, and gratings [103]. In the case of external light sources, light-emitting diode (LED) are often used [104]. Fig. 3.1 shows an example of a SSVEP response elicited by presenting three LEDs flickering at 5Hz, 7Hz, and 9Hz to the user. The top row in Fig. 1 shows the time response of the EEG signal. A 5Hz stimuli is presented during t = 5-10s, 7Hz during t = 15-20s, and 9Hz during t = 25-30s. The bottom row of Fig.1 shows the spectral power of this EEG signal. From this figure, spectral peaks corresponding to the flickering frequency of the LEDs can be observed.

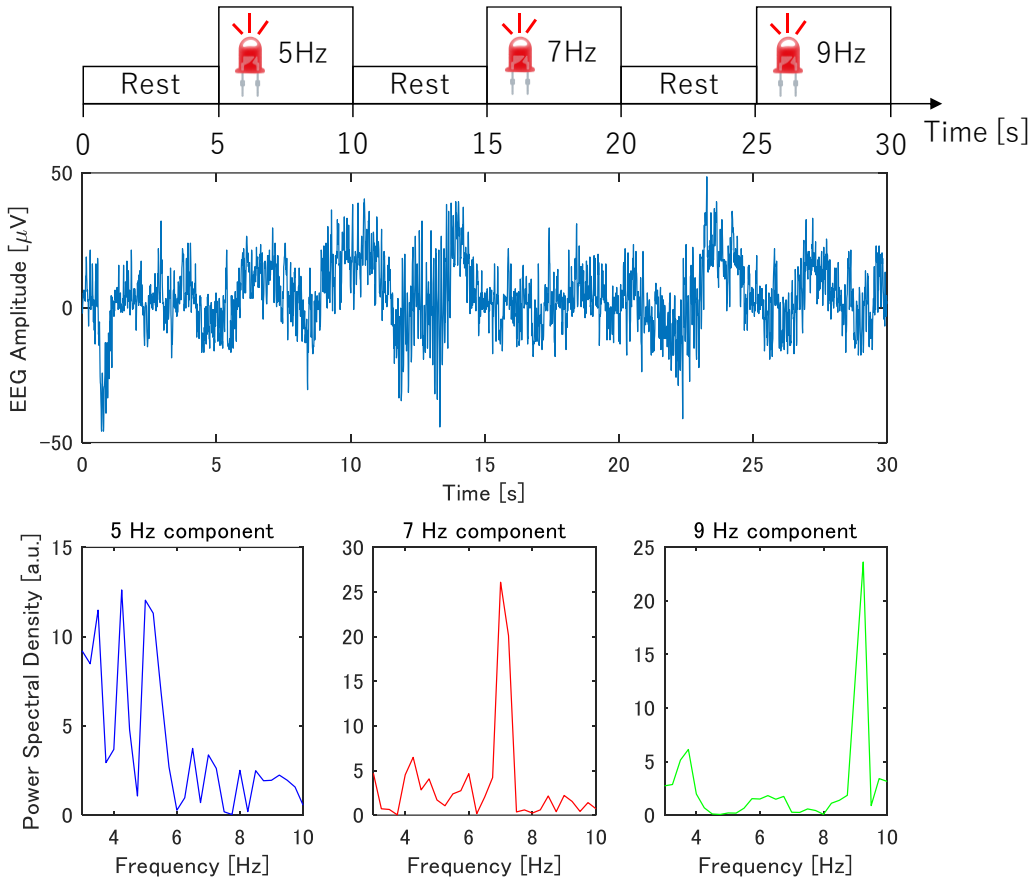

Fig. 3.1 Example of a time response of electroencephalographic signals (top subfigure) and its power spectrums while gazing at three LEDs flickering at different frequencies (lower three subfigures).

3.3 Experimental Methods

3.3.1 SSVEP-Based BMI System Architecture

The aim of this study is to classify three types of SSVEP response based on the frequency of the flickering LEDs and a rest state (no stimuli presented). A self-paced SSVEP-based BMI system is designed as illustrated in Fig. 3.2 to achieve this purpose. As depicted in Fig. 3.2, the system consists of three subsystems: the data acquisition system, the EEG signal processing system, and the interface system. The data acquisition system acquires EEG signals in a noninvasive fashion using the Emotiv EPOC+ headset. The acquired data is first sampled at 2048Hz internally and then downsampled to 128Hz before being sent wirelessly to the signal processing system. The signal processing system interprets the EEG signal and identifies the SSVEP response. The interface system consists of a PC monitor and a LED panel. The PC monitor is for displaying the signal status (for checking electrode impedance) and classification results in real-time. The LED panel is equipped with three 8×8 red LED dot matrix dis-plays for eliciting SSVEP and an Arduino for modulating the blinking frequencies. (Fig. 3.3).

Compared to other high-end EEG acquisition device, although the Emotiv EPOC+ headset offers a relatively low sampling rate at only 128Hz, there are many advantages that makes this device very attractive. The main benefit is that this device is relatively inexpensive. Another advantage is that it does not require conductive gel for the electrodes, making it easier to put on and use and saving lots of preparation time. To use the headset, users only need to apply saline solution (contact lens protection solution) to the electrodes before wearing it. In addition, Emotiv EPOC+ is able to transfer EEG data wirelessly to the computer and therefore does not restrict the user range of motion like many other clinical-grade devices. Since its wireless and compact, transport and setup are very easy even for users with little or no knowledge of BMI. This feature is very important in everyday use setting.

3.3.2 Experimental Design

In this study, three experiments are designed to evaluate several performance metrics of the SSVEP-based BMI system. The first experiment aims to evaluate the classification performance of the proposed system based on the correct and incorrect classification rates. In this experiment, participants are given the task to gaze at one of the three LED matrix displays according to the cues. Each LED is controlled by the Arduino to flicker at different frequencies. The EEG signals are recorded and analyzed to extract features that describe the brain-wave patterns elicited by each stimulus. These features will be used to train the artificial neural network (ANN) classifier and to

identify which LED the participant is gazing at. Fig. 3.4 shows the experiment protocol for each trial. In this study, rest state is also included in the classification. Therefore, the classification problem will consist of four classes. Features for rest state will be extracted from the alpha band (8-13Hz). To evaluate the classification accuracy, 5 trials of EEG data are collected for each participant. Leave-one-out cross-validation is applied to these data to compute the classification rate.

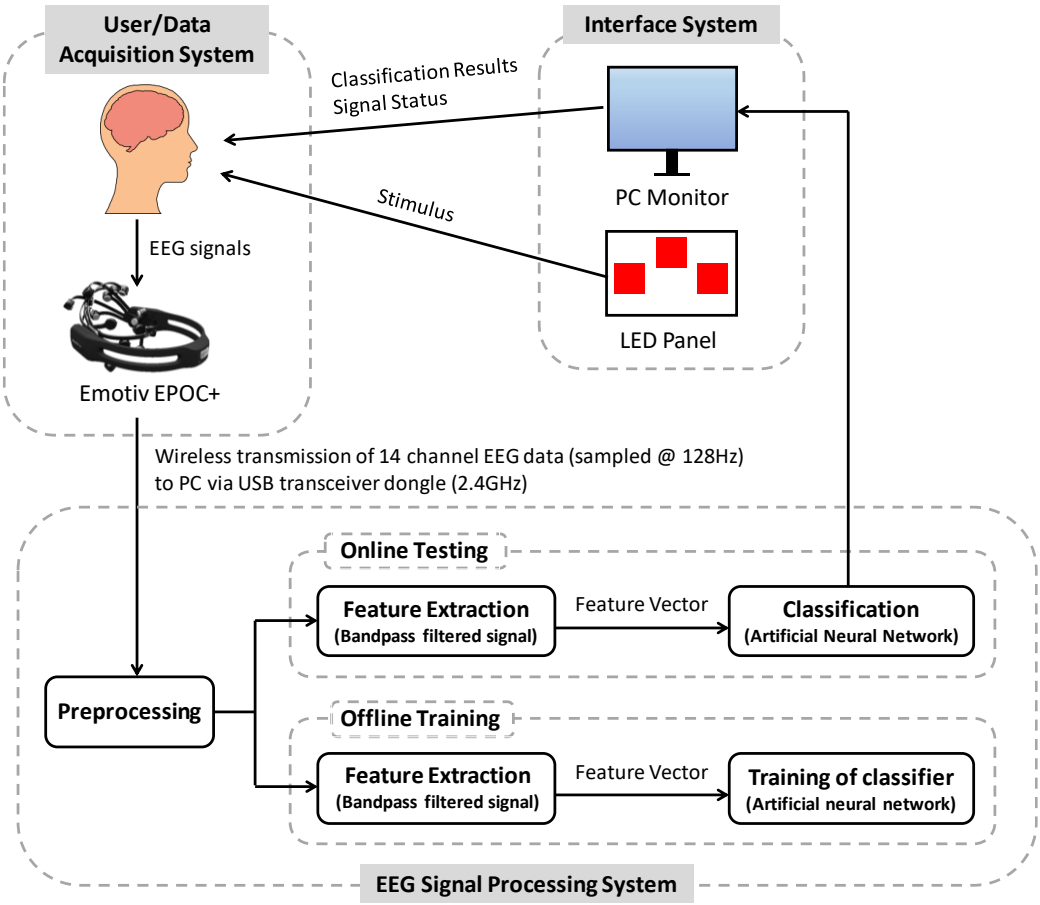

Fig. 3.2 SSVEP-based BMI system architecture

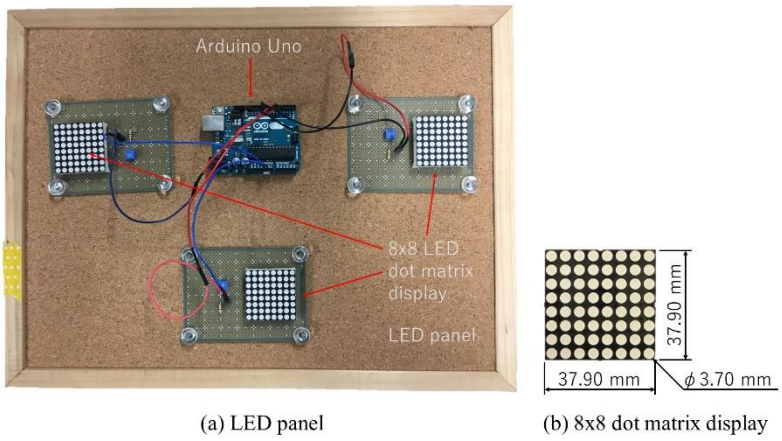

Fig. 3.3 View of the LED panel: (a) Three 8x8 dot matrix displays are used to elicit SSVEP response. The Arduino is programmed to modulate the blinking frequencies; (b) Dimensions of the dot matrix display.

The second experiment aims to evaluate the recognition speed, i.e. the time taken for the system to decide which LED the participant is gazing at. This duration of time is referred to as recognition time. In this experiment, 5 training datasets are acquired for each participant using the experimental protocol shown in Fig. 3.4. These datasets are used to train the ANN. In the evaluation stage, participants are asked to gaze at the flickering LED according to the experimental procedure shown in Fig. 3.5. During the execution of the task, the system will per-form online classification to decide which LED the participant is gazing at. The time taken for the ANN to reach a decision (recognition time) is measured and evaluated. The experiment is repeated 10 times for each flickering frequency.

The third experiment is designed to evaluate the information transfer capability of the system. The evaluation will be based on how many commands can be given out within 1 minute. In this experiment, participant will be asked to gaze at one of the three LED matrix display according to the predefined sequence. Once the system reaches a decision, an audio message saying “next” will be played and the participant can move on to select (gaze at) the next LED. This procedure is repeated for one minute. The total number of commands issued are counted at the end of each trial. Fig. 3.6 depicts the experimental protocol of a single trial. A total of 10 trials will be conducted for each participant.

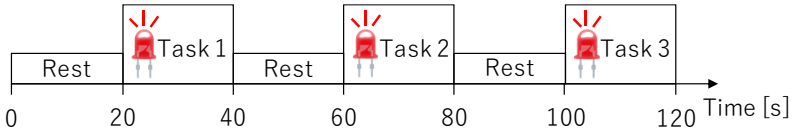

Fig. 3.4 Experimental protocol for acquiring training data. The acquired data will also be used to evaluate the classification performance.

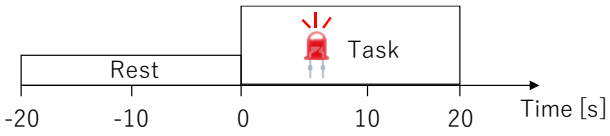

Fig. 3.5 Experimental protocol for the evaluation of recognition speed.

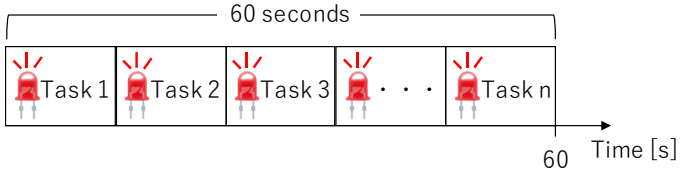

Fig. 3.6 Experimental protocol for evaluating the number of commands the BMI system can issue within one minute.

3.3.3 Preprocessing of EEG Signals

EEG signals are recorded in a noninvasive fashion on the participant's scalp using the Emotiv EPOC+ headset (Fig. 3.7(a)) and transmitted wirelessly to the computer. The headset is equipped with 14 electrodes that are arranged based on the 10-20 system as shown in Fig. 3.7(b). Out of the 14 electrodes, 2 electrodes (O1 and O2) that are positioned over the occipital region (highlighted in green) are used in this study. Two circles high-lighted in grey (CMS, DRL) indicate reference electrodes which are located behind the ears. The sampling frequency of the EEG headset is 128 Hz.

The acquired raw EEG signal is accompanied by a DC offset which needs to be removed before any analysis can be performed. This offset is removed by demeaning, i.e. subtracting the average amplitude of the raw EEG signal during the first 5 seconds from the whole signal. Next, a second order bandpass filter

$$G(s) = \frac{s^2 + 2\zeta\omega_n s + \omega_n{}^2}{s^2 + 2\zeta'\omega_n s + \omega_n{}^2} \tag{3.1}$$

is applied to the EEG signal to emphasize the frequency component of interest. Here, ω_n is the angular frequency to be emphasized, the damping coefficient ζ in the numerator is 0.6, and the damping factor ζ' in the denominator is 0.01. Next, the bandpass filtered EEG signal is full-wave rectified. By using multiple second order bandpass filter to extract the same frequency component as the stimulus, we can keep the computational cost low, which is important for implementing the algorithm on low-cost microcontrollers. Lastly, a second order lowpass filter

$$G_{LPF}(s) = \frac{(2\pi \times 4)^2}{s^2 + 2 \times 1.0 \times 2\pi \times 4s + (2\pi \times 4)^2} \tag{3.2}$$

is applied to the EEG signals. This preprocessed EEG signal will be later used in the feature extraction process.

3.4 Signal Processing Algorithm for Classification of SSVEP Responses

This study aims to develop a BMI system that is able to classify three types of SSVEP responses and rest state. In this work, features points that represent the characteristics of each SSVEP response are extracted from the preprocessed signal to form feature vectors. The type of SSVEP will be identified based on these feature vectors using an artificial neural network classifier. In this section, a detailed explanation of the proposed classification algorithm will be given. According to our preliminary experiments, the set of stimulation frequencies that can elicit strong SSVEP response vary from person to person. Therefore, the set of flickering frequencies used in this study are customized for each participant. For better understanding of the algorithm, we will assume that the flickering frequency of LED matrix displays are 7Hz, 8Hz and 13Hz.

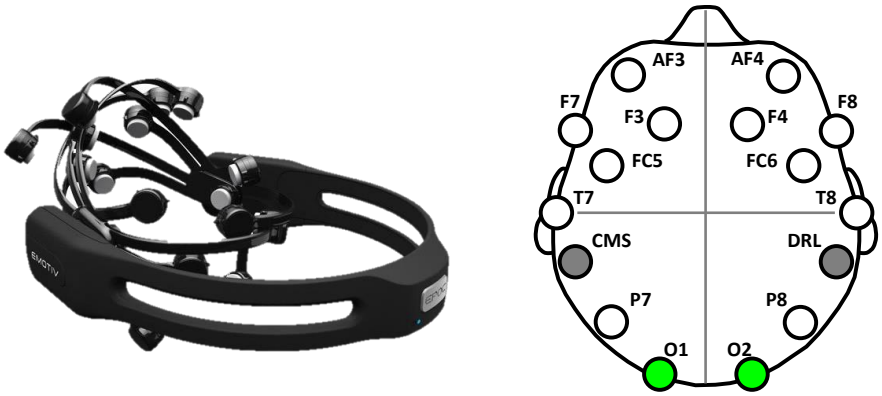

(a) Emotiv EPOC+ headset **(b) Arrangement of 10-20 electrode system**

Fig. 3.7 The EEG acquisition device and the electrode arrangement: (a) The Emotiv EPOC+ headset [105]; (b) Positioning of the electrode based on the international 10-20 system. Two green circles (O1 and O2) indicate the electrodes used in this study. Two grey circles indicate the reference electrodes. Two circles highlighted in dark grey indicate reference electrodes which are located behind the ears.

3.4.1 Feature Extraction

Let the time series data of the preprocessed EEG signal be defined as

$$\boldsymbol{x}_{f,ch}^{l} = \left[x_{f,ch}(0) \quad \cdots \quad x_{f,ch}(k) \quad \cdots \quad x_{f,ch}(n) \right]^{\mathrm{T}} \in \Re^{n+1\times 1} \tag{3.3}$$

where l represents the trial number ($l = 1, 2, \cdots, m$), k represents the discrete-time index, and n represents the final time index of the time series (the length of the vector is $n+1$). Also, $f \in \{7\,\mathbf{Hz},\ 8\,\mathbf{Hz},\ 13\,\mathbf{Hz},\ 10\,\mathbf{Hz}\}$ represents the emphasized frequency components. The 10Hz frequency component is used to detect the rest state. Furthermore, $ch \in \{\mathbf{O1}\ \ \mathbf{O2}\}$ represents the two EEG channels. Thus, as an example, $\boldsymbol{x}_{7Hz,O1}^{3}$ denotes the 7Hz time series data of channel O1 recorded on the third trial. Next, time series data of all trials (belonging to a particular frequency component) combined into one matrix can be expressed as

$$\boldsymbol{X}_{f,ch} = \left[\boldsymbol{x}_{f,ch}^{1} \quad \boldsymbol{x}_{f,ch}^{2} \quad \cdots \quad \boldsymbol{x}_{f,ch}^{m} \right] \in \Re^{n+1\times m}. \tag{3.4}$$

Then, the time series signal of each trial can be normalized by

$$\boldsymbol{d}_{f,ch}^{l} = \frac{\boldsymbol{x}_{f,ch}^{l}}{\max\left(\boldsymbol{X}_{f,ch}\right)} \in \Re^{n+1\times 1}. \tag{3.5}$$

Fig. 3.8 shows the normalized EEG signal of the O1 and O2 electrodes acquired during the third experimental trial ($\boldsymbol{d}_{f,ch}^{3}$). The feature points are selected from the normalized EEG signals. Note that $\max(\boldsymbol{X}_{f,ch})$ should be determined beforehand from *m* training datasets in order to normalized the time series of each frequency components in the online classification stage. As shown in Fig. 3.8, for each class of SSVEP response, the extracted feature points can be put together to form an 8-dimensional (4 frequency component × 2 channels) feature vector which can be expressed as

$$\boldsymbol{v}^{c} = \left[v_1^{c} \quad \cdots \quad v_i^{c} \quad \cdots \quad v_8^{c} \right], \tag{3.6}$$

where v_i^{c} is the i^{th} element of the feature vector belonging to the *c* class ($c \in \{7\,\mathbf{Hz},\ 8\,\mathbf{Hz},\ 13\,\mathbf{Hz},\ \mathbf{Rest}\}$). The feature vectors are used as the input signal to train the artificial neural network classifier.

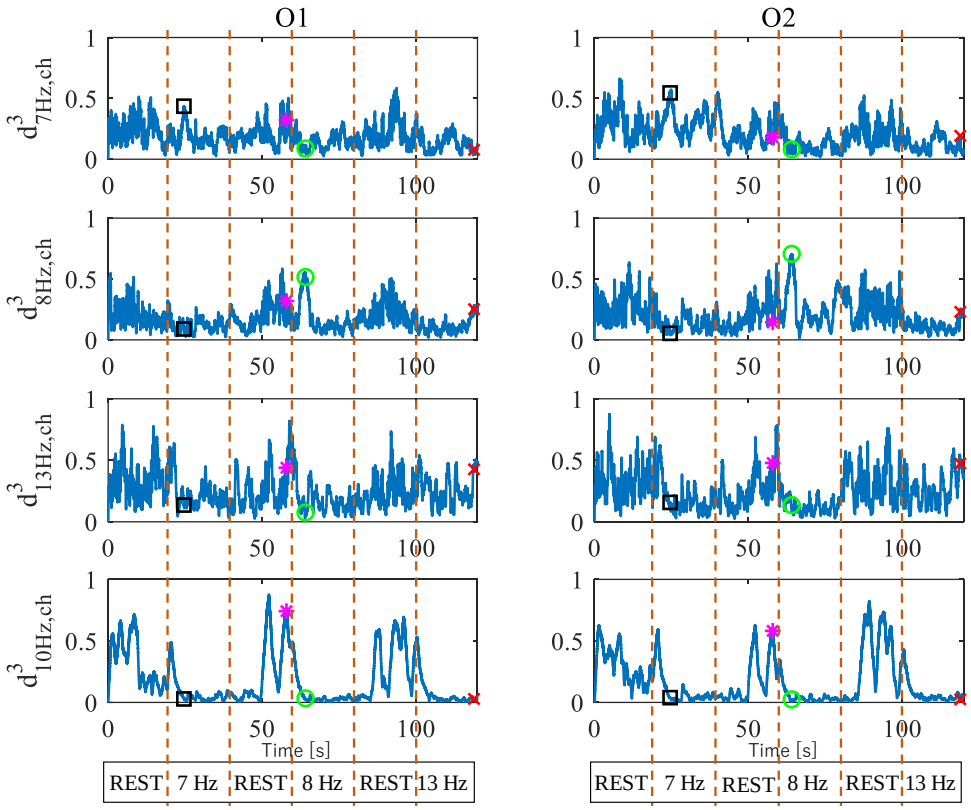

Fig. 3.8 An example of time responses of normalized preprocessed electroencephalographic signals and the selected feature points. The symbols □, ○, ×, * represents the feature points belonging to 7 Hz class, 8 Hz class, 13 Hz class and rest class, respectively.

3.4.2 Training of the Artificial Neural Network Classifier

In this study, artificial neural network (ANN) is selected as the classifier to discriminate three SSVEP brain patterns and rest state. Currently, several kinds of ANN have been proposed. In this study, a multilayered perceptron, which is a feed-forward ANN is chosen.

The multilayer perceptron is a multilayered ANN that consists of one or more hidden layers. This type of ANN is known as a supervised network because it requires a desired output (teaching signal) in order to learn. A set of learning data that consists of the feature vector and the corresponding teaching signals is used to have the perceptron acquire appropriate connection weights and threshold values of the middle layer and the output layer by machine learning. The multilayered perceptron and many other ANN learn by using an algorithm called backpropagation. With back propagation method, the input data (feature vector) is repeatedly presented to the ANN. With each presentation, the output of the ANN is com-pared to the desired output (teaching signal) and an error is computed. This error is then feedback (backpropagated) to the ANN and used to adjust weights so

that the error decreases with each iteration and the ANN model gets closer and closer to producing the desired output [106]. When performing real-time classification, these connection weights and threshold values are fixed and determined beforehand. To keep the computational cost low, an ANN with only one hidden layer is structured in this study. There are 8 neurons in the input layer, 12 in the hidden layer, and 4 in the output layer. The learning coefficient is set to 1.2. Note that the number of neurons in the hidden layer is determined by trial and error.

In the online classification stage, the classification label of a SSVEP response is deter-mined based on the integrated value of ANN outputs. More details on this procedure will be given in the next section.

3.5 Experiment

3.5.1 Experimental Conditions

In this study, the experiments were carried out with the cooperation of 3 able-bodied participants. One of the participant is female (referred to as participant A) and two are male (referred to as participant B and C) and one is female. The entire protocol and aims of the study are fully explained to them before the experiment, and all the participants signed the written informed consent. All of the experiments are conducted with the approval from Tokyo Denki University Human Bioethics Committee. Apart from participant B, all other participants had no prior experience with BMI experiments at all.

During the equipment setup, no skin preparation technique was applied to the scalp as the mimic the real-life usage scenario. The experiments are divided into training and online testing stage (with the exception of experiment 1) both conducted on the same day. Table 1 shows the number of trials performed in the training and evaluation and stage for each experiment.

Table 3.1 Experimental Procedure and Number of Trials Performed in the Training and Evaluation Stage of Each Experiment.

Experiment Number	**Number of Trials in the Training Stage**	**Experimental Procedure**	**Number of Trials in the Training Stage**	**Experimental Procedure**
1	5 (Leave-one-out cross-validation was used to evaluate the classification accuracy)			Fig. 3.4
2	5	Fig. 3.4	10	Fig. 3.5
3	5	Fig. 3.4	10	Fig. 3.6

3.5.2 Evaluation of the Classification Performance

In this experiment, EEG signals are recorded according to the procedure in Fig. 3.4 and repeated 5 times. Since the number of training data is small, leave-one-out cross-validation (LOOCV) is used to evaluate the classification performance. Here, the classification label of each task is determined based on the SSVEP class with the highest area overlap rate defined as

$$\mathbf{Area\,Overlap\,Rate} = \frac{\mathbf{Area\,of\ ANN\,output\,signal}}{\mathbf{Area\,of\ control\,signal}} \times 100[\%]. \tag{3.7}$$

If the classification label and the frequency of the stimulus match, the classification is considered correct. The accuracy of a given class will be evaluated based on the number of correct decisions. Fig. 3.9 shows the ANN output of participant B as a function of time. We will use the result from the 3rd iteration of LOOCV as an example. According to Fig. 3.9, participant B gazes at the 7Hz stimulus (task 1) during $t = 20 - 40s$. In this time frame, the area overlap rate is 70.5% for 7Hz class, 10.5 for 8Hz class, and 2.76 for 13Hz class. Clearly, the highest area overlap rate of the ANN output neuron belongs to the 7Hz class, thus, the classification result will be labeled '7Hz'. Furthermore, since the classification label matches the frequency of the stimulus, this decision is deemed correct. The area overlap rate for the remaining tasks are shown in Table 2. Based on this result, the accuracy of the 3rd iteration of LOOCV is 100%. It is worth mentioning that although rest state is included in the classification, the accuracy is not calculated because rest state is not part of the control commands. Finally, in order to evaluate the classification performance, the accuracy of all LOCCV iterations was calculated and averaged. Table 3 shows the classification performance (average accuracy) of three participants. The average accuracy across subject was 80%. Note that the frequency of the stimulus is different for each individual as mentioned previously.

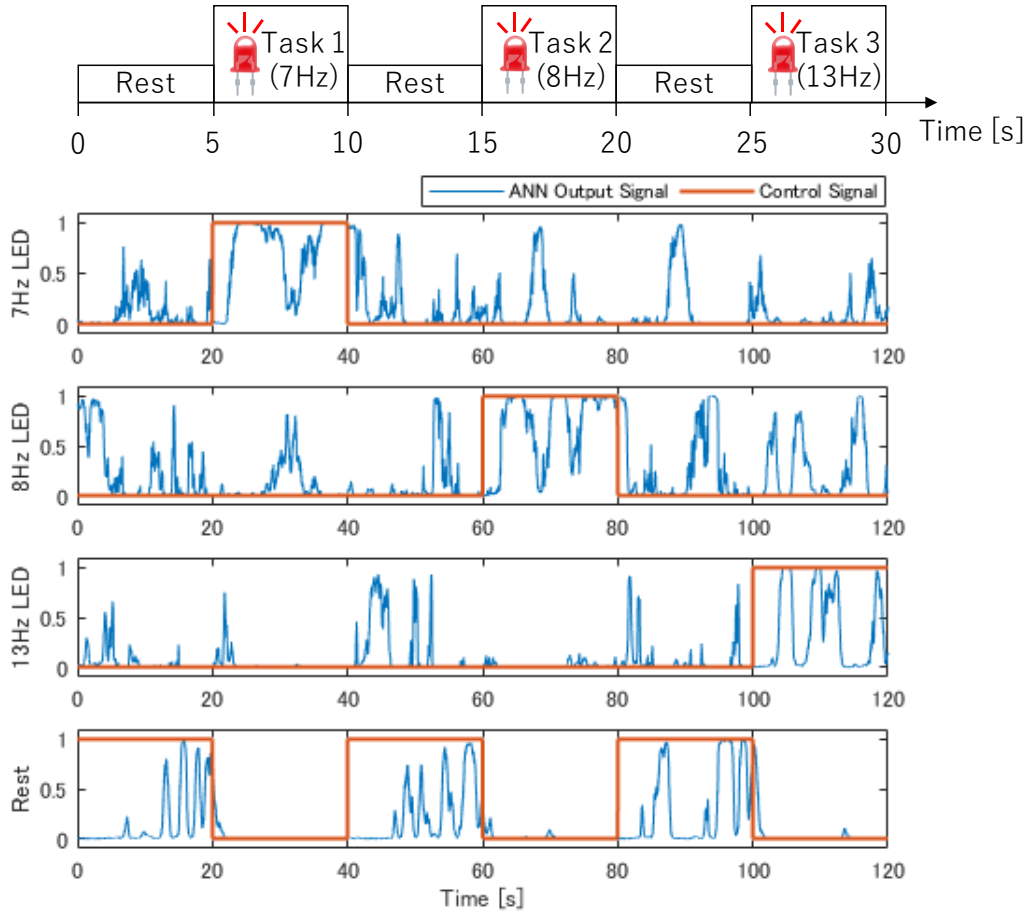

Fig. 3.9 Time responses of ANN output of participant B. From the top, output neurons corresponding to 7Hz, 8Hz, 13Hz class and rest state (in order from the top) of participant B. Leave-one-out cross-validation is performed and the result of the 3rd iteration is shown as an example. The blue line represents the classification signal. The red line represents the control signal.

Table 3.2 Area Overlap Rate of Each Tasks (LED Stimuli) in Fig. 3.9

Stimuli Frequency (Start-End Time of Task)	**ANN Output Neurons Corresponding to Three Classes**		
	7Hz	**8Hz**	**13Hz**
7Hz ($t = 20-40s$)	70.5	10.5	2.76
8Hz ($t = 60-80s$)	12.0	68.9	1.74
13Hz ($t = 100-120s$)	8.20	23.5	34.8

Table 3.3 Classification Accuracy of Three Participants [%]

Participant	**Task 1**	**Task 2**	**Task 3**	**Average**
A	80	80	80	80
B	100	100	100	100
C	40	60	80	60
Average	73.3	80	86.7	80

3.5.3 Evaluation of Recognition Speed

Other than achieving high accuracy, having a fast recognition speed is also an important factor for improving the usability of a BMI system. In this experiment, the procedure in Fig. 3.4 is repeated 5 times to acquire training data. After the ANN is trained, the experiment protocol in Fig. 3.5 is performed 10 times to evaluate the recognition speed. Here, the classification label is decided by comparing the integrated value of ANN output of each class. We will use Fig. 3.10 to explain this procedure in detail. In this example, the 7Hz stimulus was presented to the participant.

Starting from $t = 0s$, the ANN output signals (Fig. 3.10(a)) are integrated and compared with each other. At any sampling instance, if the integrated value of class is twice more than the remaining two classes, then the classification signal for that particular class will be '1'. However, if this condition is not satisfied by any class, then the classification signal belonging to the rest state will be '1'. In addition, if the classification signal of a class lasts for 3 seconds, then the classification label will belong to that particular class (Fig. 3.10(b)). Here, the time taken for the system to make a decision (referred to as decision time) is recorded and used to evaluate the recognition speed. In the example shown in Fig. 3.10(b), starting from $t = 3s$, the classification signal for 7Hz class is assigned the value '1' and lasts for more than 3s. Hence the decision time for this class is 6.09s. Note that since the classification signal for the other classes did not last 3s, no incorrect decision was made in this example.

Fig. 3.11 shows average decision time of each stimulus of 10 experiment trials. The red error bars indicate the standard deviation. The results show that the proposed method can achieve an average recognition speed of 4.74 seconds. Based on this result, it is theoretically possible for the user to issue 12.66 commands (decisions) per minute. In addition, statistical analysis result suggests that the recognition speed is different for each flickering frequency. Perhaps by searching for more suitable frequency, the recognition speed of the system could be further enhanced. As an extension to this study, a broader range of frequencies should be investigated. It would be interesting to see whether there is a relationship between recognition speed and the frequency or not.

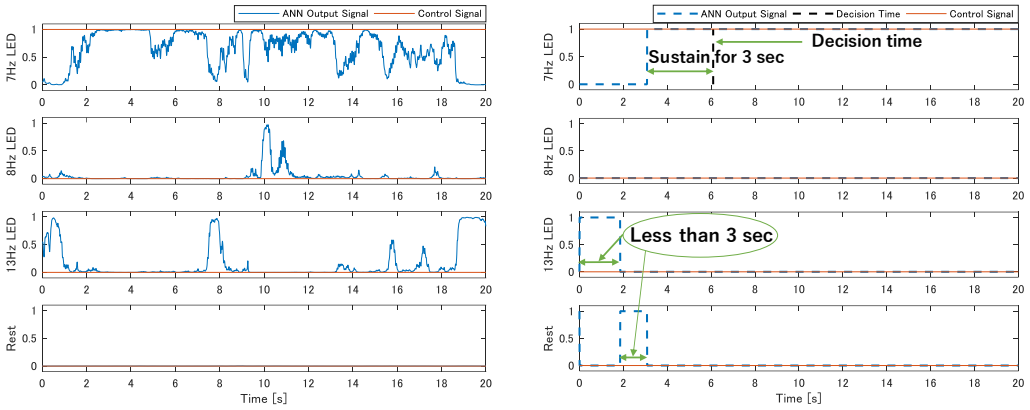

(a) Time response of ANN output **(b) Time response of the classification signal**

Fig. 3.10 Diagram illustrating the definition of decision time (recognition speed): (a) Time response of ANN output of the experiment in Fig. 3.5; (b) Time response of the classification signal derive from Fig. 3.10(a). In this example, the recognition speed of 7Hz LED stimulus is 6.09 seconds.

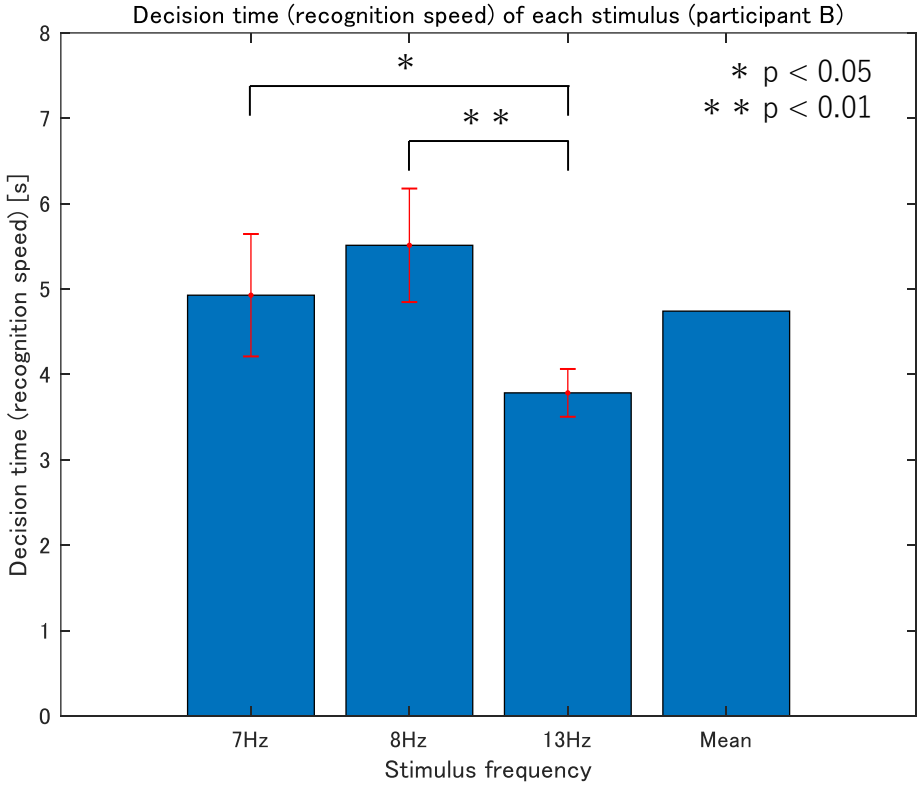

Fig. 3.11 Decision time (recognition speed) of each stimulus (participant B). The red error bars indicate standard deviation. (*) represents $p < 0.05$ and (**) represents $p < 0.01$.

3.5.4 Evaluation of Information Transfer Capability

In the previous two experiments, the evaluation of the proposed BMI system is done offline. However, since BMI systems operate in real-time, it is important to test whether the proposed algorithm will work in real-time environments. To do this, first the training data is obtained by repeating the procedure in Fig. 3.4 5 times. After the ANN is trained, the experiment protocol in Fig. 3.6 is performed 10 times to evaluate the information transfer capability. Using the same method as the second experiment, the classification label (decision) will be given to the class that can sustain the classification signal for 3 seconds (Fig. 3.10). Once a decision has been reached, the integrated value of ANN outputs will be reset to zero. Furthermore, investigation on how different time length of sustained classification signal affects the information transfer capability was also be conducted.

In this experiment, information transfer capability is evaluated based on the total number of decisions (NOD), accuracy (defined as the number of correct decisions divide by the total number of decisions), and information transfer rate (ITR). ITR is the amount of information communicated per unit time shown as bits per minute. This measure incorporates both speed and accuracy in a single value. ITR is define by Wolpaw et al. [70] as

$$\textbf{ITR [bits/min]} = \frac{60}{T}\left[\log_2 N + P\cdot\log_2 P + (1-P)\cdot\log_2\left(\frac{1-P}{N-1}\right)\right], \qquad (3.8)$$

where N is the number of possible choices (commands), P is the accuracy of classification and T (seconds/choice) is the time length of the trial or choice.

Two experiments are conducted over 2 days. On the second day, to investigate the in-fluence of time length of sustained classification signal on information transfer capability, 10 online classification trials were performed for the time length of 2 seconds and 3 seconds. Fig. 3.12 shows the information transfer capability. According to this figure, the proposed algorithm is capable of producing 5.53 commands/minute on average. Depending on condition of the user and the time length of sustained classification signal, the user can issue an average of up to 6.8 commands/minute. Compared to the theoretical value of 12.66 commands/minute reported in the previous section, the number of commands is lower in online classifications. One reason could be that during the one-minute trials, the participant was not always fully attentive to the LED stimuli. Therefore, the results reported in this study includes ‘short breaks’ in the evaluation.

Furthermore, the BMI system was able achieve a mean accuracy of 80.1%. Again, depending on the condition, an average accuracy of up to 93.5% (Day2) can be achieved. Compared

with previous studies that uses the same EEG hardware [98]-[101], this work uses a much smaller set of electrodes and offers a slightly higher accuracy. Since only two electrodes are involved in EEG recording, further reduction of hardware costs and setup time may be possible. Another advantage of this study is the simplicity of the algorithm. Compared to works like [98], [99] that uses FFT or [100] that uses wave atom transform (WAT), the computational cost of the proposed method is much lower. In addition, statistical analysis shows that shortening the time length of sustained classification signal increases the number of commands per minute but lowers the accuracy. This suggest that there is a tradeoff between number of commands and accuracy. So, depending on the target application, a different time length of sustained classification signal might be preferable over the others. For example, if the target application prefers faster response speed, then a shorter time length should be used. On the other hand, if the target application requires accurate classifications such as control of a wheelchair, then a longer time length is more suitable.

In addition to accuracy and number of commands, this work also gives an evaluation of the ITR. The mean ITR achieved by this system is 3.53 bits/minute and the highest average ITR achieved is 4.2 bits/minute. Although the ITR is relatively low compared to studies using high-end EEG device, the above results have shown that the proposed method is functional and has the potential to control external devices in real-time environment. Furthermore, the results also suggest that a consumer-grade EEG device can serve as a modality in device control and other human-machine interface applications.

The limitations of this research lie in fact that only a small number of participants were involved in the evaluation process. As an extension to this study, more participants should be recruited so that the reliability of the system can be evaluated.

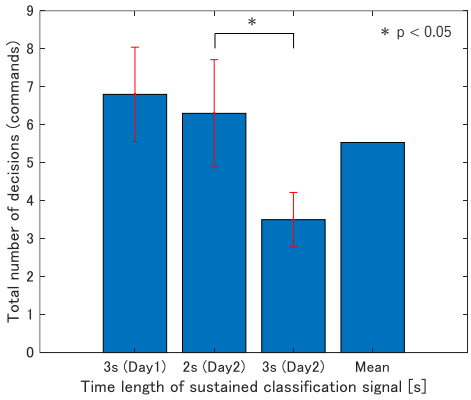

(a) Number of decisions per minute

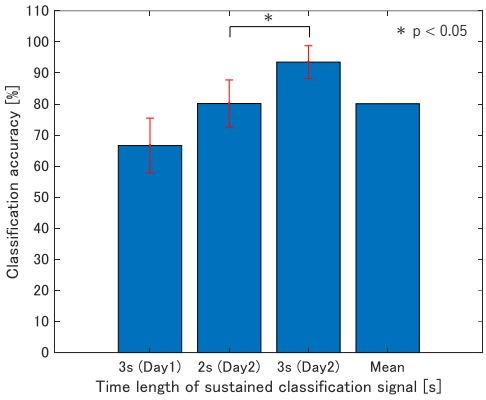

(b) Accuracy

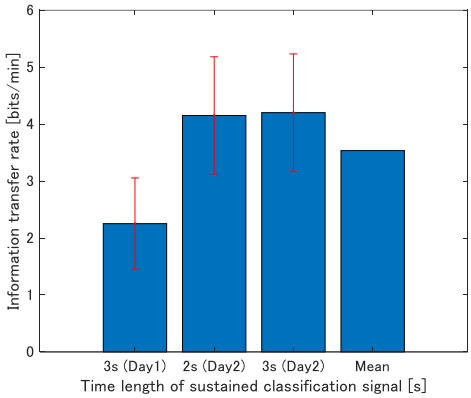

(c) Information transfer rate

Fig. 3.12 Information transfer capability of participant B: (a) The number of decision (commands per minute); (b) Accuracy of 10 trials; (c) Information transfer rate (ITR). In all three subfigures, red error bars indicate standard deviation. (*) represents $p < 0.05$.

3.6 Conclusion

In this chapter, a signal processing algorithm has been proposed for a 3-class self-paced SSVEP-based BMI system with a rest state. The function of the system is to classify the type of SSVEP response from EEG patterns in real-time. The major novelty of this study is the use of only two low-cost sensors (low sampling rate) for EEG recording. In the proposed method, multiple bandpass filters are used to extract SSVEP features and classifications are performed using artificial neural network. Experiment results show that the proposed system could achieve an average accuracy of up 93%. Also, the user is able to issue up to 6.8 commands/minute on average using this system. Furthermore, this study also presents a tradeoff between the number of commands per minute and accuracy. Using this tradeoff, the user can adjust the responsiveness and the accuracy of the system to suit the target application. Overall, the results of this study have shown the possibility of using a consumer-grade EEG device as a modality in device control and serves as a foundation for further interesting research. The discussions have also revealed the challenges towards developing a practical BMI system. An extension to this study would be to raise the overall performance by improving the feature extraction algorithm. Also, it would be interesting to investigate the characteristics of other frequencies in order to find the optimal set of frequencies that can elicit stronger SSVEP response and are more responsive.

4 Development of Motor Imagery Based Brain Machine Interface

Abstract: This chapter presents a signal processing technique for a low-cost brain machine interface (BMI) that uses spectral analysis and artificial neural network (ANN) to classify human mental states from electroencephalographic (EEG) signals. In this study, a BMI system has been prototyped to classify the intention of moving an object up, down, left, right and at rest state. EEG signals are recorded using a consumer grade EEG acquisition device. The device is equipped with 14 electrodes but only 8 electrodes are used in this study. To evaluate the system performance, online classification experiments for three subjects are conducted. True positive and false positive rates are used as an evaluation index. Experiment results show that for the classification of three mental states, the proposed method is capable of achieving an overall true positive rate of up to 67% with 15 minutes of training time by a novice BMI user. On the other hand, the overall true positive rate was below 50% for classification of five mental states. These findings strongly suggest that the BMI system can classify 2-3 mental tasks at most when using a consumer grade EEG hardware. Furthermore, offline analysis is carried out using the same EEG data to explore ways of using spectral analysis and ANN to reduce erroneous classifications. Analysis results show that by setting the classification threshold value higher, the false positive rate can be reduced. Another finding suggests that in contrast with the study results by other research teams, the use of multiple ANNs to classify three mental states do not improve the accuracy. Lastly, a hamming window size of 64 samples is found to be optimal for achieving real-time control when performing spectral analysis.

4.1 Introduction

Brain machine interface (BMI) is an emerging technology that aims to assist people with disabilities as well as the aged by allowing their users to intuitively control external devices by intent alone. BMI systems recognizes human intentions from changes in neural responses and translates them into operative control signals [1]-[3]. These brain signals can be recorded in an invasive or a noninvasive fashion, where the latter approach is preferably adopted because no surgical implantations of electrodes are required and hence extending the target user range to include healthy

people.

In a noninvasive BMI system, brain activity can be measured through electroencephalography (EEG), magnetoencephalography (MEG), functional magnetic resonance imaging (fMRI), functional near infrared imaging (fNIR), or positron emission tomography (PET), where EEG is commonly used in most BMI studies due to its high portability, inexpensiveness and high temporal resolution [36]. The traditional application of BMI is to control external devices such as a wheelchair [9]-[12] or a robot arm [107], as well as provide communication [56] for disabled users. In recent years, the use of BMI for smart home controls [14]-[17] and entertainment [18]-[21] have also been suggested which have the potential to also benefit healthy people.

However, many of these existing BMI systems are still difficult to be deployed at homes because they are very expensive in terms of cost and processing speed. Furthermore, since many BMI systems rely on large number of electrodes, the proper positioning of each electrode requires expert assistance and takes significant amount of time. Hence, most BMI systems are still unsuitable for household and daily applications. One way to counter this problem is by reducing the number of electrodes. Another way may be achieved by using a consumer grade acquisition device to lower the cost. However, obtaining a high classification rate is very challenging due to lower accuracies of the acquisition device.

This study presents a signal processing technique to classify three mental states for BMI systems that uses a consumer grade EEG acquisition device. The aim is to develop a low-cost BMI system suitable for households and daily applications. As a preliminary study, an experiment has been conducted to classify the intention of moving an object up, down, left, right and at rest state, which are basic instructions needed for controlling most electronic devices, by using only EEG signals. Specifically, the experiment is divided into two parts. The first part aims to classify three types of mental tasks (up, down and rest). The second part attempts to classify all five mental states (up, down, left, right and rest). The results are analyzed and discussed to determine the limitations of the proposed system. In this study, spectral analysis method is used in feature extraction process and artificial neural networks are employed as classifiers. This study also introduces true positive rate and false positive rate to evaluate system performance. In addition, offline analysis is carried out using the same EEG data to explore ways of reducing erroneous classifications. More specifically, the influence of the classification threshold value, the use of multiple artificial neural network for classification, and the influence of hamming window size are investigated and discussed.

This chapter is organized as follows. Section 4.2 describes the task design and experimental

procedures and setup in order to acquire EEG signals. Section 4.3 explains the necessary signal processing methods for classification of mental states. Section 4.4 shows the classification results of three and five mental states. The results will also be discussed in this section. Section 4.5 presents the findings of offline analysis. Lastly, section 4.6 concludes the study.

4.2 Experimental Design

Experiments are conducted in order to record changes in EEG signals during mental tasks. The acquired data will later be used to select informative features of each intended motion. Also, the experiment is conducted in order to evaluate the classification performance of the proposed algorithm. In this chapter, details of the experiment are described.

4.2.1 Task Design

Fig. 4.1 shows the experimental setup. In this experiment, the subjects are asked to sit comfortably and look at the display. Next, they are instructed to imagine moving the solid circle shown on the screen up, down, left or right as indicated by the imagery cues. During the task, EEG signals are acquired.

In this study, the subjects are asked to choose a mental task that is closely related to up, down, left or right movements. As such, for up or down mental tasks, the subjects may choose to imagine an object sliding up or down but asked not to choose imagery tasks such as foot imagery since they have little relation to the actual movement. The purpose is to record the “real intentions” and to observe the differences in EEG signals.

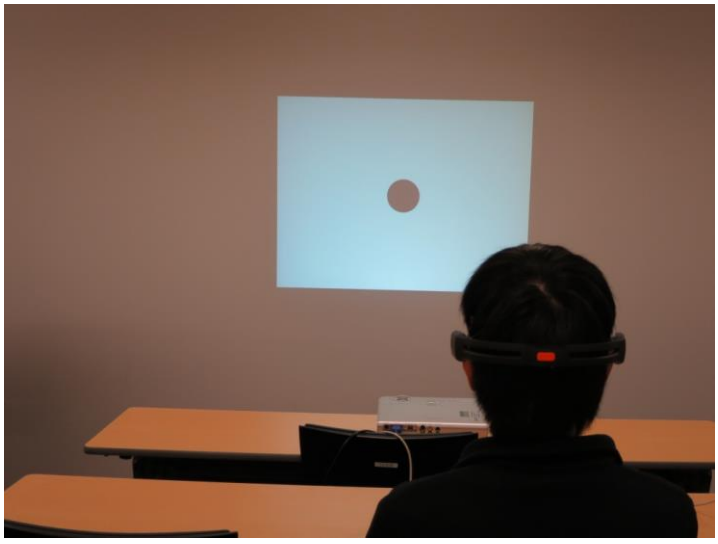

Fig. 4.1 Experimental Setup

4.2.2 Experimental Procedure

Two kinds of experiments are conducted in this study. The first one aims to correctly identify 3 mental states which are up and down intentions and rest state. In this experiment, only up and down cues are used during mental tasks trial as illustrated in Fig. 4.2 (left). The second experiment aims to classify 5 mental states which are up, down, left and right intentions and rest state. In this experiment, all four kinds of imagery cues are used as illustrated in Fig. 4.2 (right).

During the rest period, the subject gazed at a black circle that was shown at the center of the screen for 60 seconds to reduce eye movement. Next, an arrow indicating up, down, left, or right motion were presented and the subject began to perform the mental task for 10 seconds. To prevent forecasting, the mental task cues are randomized.

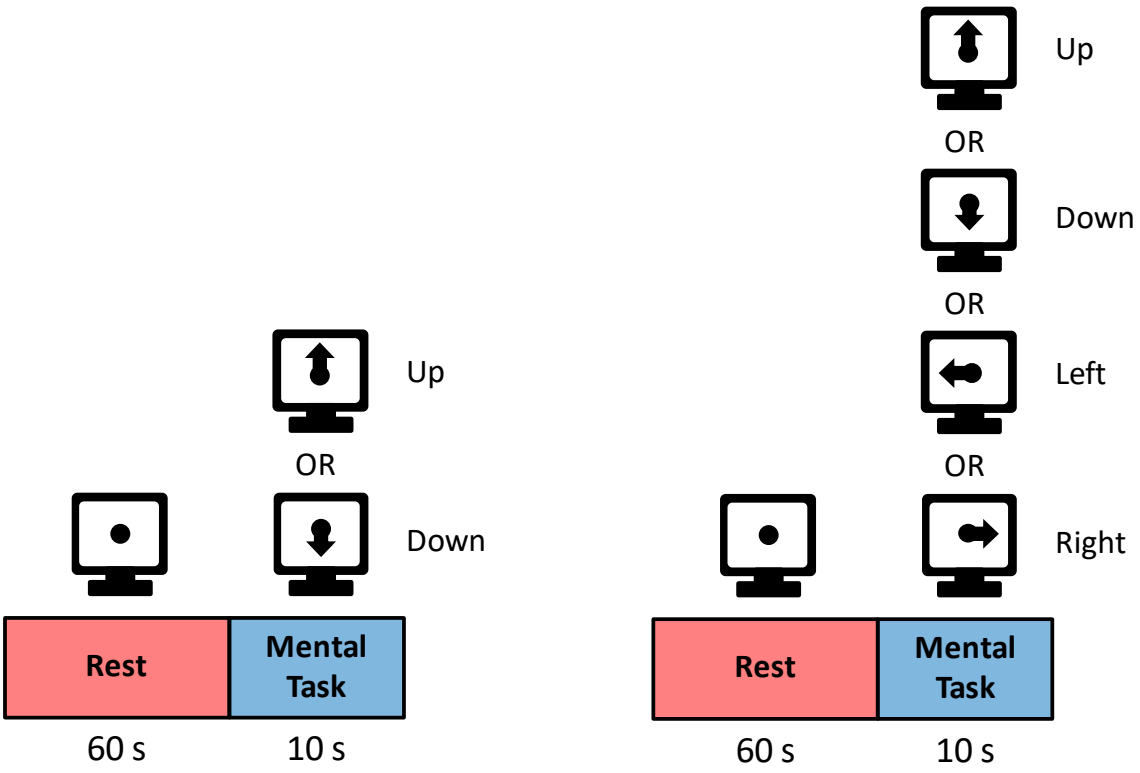

Fig. 4.2 Experiment Procedure. The illustration on the left shows the procedure for the identification of 3 mental states experiment. The illustration of the right shows the procedure for the identification of 5 mental states experiment.

4.2.3 Experimental Setup

As illustrated in Fig. 4.3, the proposed system consists of three main subsystems; the data acquisition system, the BMI system and the interface system. The data acquisition system acquires the electroencephalographic (EEG) signals in a noninvasive fashion and sends the recorded data wirelessly to the BMI system to be process. The BMI system then interprets the EEG signals and identifies the user intent. The interface system displays three types of data;

(1) Motor imagery (mental task) cues used during the offline training sessions

(2) Identification result from the BMI system during online testing sessions

(3) Signal status

In this study, the aim is to correctly identify the intention of moving an object up, down, left or right. Here, the non-control state is referred to as the "rest" state.

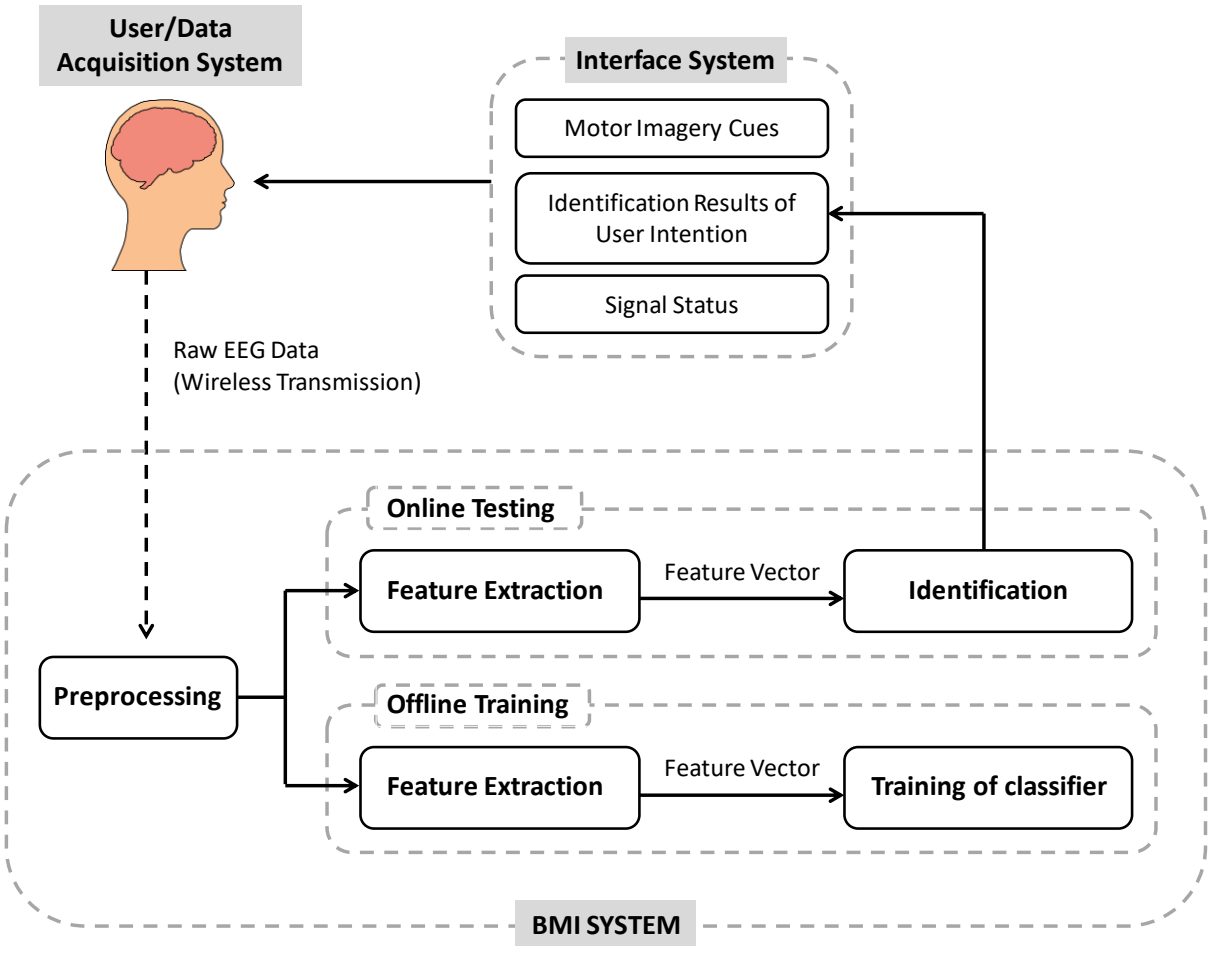

Fig. 4.3 System Architecture

EEG signals are recorded on the subject's scalp using a headset (Emotiv) equipped with 14 electrodes (AF3, F3, F7, FC5, T7, P7 O1, O2, P8, T8, FC6, F4, F8 and AF4). The electrodes are positioned based on the 10-20 system as shown in Fig. 4.4. Out of the 14 electrodes, 8 electrodes (AF3, F3, F7, FC5, FC6, F4, F8 and AF4) positioned over the frontal lobe (highlighted in light grey) are selected based on the knowledge that. the frontal lobe is responsible for thinking, planning, and the execution of cognitive tasks. Two circles highlighted in dark grey (CMS, DRL) indicate reference electrodes which are located behind the ears. The sampling frequency of the EEG headset is 128 Hz.

In most BMI studies, electrode placement is often concentrated on the primary motor cortex, e.g. C3 and C4. This is because these studies primarily focus on classifying motor imagery states by observing power changes in movement related mu (8-12 Hz) and beta (18-26 Hz) rhythms over this part of the brain, which is responsible for body/limb movements. There are two reasons why electrodes over primary motor cortex are not chosen in this study. One reason is that the Emotiv EEG headset do not provide electrodes over the primary motor cortex and since the electrode positions are fixed to the headset, they cannot be moved. The other reason is that the mental task in this study is not limited to motor imagery. For example, when the subject tries to imagine an up motion, they can choose to imagine ‘a ball sliding up’ instead of imagining ‘moving their right arm up.’ As such, electrodes placement in areas other than motor cortex is also preferred.

In this system, the recorded EEG signals are wirelessly transmitted to the PC in real-time after being converted to digital form. The headset also has a built-in 2 axis gyroscope used to monitor head movement in horizontal and vertical axes in real-time. The software development environment is MATLAB/Simulink®. The proposed algorithm is executed after being built by Simulink real-time workshop. During online testing session, identification results are feedback to the user in real-time by looking at the screen. In this way, the user can easily see whether the identification results are correct or not and allows them to modulate their brain waves accordingly. Since signal status is also visually available for the user on the screen, less preparation time is needed to setup the experiment. This also helps ensure that the acquired EEG data are reliable.

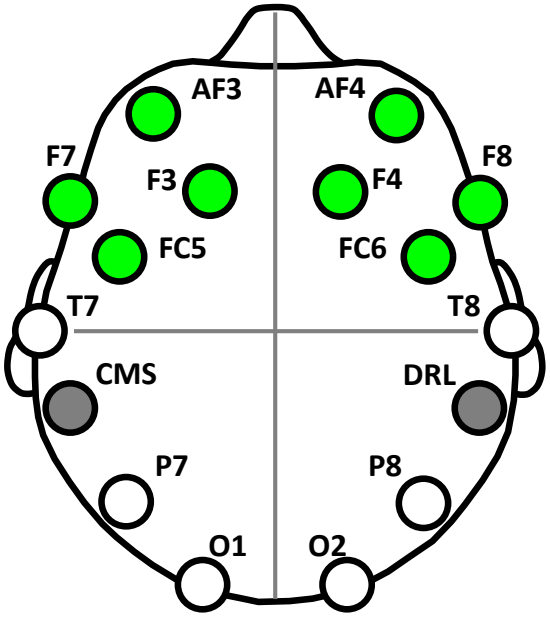

Fig. 4.4 Electrodes Position. Out of the 14 electrodes, the 8 electrodes highlighted in light grey are used in this study. Two circles highlighted in dark grey indicate reference electrodes which are located behind the ears.

4.2.4 Experimental Outline

The experiments are conducted based on the following protocols:

(1) Offline training session

(2) Selection of feature components and training of the classifier

(3) Online identification testing

During the offline training session, motor imagery (MI) cues, which indicate up or down motion, were displayed on the screen. The subjects imagine an object moving up or down according to the cues. After the offline training session, the recorded EEG data were analyzed in order to extract features that best describe each intention. Next, the classifier is trained based on the selected features. Lastly, online identification testing is conducted to evaluate the system performance.

4.3 Signal Processing

In this chapter, the proposed algorithm that is used to identify the user intent is described. According to the signal flow shown in Fig. 1, initially, the reordered EEG signals are transformed from time domain to frequency domain by performing Fast Fourier Transform (FFT) that uses a hamming window function. Next, the power spectrum densities are calculated from the FFT results. Feature vectors components that are used as the input signal of the classifier are selected from the power spectrum density. Finally, the classifier identifies the user intention and outputs the result. Here, a threshold value is established to define the identification signal. In this study, the artificial neural network is used as the classifier.

4.3.1 Preprocessing

The EEG data is stored as floating point values directly converted from the unsigned 14-bit analog-digital converter (ADC) output from the headset. This means that the (floating) DC level of the signal occurs at approximately 4200 μV where the negative voltages are transmitted as positive values less than the average level, and the positive voltages are transmitted as positive values greater than the average. Before performing FFT, it is necessary to apply some kind of DC offset removal. In this study, a 0.16 Hz first order high pass filter is applied to remove the background signal. The time taken for the DC offset to be fully removed is approximately 6 seconds. Therefore the first 10 seconds of the EEG data will be discarded during signal processing. Examples of EEG signal for up and down imagery (60 s - 70 s) task after high pass filter has been applied are respectively shown in Fig. 4.5 and Fig. 4.6.

As a preliminary stage of this study, no artifact removal algorithm has been implemented into the system. This is to minimize computation complexity as well as investigate how well the system could tolerate against artifacts such as head movements or eye blinks. During the experiments, very minor head movements were detected from the 2 axis gyroscope. Occasionally, eye blinks were also detected.

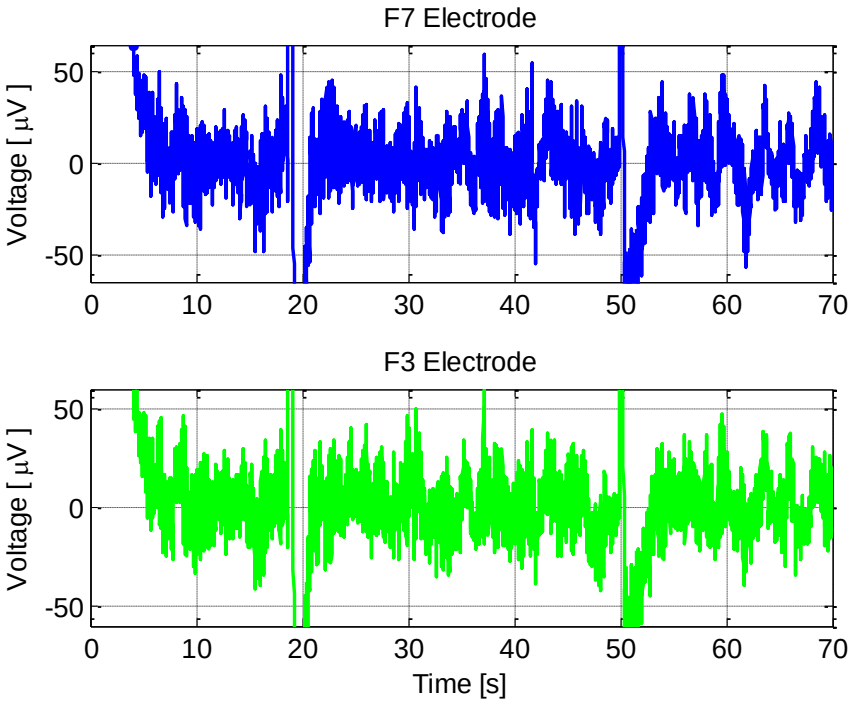

Fig. 4.5 Electroencephalograph signals during up imagery task at F7and F8 electrode. The experiment starts with a 60 seconds rest period followed by a 10 second imagery task.

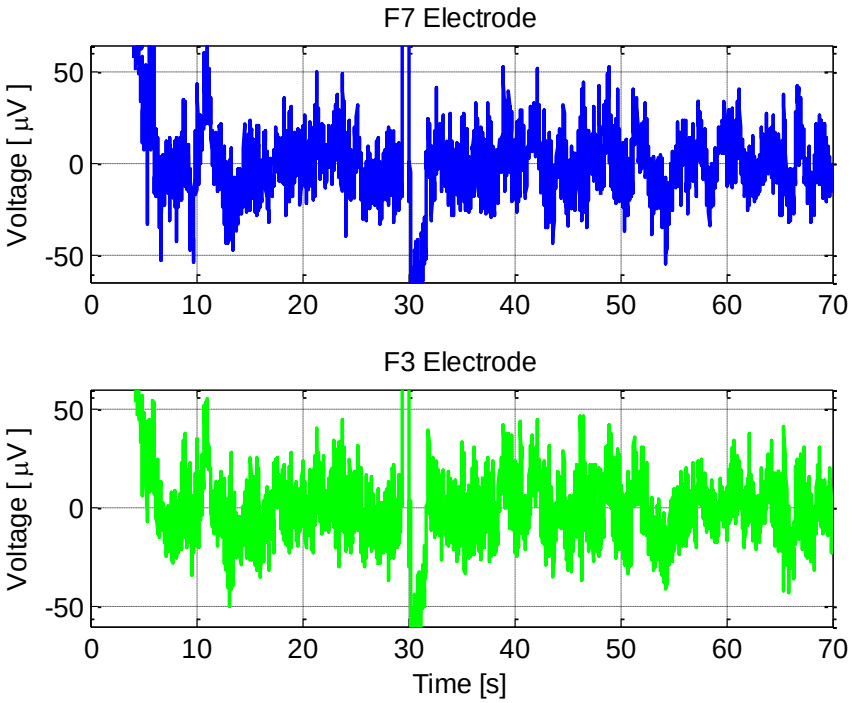

Fig. 4.6 Electroencephalograph signals during down imagery task at F7and F8 electrode. The experiment starts with a 60 seconds rest period followed by a 10 second MI task

4.3.2 Feature Extraction

After the DC offset has been removed by applying the high-pass filter, FFT is applied to the EEG signals. Then, the FFT results are used to calculate the power spectrum densities (PSD) which are used to generate the feature vector. The elements of the feature vector are made up of the spectral magnitude at 4 Hz, 10 Hz, 12 Hz, 20 Hz, 22 Hz, 24 Hz, 30 Hz and 44 Hz of each channel. Fig. 4.7 and Fig. 4.8 show an example of selected features for up and down motion and rest state at F7 electrodes and F3 electrodes respectively. These feature components are selected by looking at the spectral graph of the 8 electrodes and find the frequency where the PSD value of each intention differs from each other the most. The selected features are used to generate a 64 dimension (8 channel × 8 frequency components) feature vector. In generating the feature vector, power spectrum densities are estimated using a 64 sample hamming window with 25 % overlap transform processing and being averaged eight times. This method of using overlapping windowed FFT is known as the Welch's method. Lastly, the elements of the feature vector are normalized by the difference between the largest and smallest feature components. By this normalization, the elements of the feature vector are converted to the ratio of the spectral magnitude where the values are ranged from 0 to 1. This normalization scheme is formulated as

$$\tilde{x}_i(k) = \frac{x_i(k) - \min(x_i(k))}{\max(x_i(k)) - \min(x_i(k))} \tag{4.1}$$

where $x_i(k)$ is the i^{th} element at k^{th} sampling instance and $\tilde{x}_i(k)$ is the normalized magnitude. The normalized feature vector will be use as the input signal and to train the classifier.

Prior to conducting online identification sessions, $\min(x_i(k))$ and $\max(x_i(k))$ is calculated from feature vectors generated from EEG signals obtained during offline training sessions and relayed to the classifier as parameters.

It is important to normalize the elements of the feature vector first before feeding them into the classifier. This is because the criterion for identifying the user intent of the proposed method is based on the distributions of the input signals in the frequency domain, not based on the amplitude itself in time domain. In our previous study, offline identification tests were conducted with and without normalization of feature vectors. The results proved that normalizing the features yield much better results.

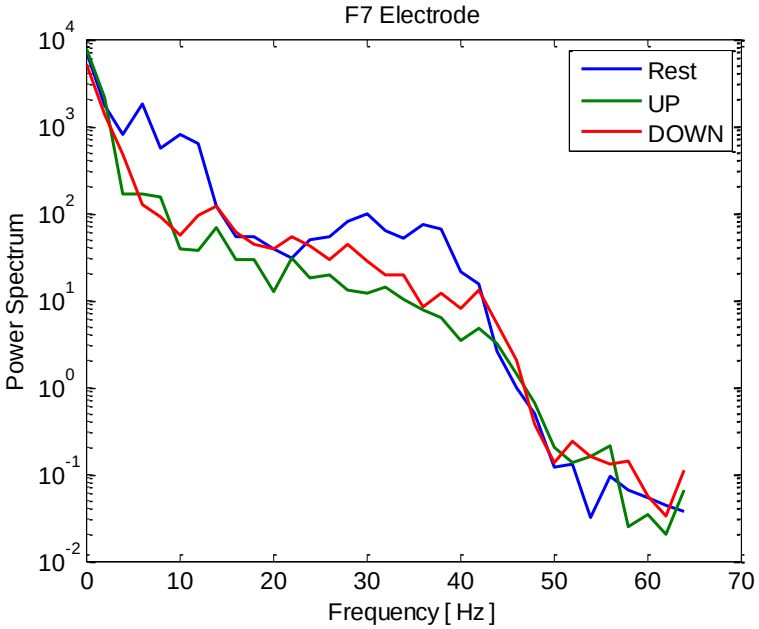

Fig. 4.7 Spectral power of F7 electrode shown as a function of frequency. In this figure, the spectral power for rest state and up imagery task is calculated by performing FFT on the EEG signals of Fig. 5 at 24 seconds and 67 seconds, respectively. Similary, spectral power for down imagery task is calculated by performing FFT on the EEG signals of Fig. 6 at 68 seconds

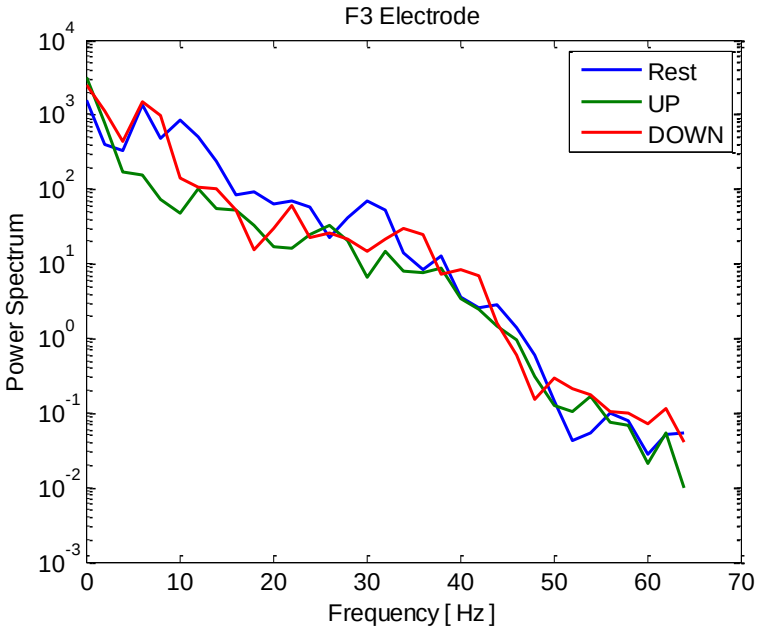

Fig. 4.8 Spectral power at F3 electrode shown as a function of frequency. In this figure, the spectral power for rest state and up imagery task is calculated by performing FFT on the EEG signals of Fig. 5 at 24 seconds and 67 seconds, respectively. Similary, spectral power for down imagery task is calculated by performing FFT on the EEG signals of Fig. 6 at 68 seconds

4.3.3 Classification of User Intentions Based on ANN Output

Several kinds of identification methods have been proposed for BMI systems. Many of those are based on linear models such as the auto aggressive (AR) models [108]-[112] or discriminant functions [8], [113]-[115]. However, it might be difficult to handle nonlinearities such as changes in subject's physiological states caused by perspiration, tiredness, emotions etc. To solve the problem, artificial neural networks (ANN), which acquire nonlinear mapping by machine learning have been put to use [116]. In this study, ANN is chosen as the classifier. In this section, the generation of neural network output signals needed in identifying the user intention is described. The output signals are generated by feeding 64 elements of the feature vector obtained from the recorded EEG signals to the ANN. Currently, many types of ANN have been suggested. In this study, a multilayered perceptron, which is a feed-forward ANN is chosen due to its implementation simplicity.

The multilayer perceptron is a multilayered ANN which consists of one or more hidden layers as shown in Fig. 4.9. This type of ANN is known as a supervised network because it requires a desired output (teaching signal) in order to learn. A set of learning data that consists of the feature vector and the corresponding teaching signals is used to have the perceptron acquire appropriate connection weights and threshold values of the middle layer and the output layer by machine learning. The multilayered perceptron and many other ANN learn by using an algorithm called backpropagation. With back propagation method, the input data (feature vector) is repeatedly presented to the ANN. With each presentation, the output of the ANN is compared to the desired output (teaching signal) and an error is computed. This error is then feedback (backpropagated) to the ANN and used to adjust weights so that the error decreases with each iteration and the ANN model gets closer and closer to producing the desired output [117]. The outline of learning procedures using the back propagation are as follows [118]:

(1) The i^{th} middle layer's output h_i is calculated using the feature vector, and the j^{th} output o_j is calculated using the middle layer's output h_i as follows:

$$h_i = \frac{1}{1+\exp(-uh_i)}$$
$$uh_i = \sum_{k=1}^{64} x_k wh_{ik} - vh_i \tag{4.2}$$

$$o_j = \frac{1}{1+\exp\left(-uo_j\right)}$$
$$uo_j = \sum_{i=1}^{6} h_i wo_{ji} - vo_j \tag{4.3}$$

where wh_{ik} is connection weight of the middle layer, vh_i is threshold of the middle layer, wo_{ik} is connection weight of the output layer, and vo_i is the threshold of the output layer.

(2) Connection weight wo_{ji} is updated by computing

$$wo_{ji} \leftarrow wo_{ji} + \alpha \times E_j \times o_j \times \left(1-o_j\right) \times h_i \tag{4.4}$$

$$E_j = o - o_j \tag{4.5}$$

where E_j is the output error of the output layer, and α is the learning constant.

(3) Then, generalized error Δ_i of the i^{th} neuron of middle layer is calculated by

$$\Delta_i \leftarrow h_i \times \left(1-h_i\right) \times wo_{ji} \times E_j \times o_j \times \left(1-o_j\right) \tag{4.6}$$

(4) Connection weight wh_{ik} of the i^{th} input of the k^{th} middle layer's neuron is updated by

$$wh_{ik} \leftarrow wh_{ik} + \alpha \times x_k \times \Delta_i \tag{4.7}$$

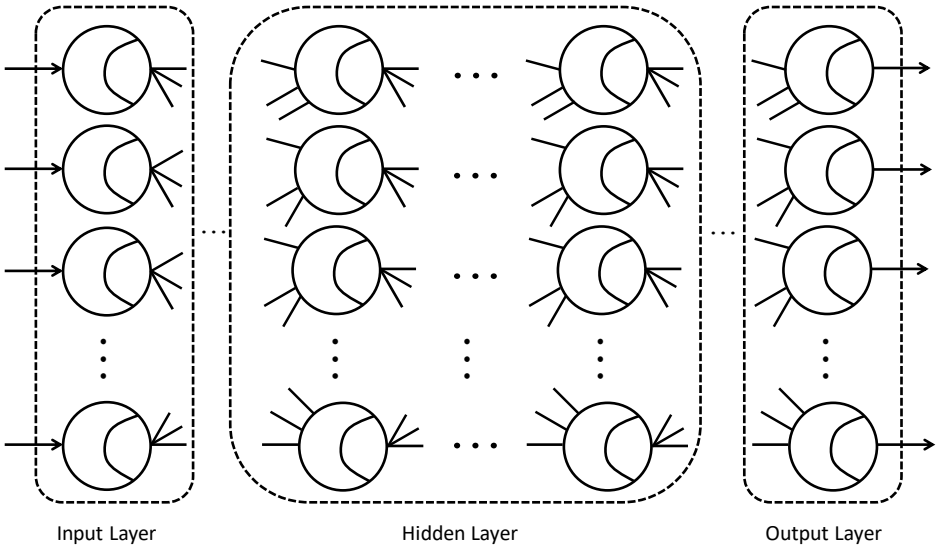

Fig. 4.9 Structure of a multilayered perceptron

Training of the ANN is performed using the above procedure while the thresholds values are also trained and updated in the same way. The training process is repeatedly conducted until the output error becomes less than 0.0001 or until the number of training iteration reaches 8000.

The identification of user intention is defined by the class with the highest ANN output. Thus the output can take one of the following states: *up*, *down*, *left*, *right* and *rest*. A threshold value of 0.5 is established to define the output. If the threshold value is not achieved by any of the classes, identification is labeled "*uncertain.*" An example showing how the identification signals are generated is shown in Fig. 4.10. Currently, the threshold value is fixed for all experiment sessions.

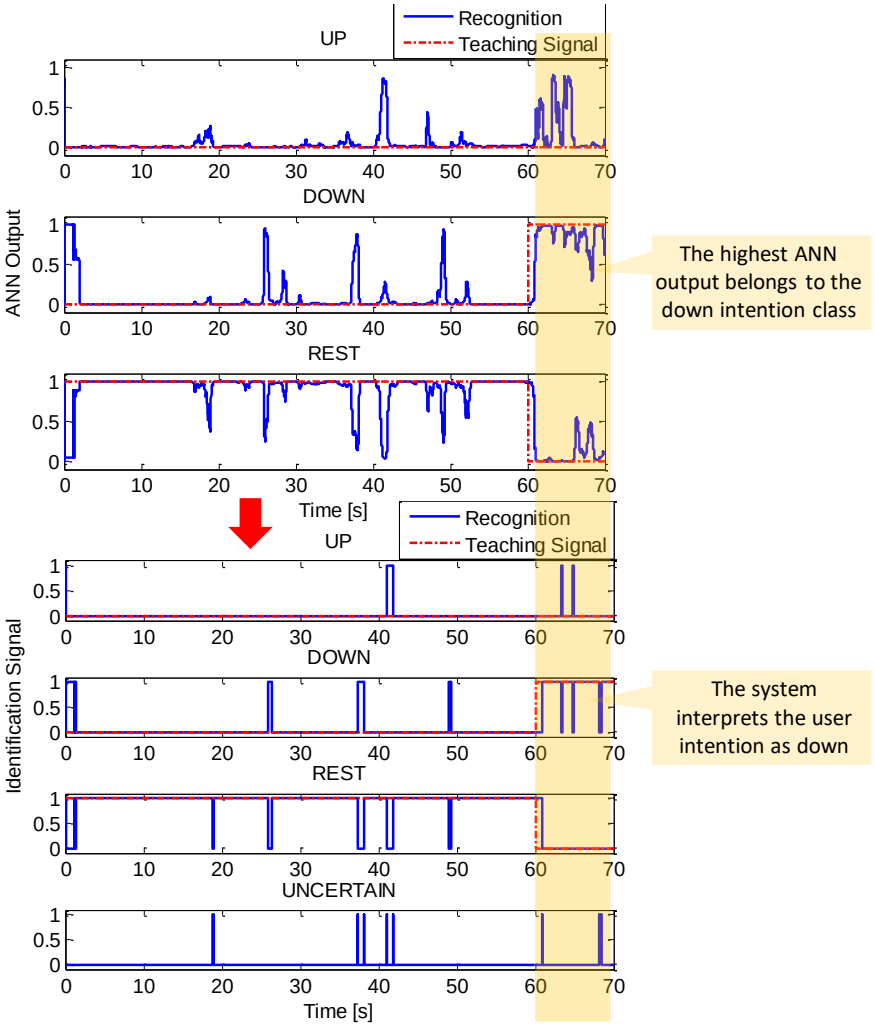

Fig. 4.10 An example of the generation of identification signals (classification of 3 mental states). The top three rows corressponds to the ANN output signal of up intention, down intention and rest state. The last four rows corresponds to the identification signal of up intention, down intention, rest state and uncertain state. At each sampling time, the ANN output signal can take one of the following states: up, down and rest. Similarly, the

identification signal can take one of the following states: up, down, rest and uncertain.

4.3.4 Definition of True Positive Rate and False Positive Rate

In this study, true positive rate (TPR) and false positive rate (FPR) are introduced to evaluate the system performance. Also, unlike other studies, each imagery tasks are evaluated separately in addition to evaluating the overall performance. Fig. 4.11 illustrates the definition of TPR and FPR. Let positive be defined as when the final classification signal is 1 and negative be defined as when the final classification signal is 0. By comparing the classification signal to the teaching signal TPR and FPR can be calculated by

$$TPR = \frac{TP}{TP + FN} \tag{4.8}$$

$$FPR = \frac{FP}{TN + FP} \tag{4.9}$$

where true positive (TP), false positive (FP), true negative (TN) and false negative (FN) are defined as follows:

- True positive is defined as the total number of samples where the classification signal says an event has occurred (ANN output value is 1) and that this statement is true (teaching signal value is 1).
- False positive is defined as the total number of samples where the classification signal says an event has occurred (ANN output value is 1) and that this statement is not true (teaching signal value is 0).
- True negative is defined as the total number of sample where the classification signal says there is no event (ANN output value is 0) and that this statement is true (teaching signal value is 0).
- True negative is defined as the total number of sample where the classification signal says there is no event (ANN output value is 0) and that this statement is not true (teaching signal value is 1).

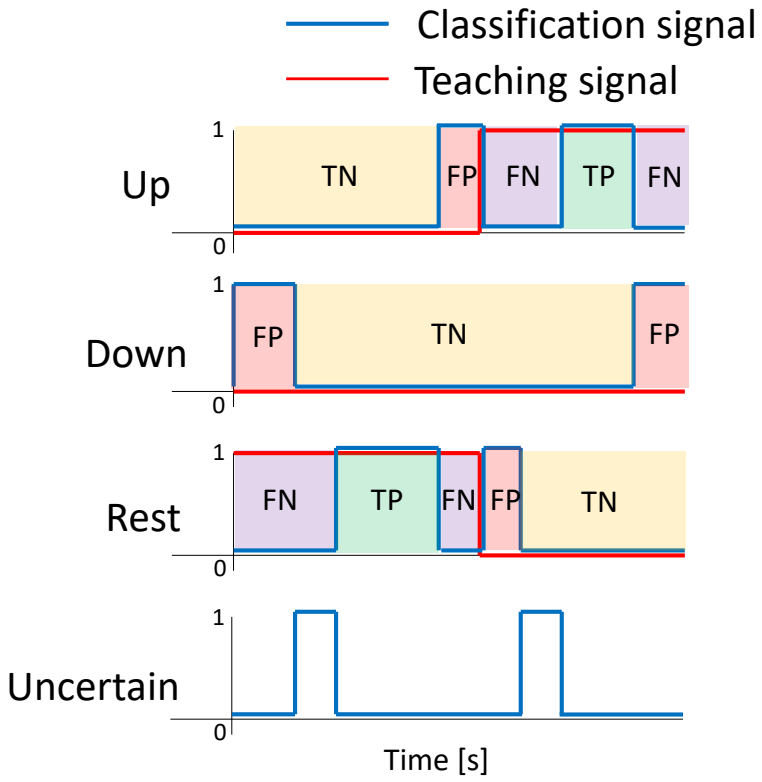

Fig. 4.11 Classification signal during up imagery task trial. From the top, classification signal of up intention, down intention, rest state and uncertain state. At each sampling time, the classification signal can take one of the following states: up, down, rest and uncertain.

4.4 Experiment

Two experiments have been conducted in order to evaluate the proposed BMI system performance. The first experiment is conducted to identify 3 mental states which are up and down intentions as well as rest state. The second experiment, aims to identify 5 mental states. In this chapter, the correct and incorrect identification rates of each experiment are evaluated and discussed.

4.4.1 Subjects

The experiments were carried out with 3 able-bodied male subjects (referred to as subject A, subject B and subject C) aged from 21 to 24 years old. Subject A took part in our previous BMI study where he performed several mental tasks trials and therefore have little experience with BMI. On the other hand, subject B and subject C have never participated in any BMI experiment before and therefore possess no prior experience with BMI at all. The entire protocol and aims of the study were fully explained to them before the experiment, and all participants signed the written informed consent. All of the experiments are conducted under the approval of Tokyo Denki University Human

Bioethics Committee（東京電機大学ヒト生命倫理委員会）.

As a measure to control and reduce any factors that might affect the subject's physiological state as much as possible, all subjects were asked to get enough sleep the day before the experiment. They are also instructed to take their meals 3 hours before the experiment begins. This is to prevent sleepiness during the experiment so that the subjects can fully concentrate on the mental tasks. It should be noted that not every subject participated in all of the three experiments.

4.4.2 Identification of 3 Mental States (Up Intention, Down Intention and Rest State)

4.4.2.1 Experimental Conditions

This experiment is conducted to evaluate the system identification performance of 3 mental states which are up and down intentions as well as rest state. All three subjects participated in this experiment. In this experiment, subject A chose to imagine pushing up the black circle presented in the visual cues with the palm of his right hand for the up intention. As for the down intention, subject A chose to imagine pushing the black circle downwards with both hands. On the other hand, subject B and subject C both chose to imagine the black circle sliding upwards for up imagery task while imagining pushing the black circle downwards with both hands for down imagery task.

As mentioned in section 4.2.4, the experiments in this study are divided into two parts both conducted on the same day. The first part is intended for determining the necessary parameters of ANN. In this part, the experiments are conducted based on the procedures described in section 4.2.2. The subject is asked to perform a total of 10 sessions (5 sessions for up intentions and 5 sessions for down intentions) of mental task. From this data, 20 sets of feature vectors (5 sets each for up and down intentions and 10 sets for rest state) are generated. All of these feature vectors are used to train the ANN. Here, the number of training sessions (epochs) are determined based on the consideration that short training time is preferable for BMI system to be easy-of-use. However, too little training sessions may result in poor identification accuracy. As a first step, the number of training session is set so that the training time required is under 15 minutes. Since each session takes about 1.5 minutes, hence the total number of training session is set to 10.

The second part of the experiment consists of online identification sessions. A total of 20 sessions (10 sessions for up intentions and 10 sessions for down intentions) is performed. Correct and incorrect identification rate is calculated from these data. Two experiments, with each one

consisting of 20 sessions are conducted over two days for each subject.

As mentioned in section 4.3.3, the identification output signals are generated by ANN. For this experiment, an ANN with 64 neurons in the input layers, 6 neurons in the middle layers and 3 neurons in the output layers are used. The learning constant in equation (4.4) and (4.7) is set to be 1.1.

The number of neurons hidden layer is determined from the results of previous offline identification experiments. In that experiment, subject A performed a total of 20 sessions (10 sessions for up intentions and 10 sessions for down intentions) of mental tasks. The experiment were carried out according to the same procedures describe in section 4.2.2. From this data, 20 sets of feature vectors (5 sets each for up and down intentions and 10 sets for rest state) were generated. Out of the 20 sets, 10 sets (5 sets each up and down intentions and 10 sets for rest state) were selected to train the ANN and the remaining 10 sets were fed into the ANN for identification. Here, the number of neurons in the hidden layer was initially set to 2. After identification of 10 sets was over, the number of neurons in the hidden layer was increased by 1. Then, the training and identification process were repeated by using the same training and identification data sets as the previous cycle. In each cycle, correct identification rates were evaluated. The above steps were repeated until identification rates declined for 3 consecutive cycles. Lastly, the identification rates were compared and the cycle with the highest identification rate was selected, which is in this case, the cycle in which the number of neurons in the hidden layer is set to 6. As a preliminary stage, in order to investigate the extent of the performance of ANN with a fix network arrangement, the number of neurons in the hidden layer is fixed in all experiment sessions for all 3 subjects. A systematic approach to optimize the number of neurons in the hidden layer is scheduled for future work.

4.4.2.2 Results

Mean and standard deviation of true positive and false positive rates of three mental states calculated from 20 trials are listed respectively in Table 4.1 and Table 4.2. The mean overall TPR is calculated by taking the average of the TPR of the three mental states from 20 trials. The mean overall FPR is calculated in the same way. Similarly, standard deviation of the overall TPR are calculated by computing the standard deviation of TPR of the three mental states from 20 trials. Standard deviation of the overall FPR is calculated in the same way.

The experimental results show that subject B performed the best in obtaining the highest overall TPR and the lowest overall FPR. On the other hand, subject C performed worst among the

three subjects in obtaining the lowest overall TPR and the highest overall FPR. According to Table 4.1, subject B were able to achieve an overall TPR of 67% on the first day despite being a first-time user and had little training time. Furthermore, all three subjects performed better on the second day. The TPR of each mental task were also better on the second day with the exception of down mental task for subject B and C. Also, the overall TPR improved and the overall FPR lowered (Table 4.2) for all subjects. One reason for this improvement is that the subjects became accustom to the task and the way to modulate their brain waves. This suggests that training of each individual can potentially improve the performance. At the end of the second day, the performances of subject A, subject B, subject C are 60 %, 67 %, 42%, respectively.

Also, according to Table 4.1, subject B performed better on the down imagery task than that of the up imagery task. Whereas, subject A performed better on the up imagery task than that of the down imagery task. This suggests that a certain individual may perform well on a certain imagery task but not on the others depending on his/her aptitude. This also suggests that the selection of mental tasks that are easy for the user to execute are extremely important in order to achieve high accuracy.

As shown in Table 4.2, the FPR of rest state for all subject is relatively high compared to the FPR of up or down intentions. This may be due to the fact that during the imagery tasks (duration of 10 seconds), each subject was unable to sustain the imagery intention for long periods of time and for most of the time, he remained in a relaxed state. For example, on day 2, the FPR of rest state for subject B is 22%. Furthermore, from Table 4.1, the TPR rates of up and down intention are 43% and 54%, respectively. Therefore, in this case, subject B could focus and sustain his mental tasks for only about 5 seconds on average. Generally, sustaining the imagery intention for 10 seconds is a difficult task because it requires a lot of continuous concentration as well as a stable physiological condition. The same is true for rest state. Keeping a relaxed state of mind for 50 seconds while not being engaged in any task proved to be uneasy especially for subject C. From the above results, it is clear that the physical and mental conditions of the subject greatly influence the performance of the BMI system.

Although the overall accuracy presented in this work may sound slightly lower than those in some other studies, the difficulty of each tasks are in fact much higher than other studies. More specifically, the duration of mental tasks in other studies are usually around 3-5 seconds [119] whereas the tasks are twice longer (10 seconds) in this study. In addition, the rest period is considered to be especially long. Therefore, to obtain higher accuracy, the subjects will have to sustain their mental task for longer periods of time for which it is difficult to achieve. So, by

considering these facts, all the three subjects have performed well.

Based on the above results, the proposed BMI system has basically worked well. Also, one subjects was able to achieve an overall TPR of 67% with 10 sessions (15 minutes) of training. The extension to this study would be to improve the basic performance by improving the feature selection algorithm and tuning the ANN parameters. It would also be interesting to investigate on how the number of training datasets affect the classification accuracy in order to determine the optimal number of training datasets.

Table 4.1 True Positive Rates of Three Subjects (Classification Threshold Value is 0.5)

Intention	**Classification Results (Mean ± Standard Deviation) [%]**					
	Subject A		**Subject B**		**Subject C**	
	Day 1	**Day 2**	**Day1**	**Day2**	**Day 1**	**Day 2**
Up	35.11 ± 11.75	61.00 ± 15.13	34.00 ± 10.64	43.48 ± 12.73	15.16 ± 11.87	39.24 ± 13.51
Down	15.81 ± 6.44	35.19 ± 3.98	80.78 ± 14.10	54.24 ± 16.45	74.91 ± 10.54	39.59 ± 12.02
Rest	42.00 ± 13.22	72.37 ± 11.43	62.40 ± 9.06	85.70 ± 8.03	37.82 ± 10.69	45.48 ± 15.49
Overall	**33.73 ± 15.54**	**60.23 ± 18.87**	**59.89 ± 19.98**	**67.28 ± 22.23**	**41.43 ± 24.18**	**42.45 ± 14.20**

Table 4.2 False Positive Rates of Three Subjects (Classification Threshold Value is 0.5)

Intention	**Classification Results (Mean ± Standard Deviation) [%]**					
	Subject A		**Subject B**		**Subject C**	
	Day 1	**Day 2**	**Day1**	**Day2**	**Day 1**	**Day 2**
Up	30.93 ± 15.82	15.32 ± 12.42	17.79 ± 7.35	9.26 ± 4.95	7.60 ± 5.01	25.99 ± 9.28
Down	15.30 ± 6.76	8.62 ± 5.07	14.79 ± 7.78	1.06 ± 1.07	45.82 ± 14.03	18.78 ± 12.82
Rest	30.66 ± 21.34	19.65 ± 10.79	14.11 ± 7.31	22.75 ± 19.27	12.88 ± 11.21	20.97 ± 15.09
Overall	**25.63 ± 16.98**	**14.53 ± 10.64**	**15.56 ± 7.40**	**11.02 ± 14.46**	**22.10 ± 20.07**	**21.92 ± 12.78**

4.4.3 Identification of 5 Mental States

4.4.3.1 Experimental Conditions

This experiment is conducted to evaluate the system identification performance of 5 mental states which are up, down, left and right intentions as well as rest state. Two subjects (subject B and subject C) participated in this experiment. In this experiment, subject B and subject C chose to imagine pushing up the black circle presented in the visual cues with the palm of his right hand for the up intention. As for the down intention, both subjects chose to imagine pushing the black circle downwards with both hands. For left intention, subject B and subject C both chose to imagine sliding the black circle towards the left side with their left hand. Lastly, for right intention, both subjects chose to imagine moving the black circle toward the right side in a spiral motion with their right hand.

The experiments are conducted using the same procedure as the previous experiments (section 4.4.2). During the offline training sessions, the subject is asked to perform a total of 20 sessions (5 sessions for each intention) of mental task. From this data, 40 sets of feature vectors (5 sets for each intention and 20 sets for rest state) are generated. All of these feature vectors are used to train the ANN. For the online identification sessions, the subject is asked to perform a total of 20 sessions (5 sessions for each intention). Correct and incorrect identification rate is calculated from these data. It should be noted that the number of experiment sessions for each intention is reduced to 5 instead of 10. The reason is that too many experiment sessions will lengthen the experiment duration in which user could become too tired. This could greatly affect and lower the system performance.

In this experiment, an ANN with 64 neurons in the input layers, 6 neurons in the middle layers and 5 neurons in the output layers are used. The learning constant in equation (4.4) and (4.7) is set to be 1.1.

4.4.3.2 Results

Mean and standard deviation of correct identification rates for the 20 sessions are listed in Table 4.3. Also, mean and standard deviation of incorrect identification rates are listed in Table 4.4. According to Table 4.3, the overall performance of both subjects is below 50 %. Also, the correct identification rate of each individual intention is also low. Furthermore, according to Table 4.4, both subject obtained a very high overall incorrect identification rate. These results show that the proposed BMI system failed to classify 5 mental states. One reason for this failure may be that the feature extraction algorithm could not find distinct features for all 5 mental states. More work need to be done in implementing a more advanced algorithm. Another reason may be due to the experience of the user. Since this is the first time that both subjects tried to execute 4 different imagery tasks, the subjects are still inexperience in modulating their brain waves. As a result, they failed to create 5 distinct brain wave patterns which made the classifier unable to correctly identify the intentions. Hence, training the user to modulate their brain waves is also an important part in raising the system performance. Currently, it is not clear which reason leads to this failure. The future work would be to investigate and make clear the reason as well as propose a suitable countermeasure.

Table 4.3 Correct Identification Rates of Five Mental States

Intention	**Identification Results (Mean ± Standard Deviation) [%]**	
	Subject B	**Subject C**
Up	2.20 ± 4.03	15.84 ± 9.26
Down	0.0 ± 0.0	47.81 ± 25.84
Left	18.05± 8.67	17.25 ± 13.32
Right	16.02 ± 14.78	26.20 ± 9.67
Rest	55.72 ± 22.77	12.67 ± 16.75
Overall	**47.94 ± 18.45**	**15.02 ± 14.65**

Table 4.4 Incorrect Identification Rates of Five Mental States

Intention	**Identification Results (Mean ± Standard Deviation) [%]**	
	Subject B	**Subject C**
Up	3.25 ± 5.45	8.65 ± 3.06
Down	2.51 ± 3.07	38.78 ± 15.78
Left	21.96 ± 6.74	5.75 ± 3.78
Right	16.65 ± 22.17	25.89 ± 7.17
Rest	16.06 ± 12.10	4.89 ± 8.14
Overall	**45.20 ± 20.57**	**76.59 ± 18.03**

4.5 Offline Analysis

Offline analysis is conducted using the same EEG data recorded from experiments in section 4.2 to investigate the influence of the classification threshold value, the use of multiple ANN for classification, and the influence hamming window size.

4.5.1 Influence of the Classification Threshold Value

In order to investigate how different threshold affect the system performance, first, the threshold value was altered from 0.0 to 1.0 as shown in Table 4.5. Next, the same EEG data recorded during online classification sessions on the second day were fed into the BMI system to be classified. Here, the set of ANN parameters are exactly the same as the one used in experiment. Mean overall TPR and FPR are calculated based on the results. In addition, the receiver operating characteristic (ROC) curve is plotted based on the results of Table 4.5. Table 4.5 shows the TPR and FPR of each threshold value. Fig. 4.12 shows the ROC curve of 3 subjects.

Table 4.5 shows that the lower the threshold value is, the higher the TPR and FPR becomes. On the contrary, when higher threshold value is set, the TPR decreases, but in return, the FPR improves. The above results show that there is a tradeoff relationship between TPR and FPR and that high threshold value is the key to reduce FPR. So, depending on the target application a different threshold value might be preferable over the others. For example, if the application is the type where high FPR would pose a serious problem such as controlling a wheelchair, then using a high threshold value could help reduce the FPR.

Furthermore, by looking at Fig. 4.12, the ROC curve of subject B is the furthest away (towards the upper left corner) from the black straight line. This means that subject B performed best amongst the 3 subjects. On the other hand, subject C has the worst performance. In addition, a relatively large improvement in FPR can be seen in all three subject when the classification threshold value is set 0.8. However, on the contrary, TPR declines significantly.

Table 4.5 True Positive Rates and False Positive Rates of Each Classification Threshold Value

Threshold Value	Classification Results [%]					
	Subject A		Subject B		Subject C	
	TPR	FPR	TPR	FPR	TPR	FPR
0.0	64.07	16.68	72.43	13.56	47.13	25.42
0.2	64.04	16.82	72.20	13.37	47.10	25.40
0.4	62.24	15.65	69.44	11.95	44.75	23.56
0.5	60.23	14.53	67.28	11.02	42.45	21.92
0.6	57.36	13.19	65.00	9.85	39.76	19.94
0.8	47.54	9.50	57.87	7.49	31.90	14.94
1.0	0.0	0.0	0.0	0.0	0.0	0.0

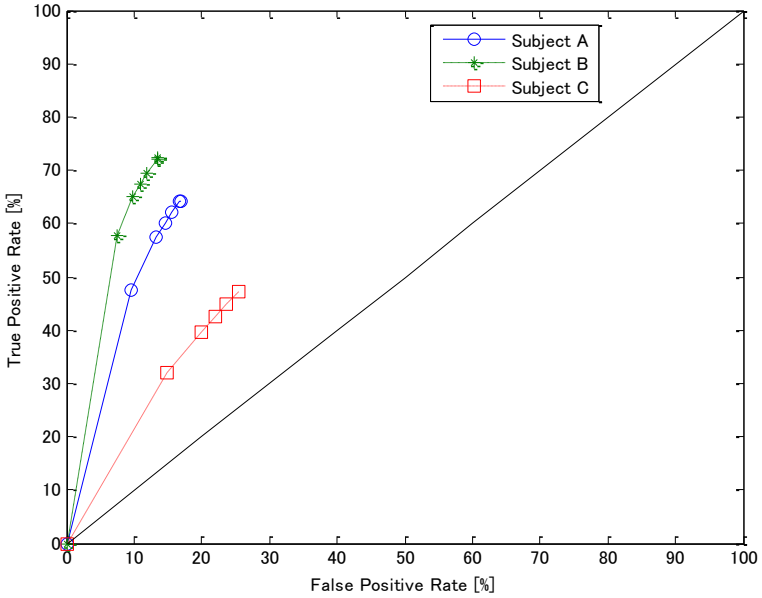

Fig. 4.12 ROC curve of 3 subjects. The further away (towards the upper left corner) the curve is from the black straight line, the better the peformance. Subject B performed best among the 3 subjects while subject C performed worst.

4.5.2 Multiple ANN Classification Scheme

Most researches on classification problems involving ANN classifiers are often focused on the design of efficient learning algorithms to train a single ANN to solve a specific problem. However, in multiclass classification problems, the accuracy of the classifier tends to degrade as the number of classes involved in the classification task increases. According to the report of some studies, the use of multiple ANN may help increase the classification accuracy [120]-[122]. In order to test the validity of this idea, the use of two and three ANNs to classify three mental states are explored. In each classification scheme, ANN are structured as shown in Fig. 4.13.

In the two ANN classification scheme, the first ANN is use to classify whether the intent belongs to the mental task category or the rest state category. If the output is labeled “rest”, then the final result will be classified as rest. On the other hand, if the output is labeled “task”, then the second ANN will determine whether the intention belongs to up category or the down category. As with the single ANN classification scheme, a classification threshold value of 0.5 is adopted in both ANNs to define the final classification output. If the threshold value is not achieved by any of the categories, classification will be labeled as “uncertain.”

Similarly, in the three ANN classification scheme, each ANN is used to perform binary classification. The first ANN is used to classify between up or down intentions. The second one is used to classify between down intention and rest state. The last ANN is used to classify between up intention and rest state. Hence, each class has two ANNs that is responsible for determining the final classification output. In this scheme, the final classification output is defined by the class with classification label from two ANNs. For example, in order for the final output to be labeled “rest”, the classification output of two ANNs associating must all belong to the rest class. If none of the three class is able to obtains two classification labels, then the final output will be labeled as uncertain. Again, a threshold value of 0.5 is adopted in all of the ANN.

To evaluate the effectiveness of this method, the same EEG data recorded on the second day were fed into the BMI system to be classified. Here, all the ANNs in both classification scheme consist of 64 neurons in the input layer, 6 neurons in the middle layer and 2 neurons in the output layers. The learning constant for both ANN are 1.1. The ANNs are trained using the training data set recorded on the second day.

Mean and standard deviation of true positive and false positive rate for the 20 sessions are listed respectively in Table 4.6 and Table 4.7. In contrast to the findings of other studies, the results

show that using multiple ANN to classify three mental state do not improve the accuracy. As shown in Table 4.6, the accuracy of subject A declined significantly in both classification schemes; the true positive rate lowered and false positive rate increased. For subject B and C, the accuracy appears to decline slightly. This result suggests that in contrast with the results from studies mentioned above, using multiple ANN do not improve the classification accuracy.

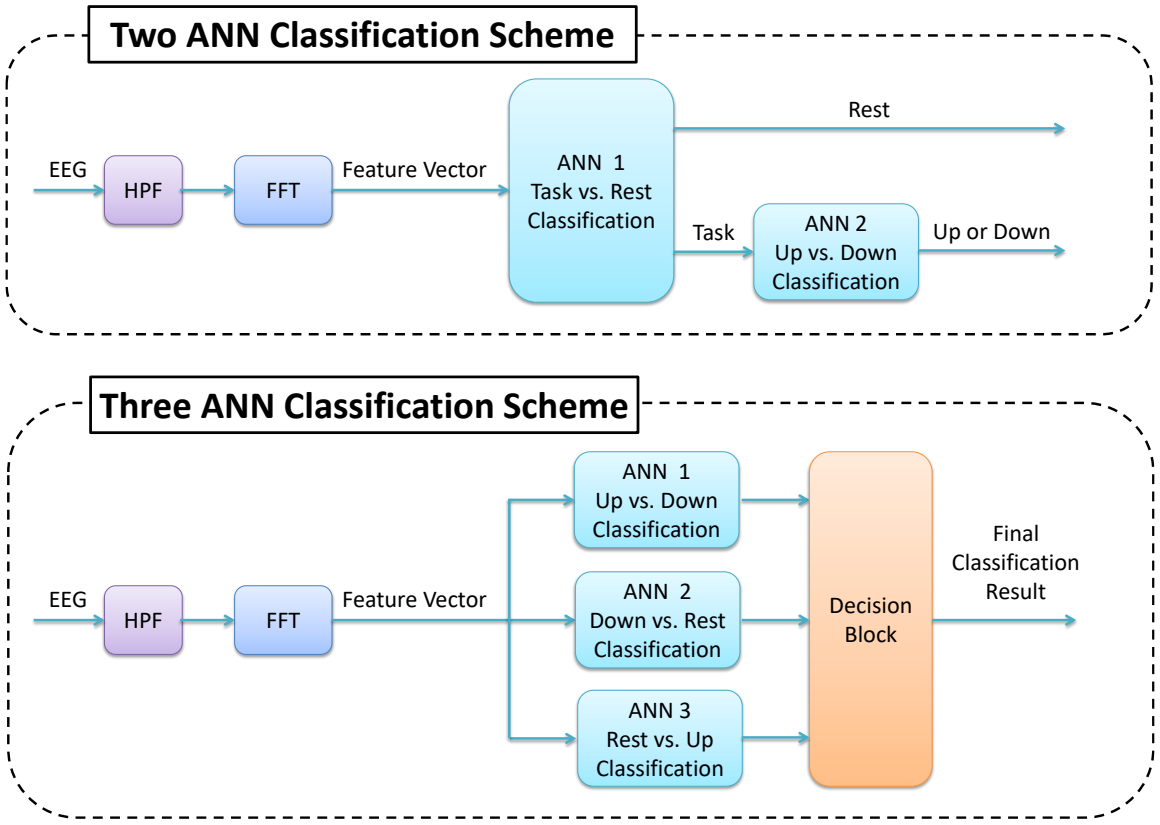

Fig. 4.13 Classification scheme using multiple artificial neural networks.

Table 4.6 True Positive Rates of Each Classification Scheme (Single ANN and Two ANN)

Intention	Classification Results (Mean) [%]								
	Subject A			Subject B			Subject C		
	Single ANN	Two ANNs	Three ANNs	Single ANN	Two ANNs	Three ANNs	Single ANN	Two ANNs	Three ANNs
Up	61.00	61.38	48.73	43.48	33.45	34.37	39.24	56.50	79.52
Down	35.19	48.69	58.02	54.24	45.82	51.79	39.59	29.35	19.04
Rest	72.37	18.59	29.99	85.70	91.44	90.94	45.48	47.44	43.90
Overall	**60.23**	**36.81**	**41.68**	**67.28**	**65.54**	**67.01**	**43.45**	**45.19**	**46.59**

Table 4.7 False Positive Rates of Each Classification Scheme (Single ANN and Two ANN)

Intention	Classification Results (Mean) [%]								
	Subject A			Subject B			Subject C		
	Single ANN	Two ANNs	Three ANNs	Single ANN	Two ANNs	Three ANNs	Single ANN	Two ANNs	Three ANNs
Up	15.32	34.16	22.51	9.26	8.59	7.79	25.99	38.89	46.27
Down	8.62	46.33	35.42	1.06	3.85	2.19	18.78	15.83	7.06
Rest	19.65	5.28	7.71	22.75	30.99	36.00	20.97	21.14	24.24
Overall	**14.53**	**28.59**	**21.88**	**11.02**	**14.48**	**15.33**	**21.92**	**25.12**	**25.86**

4.5.3 Influence of Hamming Window Size

In this section, the size of hamming window used when performing FFT are altered in order to investigate how it affects the system performance. The same EEG data recorded on the second day of subject B is use in this analysis. The overlap percentage of 25% is fixed for all window size. In addition, the same frequency components are selected to construct the feature vector for all window size. Mean and standard deviation of true positive and false positive rate for each window size are listed respectively in Table 4.8. In this study, window size smaller than 64 samples are omitted because the classification fails or the accuracy are too low (less than 20%). Also, window size larger than 256 samples (2 seconds) are omitted either because the classification fails (the accuracy is too low) or because the time taken to gather enough data sample for FFT processing is too long and therefore rendering the system unable to control the devices in real time.

As shown in Table 4.8, the overall accuracy improves slightly as well as the overall FPR when the window size is set to 128 sample. However in general, no significant change in accuracy between these three windows size. Thus, considering real time control properties, a window size of 64 sample is most suitable.

Table 4.8 True Positive and False Positive Rates of Each Window Size (Subject B Only)

Intention	Classification Results (Mean ± Standard Deviation) [%]					
	64 sample window (default)		128 sample window (default)		256 sample window (default)	
	TPR	FPR	TPR	FPR	TPR	FPR
Up	43.48 ± 12.73	9.26 ± 4.95	61.88 ± 26.86	15.47 ± 8.29	54.21 ± 32.30	9.99 ± 7.20
Down	54.24 ± 16.45	1.06 ± 1.07	45.02 ± 22.59	0.24 ± 0.67	35.97 ± 24.27	0.22 ± 0.71
Rest	85.70 ± 8.03	22.75 ± 19.27	82.57 ± 11.27	15.82 ± 14.77	88.47 ± 8.52	25.36 ± 19.06
Overall	**67.28 ± 22.23**	**11.02 ± 14.46**	**68.01 ± 24.50**	**10.51 ± 12.09**	**66.78 ± 30.61**	**11.86 ± 15.58**

4.6 Conclusion

This chapter presents a signal processing technique using spectral analysis and artificial neural network for a low-cost BMI system. As a preliminary study, experiments have been conducted to classify up and down intentions as well as rest state. Experimental results have shown that the proposed BMI system has basically worked well. The system is able to achieve an overall true positive rate of up to 67 % with 5 trials (15 minutes) of training by a novice user. Furthermore, offline analysis is carried out using the same EEG data recorded from the previous experiments. Analysis results show that by setting the classification threshold value higher, the erroneous classification can be reduced. Another finding shows that in contrast with the study results reported by other research groups, the use of multiple ANNs to classify three mental states do not improve the accuracy. Lastly, the optimal hamming window size is 64 samples for achieving real-time control.

5 Development of Electromyogram-based Brain Machine Interface for Multi-Degree Myoelectric Prosthetic Hand Control

Abstract: Myoelectric prosthetic hand is a powerful tool developed to help people with upper limb loss restore the functions of a biological hand. Recognizing multiple hand motions from only few electromyography (EMG) sensors is one of the requirements for the development of prosthetic hands with high level of usability. This task is highly challenging because both classification rate and misclassification rate worsen with additional hand motions. This chapter presents a signal processing technique that uses spectral features and artificial neural network to classify 17 voluntary movements from EMG signals. The main highlight will be on the use of a small set of low-cost EMG sensor for classification of a reasonably large number of hand movements. The aim of this work is to extend the capabilities to recognize and produce multiple movements beyond what is currently feasible. This work will also show and discuss about how tailoring the number of hand motions for a specific task can help develop a more reliable prosthetic hand system. Online classification experiments have been conducted on seven male and five female participants to evaluate the validity of the proposed method. The proposed algorithm achieves an overall correct classification rate of up to 83%; thus, demonstrating the potential to classify 17 movements from 6 EMG sensors. Furthermore; classifying 9 motions using this method could achieve an accuracy of up to 92%. These results show that if the prosthetic hand is intended for a specific task; limiting the number of motions can significantly increase the performance and usability.

5.1 Introduction

The hand is one of the most important parts of the human body. It is responsible for almost all of the intellectual activities of our daily living [123] The dexterity of the hand not only enables us to perform delicate tasks but to also regard that object as a part of our body and manipulate it to execute new tasks that are not possible with the hand alone. Also, the fingertip is equipped with fine sensors that allow the sensing of pressure, temperature, pain etc. For these reasons, amputation of the hand generates both psychological trauma and functional impairment because the person becomes unable to perform most daily tasks and baffled by the change in their appearance [124]. According to the 2006 survey on persons with physical disability conducted by the ministry of health, labour and welfare of Japan, there are approximately 80 thousand upper limb amputees in Japan [125]. Prosthetic arm/hand were developed to help these people by restoring as much as possible the functions of a biological hand and natural appearance. Myoelectric prosthetic hand/arm is a type of externally powered prostheses that is controlled by electrical signals generated during voluntary muscle contraction. The measuring of muscle activity via electric potential is referred to as electromyography (EMG). Since EMG signals can be recorded by placing surface electrodes on top of the skin, it is possible to use this electrical potential to provide a signal for control of prosthetic limbs that is relatively intuitive and non-invasive.

Over the past decades, extensive research on myoelectric prosthetic hand/arm have been conducted by many research groups across the globe, improving the overall functionality and reliability of myoelectric hands rapidly each year. However, despite these technological advances, the capability to recognize and produce extensive movements of many existing myoelectric hands is still primitive. The limited capability to execute many movements or to provide the user with the control of multiple degrees of freedom (DOF) consequently limits the number of task the user can perform, and is one of the cause that leads to rejection or abandonment of a prosthesis [126], [127]. Recently, due to huge progress in the mechanical development of prosthetic hands, several complex, articulated (multi degree of freedom) myoelectric hands have become available on the market. The Bebionic hand [128] and the iLimb hand [129] are examples of articulated prosthetic hands. Other multi-DOF prosthetic hands like the Vanderbilt hand [130], the UNB hand [131], the Yale hand [132], Smart hand [133], the DLR/HIT hand [134], the Keio hand [135], and the 6 DOF hand [136] are also being developed as research devices.

With the emerging of complex multi-DOF prosthetic hands, development of a control system that can distinguish and produce large number of movements are needed to allow the execution of more complex daily tasks. This study presents a signal processing technique to classify

17 forearm motions (with a rest state included) using 6 EMG sensors. The aim is to explore and determine the extent of hand movement recognition capabilities for myoelectric prosthetic hands with the currently available hardware. The novelty of this work is providing the basic methodology to classify not only wrist movements (grasping, opening, flexing, etc.) but also individual flexion and extension control of the five fingers. It will extend the capabilities of recognizing multiple motions beyond what is currently feasible (3-10 motions) [137]-[141]. The experiments will be conducted on fully-limbed participants as we believe that this defines the upper bound. Furthermore, this work will also show and discuss about how tailoring the number of hand motions for a specific task can help increase the performance and usability of the prosthetic hand system.

This chapter is organized as follows. Section 5.2 gives a literature review of EMG based pattern recognition and highlights the features of this study. Section 5.3 describes the system architecture and the procedures needed to acquire EMG signals. Details on the necessary preprocessing steps are also given in this section. Section 5.4 explains in detail, the feature extraction method using spectral analysis and classification algorithm using artificial neural network. Section 5.5 gives an evaluation of the proposed algorithm. The classification accuracy of the proposed system will be given and discussed. Section 5.6 concludes this study.

5.2 Related Works

To myo-electrically control a dexterous hand it is necessary to map EMG signals (corresponding to different muscle contractions) to the different existing degree of freedom using pattern recognition based algorithms. To this aim, researchers have been working on various aspects of EMG classification techniques such as electrode placement, selection of suitable feature extraction techniques, and selection of suitable classification algorithms to improve the classification accuracy and increase the number of controllable functions (motions).

Electromyography are usually performed by placing several electrodes on the skin. Over the past decades, different electrode placement strategies have been investigated. Some researches study the use of multichannel electrode arrays [142] or high-density EMG (large number of electrodes) strategy [143], [144], while others explore the precise anatomical positioning approach [140], [145].

In the pattern recognition based control approach, feature extraction and classification are the two important steps in achieving higher classification performance. The feature extraction process involves the transforming of raw EMG signals into feature vector that are assigned to represent different motions. Several features extraction methods have been suggested and these

features can be sorted into time domain features [139], frequency domain features [140], and time-frequency domain features [146]. Time domain features are generally evaluated based on signal amplitude that varies with time. On the other hand, frequency domain features contain the power spectrum density of the signals and are computed by parametric methods or a periodogram. Time-frequency domain features contains the combination of temporal and frequency information. These features can characterize varying frequency information at different time locations, providing plentiful non-stationary information of the EMG signals. A list of specific features in each category can be found in [84]. Classification of arm/hand motions based on the extracted features can be performed by a large variety of methods such as linear discriminant analysis [147], support vector machines [18], or artificial neural networks [139].

Using these state-of-the-art approaches, many studies concentrate on the forearm and wrist movements such as flexion/extension, pronation/supination, and sometimes hand grasping/opening (all fingers simultaneously). However, since these systems can only produce a small number of motions, they have yet to fully mimic the human hand. With increasing number of multi-DOF prosthetic hands on the market, additional motions are needed to dexterously control these devices in daily activities. In one survey, ten participants with upper limb deficiency were asked what movements or features useful in a future prosthetic hand [148]. All participants wanted to point with the extended finger, 90% of them desired individual control of fingers, and 70% responded that wrist flexion and extension would be beneficial.

Control of the fingers using EMG is extremely challenging compared to forearm/wrist movements. This is because the amplitude of EMG signal for finger movements are generally smaller than those of arm/wrist movements. Furthermore, since the muscles controlling the finger movements lie in the intermediate and deep layers of the forearm [149], attenuation of EMG signals caused by forearm tissues can be observed. Therefore, multiple electrodes are needed to provide enough information to distinguish the intended movement. In recent years, studies on finger movement control have started to appear in literature. However, the number of available literature is still relatively small compared to studies on classification of arm/wrist movements. Furthermore, arm/wrist movement and finger movements are rarely investigated together. However, both wrist and finger movements are needed in daily activities and thus, it is desirable to develop a system that can classify both wrist and finger movements.

Fig. 5.1 shows an overview of recent studies on EMG based pattern recognition. The number of electrodes used in the study is plotted against the number of classes. As can be seen, the number of electrode is greater than or equal to the number of classes in nearly all of these researches.

Also, almost all of the current works only deals with small number of classes (less than 10) [133], [139]-[142], [145], [150], [151]. Only an extremely small number of studies have reported classification results for more than 10 classes but they require large number of electrodes [143], [152]-[154]. However, this option may not be possible with an amputee. This is because using large number of electrodes requires a large surface on the forearm, which may not be available in the case of amputees. Furthermore, having large number of electrodes will increase the cost and complexity of the required hardware as well as increase the computation load which slows down the processing speed of the system [155]. As such, it is desirable to reduce the number of electrode but at the same time have the ability to classify large number of movements. It is also worth noting that most existing researches involve sophisticated clinical grade sensor equipment that are expensive, making practical social use difficult or prohibitive.

For the purpose of developing a low-cost EMG control system that can classify large numbers of movements, this study presents a signal processing technique to classify 17 wrist and finger movements (with a rest state included) using 6 consumer grade EMG sensors. This study will tackle the following research questions:

(1) How well can the state-of-the-art classification scheme classify 17 types of movements?
(2) Can a consumer grade EMG sensor serve as a modality in myoelectric prosthetic control?
(3) How long can the user control the prosthetic hands until the accuracy drops significantly?

To answer the first question, evaluation of a classification scheme using spectral features and multilayer perceptron as the classifier will be performed and discussed. To answer the second question, a consumer grade acquisition device (sampling frequency of 200Hz) will be used in the experiment. The answer to these two questions will give us an idea of the extent of hand movement recognition capabilities with limited hardware. The answer to the third question will give us a hint of when classifiers may need to be recalibrate.

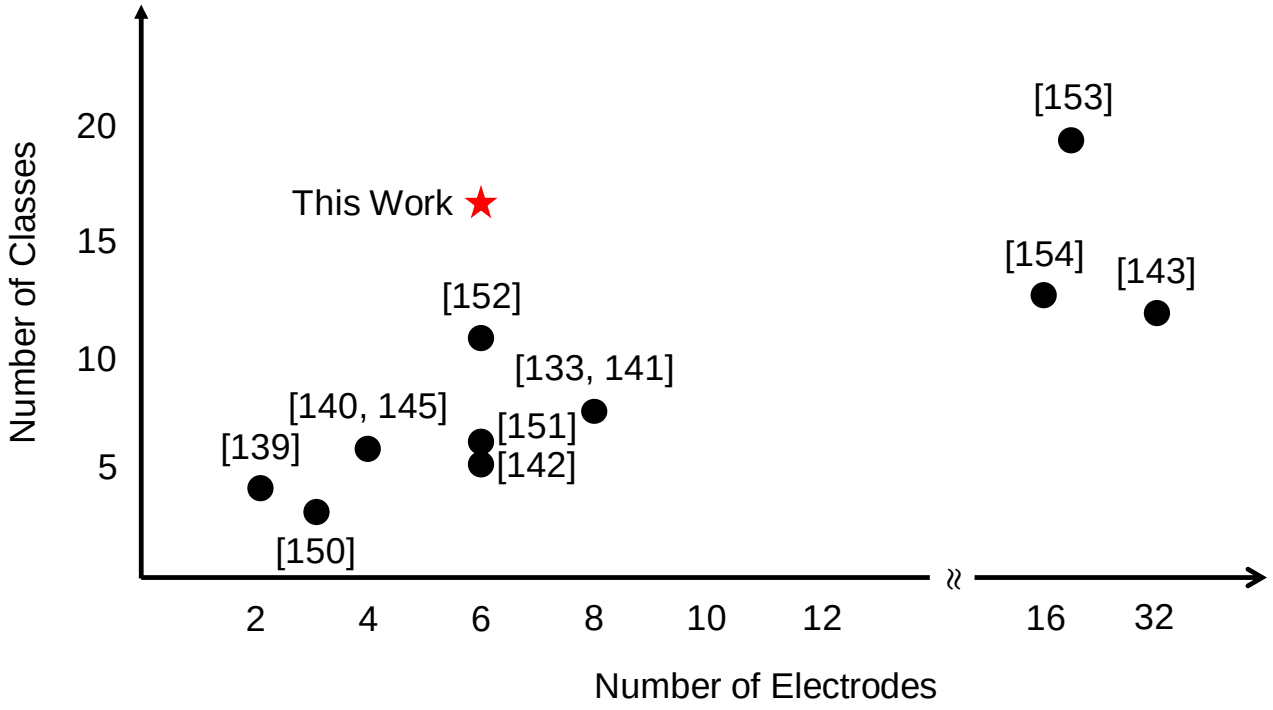

Fig. 5.1 Overview of current EMG based pattern recognition studies illustrating the number of electrodes used and the number of movements classified.

5.3 Data Acquisition and Preprocessing of EMG Signals

The aim of this study is to classify 17 types of motion from EMG signals. The 17 motions include 6 forearm/wrist movements (pronation, supination, flexion, extension, hand grasping and hand opening) as shown in Fig. 5.2, flexion and extension of the five fingers, and a rest state (no movement). In this work, an EMG-based control system is designed as illustrated in Fig. 5.3 to achieve the aim of classifying these 17 motions. As depicted in Fig. 5.3, the system consists of three subsystems: the data acquisition system, the EMG signal processing system, and the interface system. The data acquisition system records EMG signals in a noninvasive fashion using six EMG sensors (IDPAD series manufactured by Oisaka Electronic Equipment Ltd.). These signals are sampled at 200 Hz using a 12-bit analog-digital converter (ADC) and then sent to the signal processing system to undergo further processing. The EMG signal processing system processes the EMG signal and classifies the arm/hand motion. The interface system displays EMG signal waveform, movement cues, as well as classification results in real-time. The software is developed using MATLAB/Simulink® environment. The proposed algorithm is executed after being built by Simulink real-time workshop.

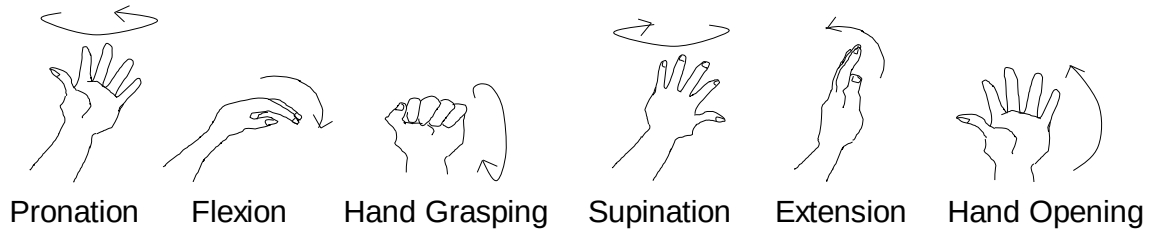

Fig. 5.2 Six forearm motions.

In this study, six EMG sensors are positioned on the flexor carpi radialis muscle, flexor carpi ulnaris muscle, flexor digitorum profundus muscle, flexor pollicis longus muscle, extensor carpi radialis longus muscle and extensor pollicis longus muscle of the left arm as shown in Fig. 5.4 [156]. The functions of each muscle are summarized in Table 5.1. Muscles acting on the hand can be divided into two groups: extrinsic and intrinsic muscles. Intrinsic muscles of the hand are muscles which are located within the hand itself. On the other hand, extrinsic muscles are located in the anterior and posterior compartments of the forearm. Extrinsic muscles are responsible for crude movements of hand whereas intrinsic muscles control fine movements. Controlling the prosthesis using intrinsic hand muscles has the advantage of providing finger control independent of wrist motion [153], but depending on the level of amputation, the required region may not be available. For this reason, this study will only concentrate on extrinsic muscles.

According to the standards for reporting EMG data, significant EMG activity occurs in the 5-450Hz bandwidth [157]. To analyze EMG signals in this bandwidth, most studies uses a clinical grade EMG acquisition device which samples data at 1000Hz or higher. However, these instruments are expensive, making practical social use difficult or prohibitive. To overcome this issue, this study takes on the challenge of using a relatively low-cost consumer grade EMG sensor with lower sampling rate to decode large number of wrist and finger motions. The results of this work will help determine the validity of low cost EMG sensors as a modality in myoelectric prosthetic control.

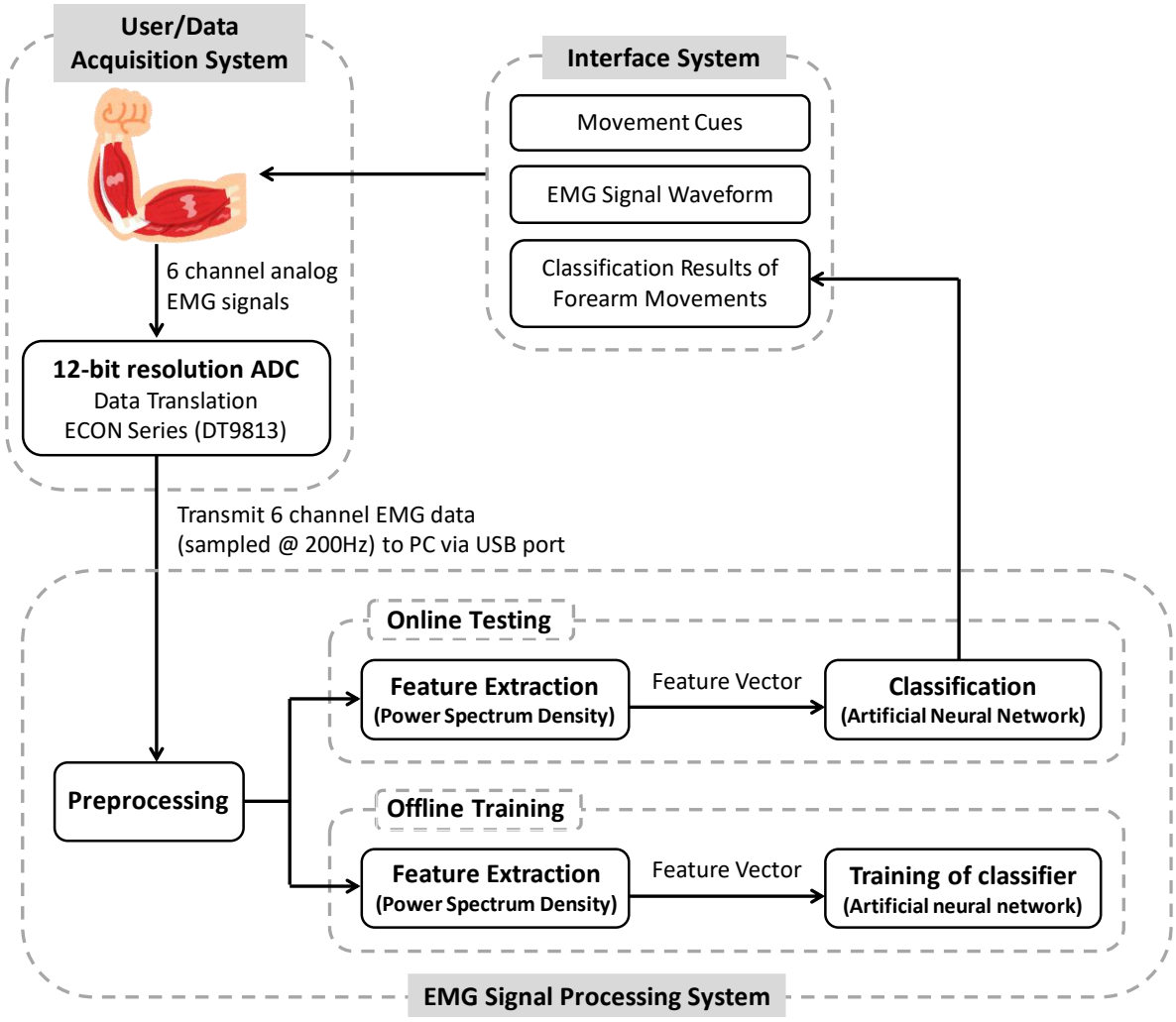

Fig. 5.3 System Architecture.

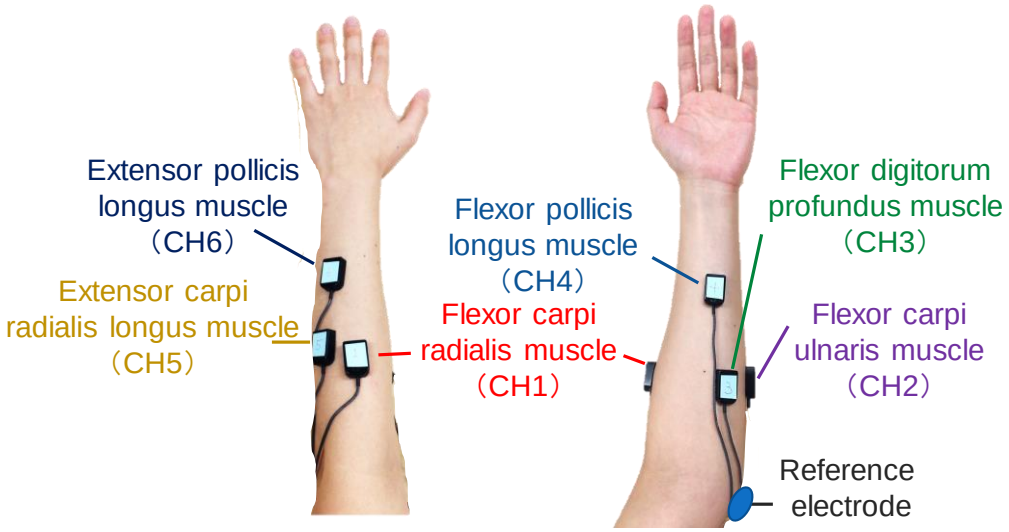

Fig. 5.4 Electrode positions. The positions of the six electrodes are selected with reference to previous work [156].

Table 5.1 Muscle of the Forearm and Their Functions.

Channel Number	Muscle	Function
1	Flexor carpi radialis muscle	Flexion of the hand at the wrist, pronation of the forearm (works along with other muscles which pronate the forearm)
2	Flexor carpi ulnaris muscle	Flexion of the hand at the wrist
3	Flexor digitorum profundus muscle	Flexion of the fingers (excluding the thumb)
4	Flexor pollicis longus muscle	Flexion of the thumb
5	Extensor carpi radialis longus muscle	Extension of the wrist, assists movements of the digits
6	Extensor pollicis longus muscle	Extension of the thumb

The acquired raw EMG (rEMG) signals comes with a DC offset of 2.5V which needs to be removed before any analysis can be performed. The offset is removed by demeaning, i.e. subtracting the average amplitude of rEMG signal during the first 10 seconds from the whole signal. The preprocessed EMG (pEMG) signals will be later used in the feature extraction process. An example of raw EMG signals during the execution of 17 motions is shown in Fig. 5.5.

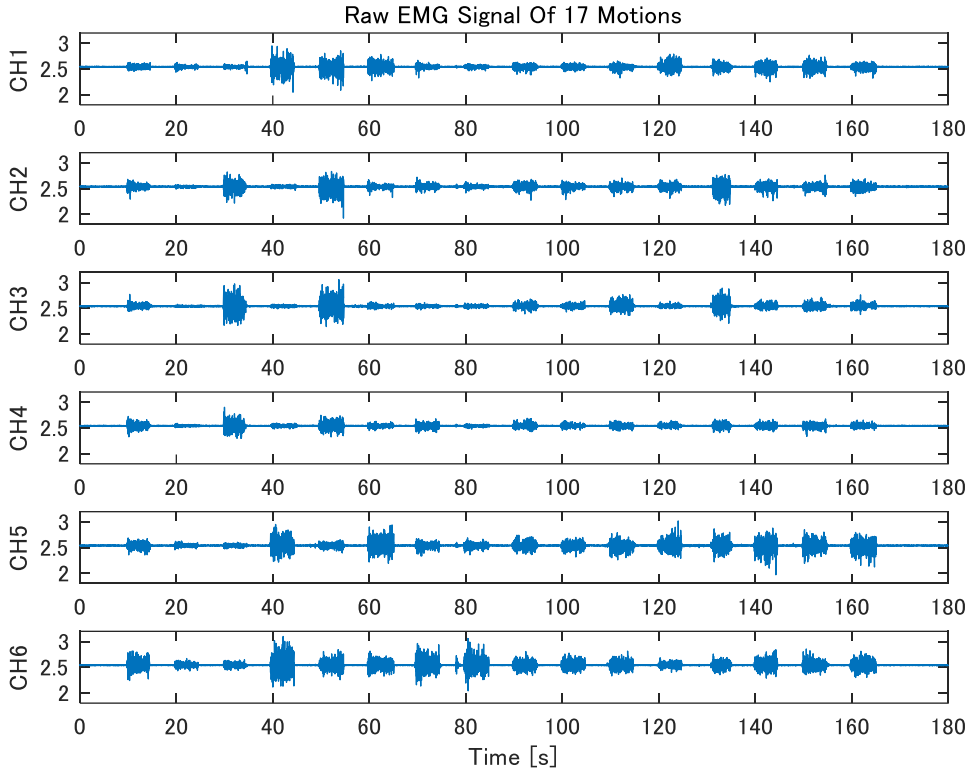

Fig. 5.5 An example of raw EMG (rEMG) signal during the execution of 17 motions. The channels are layout in ascending order starting from the top.

5.4 Signal Processing Algorithm for Classification of 17 Motions

In this section, the proposed signal processing algorithm to classify 17 motions is described. In this method, the pEMG signals are transformed from time domain to frequency domain by performing fast Fourier transform (FFT) that uses a hamming window function. Next, power spectrum densities (PSDs) are calculated from the FFT results. Feature points that best characterize each motion are selected from the power spectrum densities for each channel to form feature vectors. Finally, the 17 motions are classified by feeding the feature vectors into the artificial neural network (ANN) classifier. The details of the proposed method are described in the following sections.

5.4.1 Feature Extraction Based on Spectral Analysis

After removing the DC offset, PSDs are calculated by applying FFT to the pEMG signals. In this step, a 32-sample hamming window with 75% overlap is used when performing FFT. Next, feature points for each motion are extracted from the PSDs to construct a feature vector. In this study, spectral magnitudes at 6 frequencies are used as features. Considering the fact that the Nyquist frequency is 100Hz (sampling frequency of the equipment is 200Hz) and the frequency resolution is 6.25Hz, one frequency is chosen from each of the following frequency range: 10-20Hz, 20-30Hz, 30-40Hz, 60-70Hz, 70-80Hz, 80-90Hz. The 40-50Hz and 50-60Hz frequency ranges are not considered because they contain the frequencies of the power-line interferences. Based on the selection results, the elements of the feature vectors are made up of log-transformed spectral magnitude at 18.75Hz, 25Hz, 31.25Hz, 68.75Hz, 75Hz, 81.25Hz of each channel. Thus, the feature vector of j^{th} motion is a 36-dimensional vector and can be expressed as

$$\boldsymbol{f}^{j} = [\, f_1^{j} \quad \cdots \quad f_i^{j} \quad \cdots \quad f_{36}^{j} \,] \in \Re^{1\times 36}, \tag{5.1}$$

where f_i^{j} is the i^{th} element of the feature vector of j^{th} motion. Fig. 5.6 and Fig. 5.7 shows an example of normalized PSDs of all 17 motions derived from pEMG signals on channel 2 and channel 5.

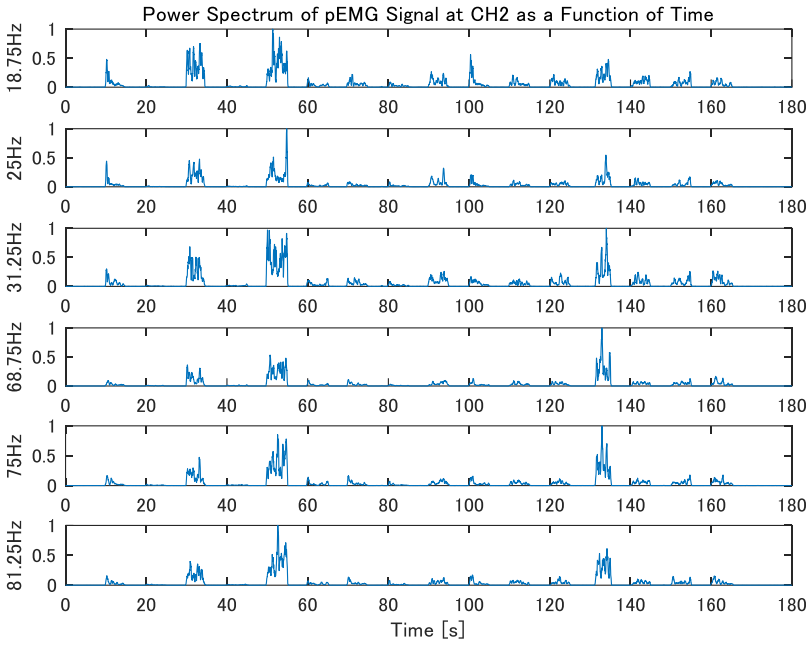

Fig. 5.6　An example of PSDs prior to log transform of 17 motions shown as a function of time. The PSDs are derived from pEMG signals on channel 2. In order from the top, PSDs at 18.75 Hz, 25 Hz, 31.25 Hz, 68.75 Hz, 75 Hz, 81.25 Hz. Note that the PSDs are normalized for better visualization.

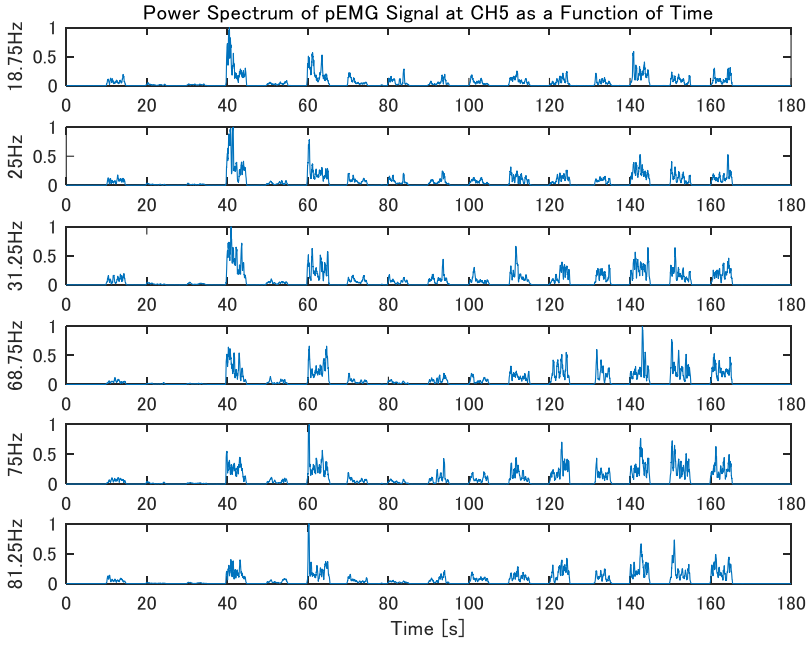

Fig. 5.7　An example of PSDs prior to log transform of 17 motions shown as a function of time. The PSDs are derived from pEMG signals on channel 5. In order from the top, PSDs at 18.75 Hz, 25 Hz, 31.25 Hz, 68.75 Hz, 75 Hz, 81.25 Hz. Note that the PSDs are normalized for better visualization.

Let m be the number of sets of training data used in the training process, with each set containing EMG signals of all 17 motions (1 trial for each motion). Then, from a single set of training data, a matrix consisting of feature vectors of each motion can be derived and defined as

$$\boldsymbol{F}_n = \begin{bmatrix} \boldsymbol{f}^1 \\ \vdots \\ \boldsymbol{f}^j \\ \vdots \\ \boldsymbol{f}^{17} \end{bmatrix} \in \Re^{17\times 36}, \quad n \in \{1,2,\cdots,m\}. \tag{5.2}$$

Furthermore, using (2), a feature matrix containing all feature vectors derived from m sets of training data can be expressed as

$$\begin{aligned} \boldsymbol{F} &= \begin{bmatrix} \boldsymbol{F}_1 \\ \vdots \\ \boldsymbol{F}_n \\ \vdots \\ \boldsymbol{F}_m \end{bmatrix} \in \Re^{17m\times 36} \\ &= \begin{bmatrix} \boldsymbol{f}_1 & \cdots & \boldsymbol{f}_i & \cdots & \boldsymbol{f}_{36} \end{bmatrix} \end{aligned}, \tag{5.3}$$

where $\boldsymbol{f}_i$ is a 17m dimension column vector. Next, the feature matrix (3) is normalized by

$$\tilde{\boldsymbol{F}} = \begin{bmatrix} \dfrac{\boldsymbol{f}_1}{\min(\boldsymbol{f}_1)} & \cdots & \dfrac{\boldsymbol{f}_i}{\min(\boldsymbol{f}_i)} & \cdots & \dfrac{\boldsymbol{f}_{36}}{\min(\boldsymbol{f}_{36})} \end{bmatrix} \in \Re^{17m\times 36} \tag{5.4}$$

and use as the input signal to train the ANN classifier. In the online classification stage, the feature vector at k^{th} sampling instance are given by

$$\hat{\boldsymbol{f}}(k) = \begin{bmatrix} \dfrac{\hat{f}_1(k)}{\min(\boldsymbol{f}_1)} & \cdots & \dfrac{\hat{f}_i(k)}{\min(\boldsymbol{f}_i)} & \cdots & \dfrac{\hat{f}_{36}(k)}{\min(\boldsymbol{f}_{36})} \end{bmatrix} \in \Re^{1\times 36}. \tag{5.5}$$

Note that $\min(\boldsymbol{f}_i)$ should be determined beforehand from m training data sets.

5.4.2 Training of Artificial Neural Network Classifier

A feature vector of a given motion consists of 36 elements as denoted in (1). Since there are 17 motions, a data set can produce 17 feature vectors (one feature vector for each motion). In the training stage, feature matrix generate from m data sets are used to train the classifier as defined in (4). Thus, the teaching signal $\boldsymbol{T}$ is given by

$$\boldsymbol{T} = \begin{bmatrix} \mathrm{I}_{17} & \mathrm{I}_{17} & \cdots & \mathrm{I}_{17} \end{bmatrix}^{\mathrm{T}} \in \Re^{17m\times 17}. \tag{5.6}$$

In this study, the artificial neural network (ANN) is chosen as the classifier to discriminate the 17 motions. Currently, several kinds of ANN have been proposed. In this study, a multilayered perceptron, which is a feed-forward ANN is chosen.

The multilayer perceptron is a multilayered ANN which consists of one or more hidden layers. This type of ANN is known as a supervised network because it requires a desired output (teaching signal) in order to learn. A set of learning data that consists of the feature vector and the corresponding teaching signals is used to have the perceptron acquire appropriate connection weights and threshold values of the middle layer and the output layer by machine learning. The multilayered perceptron and many other ANN learn by using an algorithm called backpropagation. With back propagation method, the input data (feature vector) is repeatedly presented to the ANN. With each presentation, the output of the ANN is compared to the desired output (teaching signal) and an error is computed. This error is then feedback (backpropagated) to the ANN and used to adjust weights so that the error decreases with each iteration and the ANN model gets closer and closer to producing the desired output [117], [118]. When performing real-time classification, these connection weights and threshold values are fixed and determined beforehand. To keep the computational cost low, an ANN with only one hidden layer is structured in this study. Table 5.2 shows the number of neurons in the input, hidden and output layer along with the learning coefficient of each classification scenarios (see section 5.1.2). Based on our experience [156] and also suggested by [158], overfitting may occur in ANN if the training iteration (epoch) is too long. To prevent this, the training process is terminated when the error reaches 0.001 or when the number of training epoch reaches 2000. It is also worth noting that the number of neurons in the hidden layer for each classification scenarios are determined based on our experience and trial and error. More specifically, the number of neurons that produces the lowest training error is selected. In the case that the training error reaches 0.001 for two or more neuron arrangements, the number of neurons that requires the least training epoch will be chosen.

Furthermore, a classification label of a motion at any given sampling instance is defined by the class with the highest ANN output. Thus, the classification output corresponding to the discriminated motion will have a value of 1 while classification output for other motions will have a value of 0.

5.5 Online Classification Experiment

In this section, experimental conditions necessary to perform online classification of 17 motions are described. The aim of this experiment is to clarify how well the proposed algorithm works based on the following three criteria:

(1) Classification accuracy of 17 motions
(2) Classification accuracy without re-training the classifier
(3) Classification accuracy of 9 motions (motions that are required to complete most daily tasks).

The results of the experiment are evaluated and discussed.

5.5.1 Experimental Conditions

5.5.1.1 Participants

In this study, the experiments were carried out with cooperation of 12 able-bodied participants (referred to as participant A to L) in their twenties. 7 were males (participant A, D, E, G, H, I, and L) and 5 were females (participant B, C, F, J and K). The entire protocol and aims of the study are fully explained to them before the experiment, and all participants signed the written informed consent. All of the experiments are conducted with the approval from Tokyo Denki University Human Bioethics Committee. Apart from participant A and B, all other participants had no prior experience with myoelectric control experiments at all.

During the electrode placement, no particular skin preparation technique was applied to the forearm as to mimic the real-life usage scenarios. Also, hair on the forearms of male participants were not shaved according their request.

5.5.1.2 Experiment Protocol

In the experiment, participants were seated in front of a monitor and we asked to perform the 17 movements in order as shown in Fig. 5.8. During the experiment, visual and audio cues were presented to the participants. In each experimental run, participants were asked to perform each motion once and sustain that motion for 5 seconds. They were also instructed to execute each motion naturally and not forcefully. For flexion and extension movements of middle, ring, and little finger, it is generally difficult to independently move each finger without simultaneously moving the other two. The participants were informed that it is perfectly fine if the other fingers were to also move.

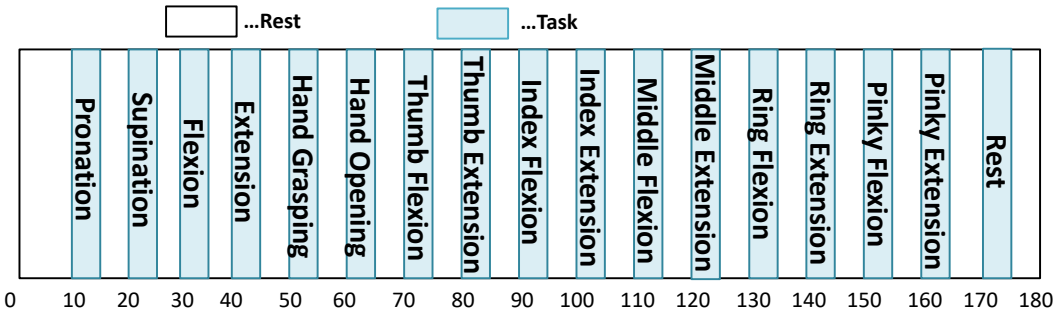

Fig. 5.8 Execution sequence of 17 motions (including rest state). Each motion is executed for five seconds with a five second resting interval in between each motion. The total duration of each run is 180 seconds. The feature point for rest state is selected between 170 to 175 seconds.

The experiment is divided into training and online testing stage both conducted on the same day. First, five sets of data were acquired for training the ANN and later, 10 sets of testing data were recorded for evaluation. The same experiment is repeated again on a different day for participants A, B, E and H. There was a 4-day gap in between day 1 and day 2 for participant A, a 2-day gap for participant B, and a 6-day gap for participant E and H. To address the research questions, four online and pseudo-online classification scenarios are designed as describe below. Details of each classification scenarios can also be found in Table 5.2. The results are evaluated and discussed in the next section.

(1) Classification of 17 voluntary movements: This classification scenario aims to evaluate the classification performance of the proposed system. The result of this experiment will give us a hint of the extent of using state-of-the-art pattern recognition scheme to classify 17 types of motions. It will also help demonstrate the validity of low-cost hardware as a modality for myoelectric control. In this experiment, ANN is trained using all five training data sets and the accuracy is evaluated using all 10 testing data sets.

(2) Classification of 17 movements using testing data obtain on a different day: This classification scenario aims to determine how well the proposed method can perform without having to re-train the classifier. To do so, the ANN parameters from day1 are used to classify the testing data obtained in day 2, and vice-versa.

(3) Classification of 9 movements: This scenario is intended to see how much the accuracy improves when the number of classes are reduced to nine. The 9 motions involved in this classification scenario are pronation, supination, hand grasping, hand opening, flexion and extension of thumb and index finger, and a rest state. These motions were selected because they are the basic hand/arm movements needed to carry out most daily

tasks, e.g. turning a door knob, grabbing and relocating an object, picking up a small object. The same EMG data involved in the previous classifications are used in this scenario. Since both training and testing data sets contains EMG signals for 17 motions, the epoch of the non-target motions along with subsequent rest period was cut off and the remaining epoch were merged together to form a new time series data set lasting 100 seconds.

(4) Classification of 9 movements using testing data obtain on a different day: Similar to the scenario 2, this scenario hopes to test the functionality of the proposed algorithm without having to re-train the classifier.

Table 5.2 Details of Each Classification Scenarios

Classification Scenario	**Number of Motions**	**Training Data**	**Testing Data**	**Participant**	**Number of Neurons in the Input Layer / Hidden Layer / Output Layer**	**Learning Coefficient**
1	17	Day 1	Day 1	A	36 / 20 / 17	1.2
		Day 2	Day 2	A	36 / 20 / 17	
		Day 1	Day 1	B	36 / 20 / 17	
		Day 2	Day 2	B	36 / 20 / 17	
		Day 1	Day 1	C	36 / 24 / 17	
		Day 1	Day 1	D	36 / 20 / 17	
		Day 1	Day 1	E	36 / 24 / 17	
		Day 2	Day 2	E	36 / 20 / 17	
		Day 1	Day 1	F	36 / 16 / 17	
		Day 1	Day 1	G	36 / 20 / 17	
		Day 1	Day 1	H	36 / 18 / 17	
		Day 2	Day 2	H	36 / 18 / 17	
		Day 1	Day 1	I	36 / 20 / 17	
		Day 1	Day 1	J	36 / 22 / 17	
		Day 1	Day 1	K	36 / 24 / 17	
		Day 1	Day 1	L	36 / 20 / 17	
2	17	Day 1	Day 2	A	36 / 20 / 17	1.2
		Day 2	Day 1	A	36 / 20 / 17	
		Day 1	Day 2	B	36 / 20 / 17	
		Day 2	Day 1	B	36 / 20 / 17	
		Day 1	Day 2	E	36 / 24 / 17	
		Day 2	Day 1	E	36 / 20 / 17	
		Day 1	Day 2	H	36 / 18 / 17	
		Day 2	Day 1	H	36 / 18 / 17	
3	9	Day 1	Day 1	A	36 / 14 / 9	1.2

		Day 2	Day 2	A	36 / 12 / 9	
		Day 1	Day 1	B	36 / 14 / 9	
		Day 2	Day 2	B	36 / 16 / 9	
		Day 1	Day 1	C	36 / 20 / 9	
		Day 1	Day 1	D	36 / 14 / 9	
		Day 1	Day 1	E	36 / 16 / 9	
		Day 2	Day 2	E	36 / 14 / 9	
		Day 1	Day 1	F	36 / 12 / 9	
		Day 1	Day 1	G	36 / 18 / 9	
		Day 1	Day 1	H	36 / 20 / 9	
		Day 2	Day 2	H	36 / 16 / 9	
		Day 1	Day 1	I	36 / 20 / 9	
		Day 1	Day 1	J	36 / 16 / 9	
		Day 1	Day 1	K	36 / 14 / 9	
		Day 1	Day 1	L	36 / 18 / 9	
4	9	Day 1	Day 2	A	36 / 14 / 9	1.2
		Day 2	Day 1	A	36 / 12 / 9	
		Day 1	Day 2	B	36 / 14 / 9	
		Day 2	Day 1	B	36 / 16 / 9	
		Day 1	Day 2	E	36 / 16 / 9	
		Day 2	Day 1	E	36 / 14 / 9	
		Day 1	Day 2	H	36 / 20 / 9	
		Day 2	Day 1	H	36 / 16 / 9	

In this study, the evaluation of classification accuracy is based on correct and incorrect rates. Since the ANN has the same number of output neurons as the number of motions, the correct and incorrect rates for each motion are calculated from the output neuron belonging to the motion of interest (Fig. 5.9). Correct classification rate is given by

$$\mathbf{CorrectRate} = \frac{\mathbf{Number\ of\ correct classification}}{\mathbf{Total\ number\ of\ classification samples}} \times \mathbf{100\%} \tag{5.7}$$

On the other hand, incorrect classification rate is calculated by

$$\mathbf{IncorrectRate} = \frac{\mathbf{Number\ of\ erroneous classification}}{\mathbf{Total\ number\ of\ classification samples}} \times \mathbf{100\%} \tag{5.8}$$

Fig. 5.9 shows an example of a classification output. We will use this example to demonstrate how correct and incorrect rates are calculated using (7) and (8). In this example, correct classification label of pronation movement is indicated by the green circle. Three red circles indicate the incorrect classification label of pronation movement. Since the ANN classifier gives a decision every 0.005 seconds (200 Hz), and each movement is sustained for 5 seconds, the total number of classification

samples for each motion is 1000. In the example shown in Fig. 5.9, 904 samples out of 1000 samples were correctly classified for pronation movement, thus, the correct rate becomes 90.4%. On the other hand, 1/1000 samples (0.1%) were misclassified as supination movement, 19/1000 samples (1.9%) were misclassified as middle finger flexion movement, and 76/1000 samples (7.6%) were misclassified as rest state. Adding up these numbers will give an incorrect rate of 9.6% for middle finger flexion movement.

5.5.2 Results and Discussions

5.5.2.1 Classification of 17 Voluntary Movements

This classification scenario provides some answers to all of the three research questions. The questions are:

(1) How well can the state-of-the-art classification scheme classify 17 types of movements?
(2) Can a consumer grade EMG sensor serve as a modality in myoelectric prosthetic control?
(3) How long can the user control the prosthetic hands until the accuracy drops significantly?

First, let's answer question number 1 and 2. According to Fig. 5.10, under the condition that training and testing are done on the same day, an overall correct rate of 63.8% across subject can be achieved for classification of 17 motions using the proposed method. Also, depending on the participant and the muscle condition, the system can accomplish a correct rate of 82.9% (participant E) or an average accuracy of up to 76.1% (participant H). Furthermore, the statistical results in Fig. 5.11 suggests that improvement in accuracy may be due to the fact that the user has gained more experience from the training on the previous day. However, since the current work only compares the accuracy between two days, it is still too early to draw a decisive conclusion based on the current results. As an extension to this study, more experiments should be conducted for multiple days. It would be interesting to observe how long this trend will persist and how long can the training effect last. Based on the above results combined with the fact that the user can promptly modify any erroneous actions executed by the prosthetic hand by looking at the actual output, the proposed method is functional and has demonstrated the potential to classify 17 motions using six EMG sensors. Furthermore, the results also suggest that a consumer-grade EMG sensor can serve as a modality in myoelectric prosthetic control and other human-machine interface applications.

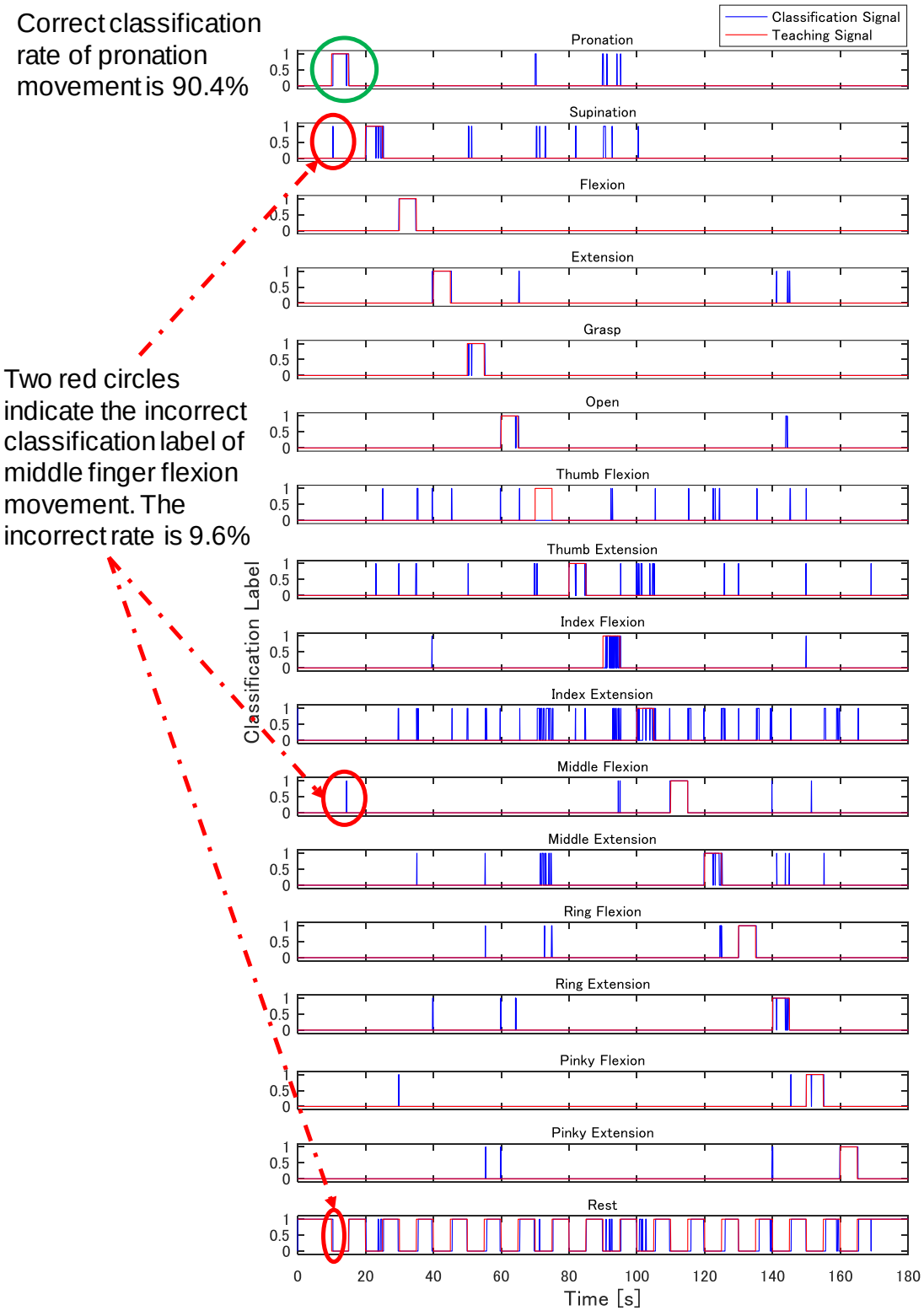

Fig. 5.9 Example of a classification output. The blue line indicates the classification signal. The red line indicates teaching signals. The green circle represents correct classification label of pronation movement as an example. The red circle indicates the incorrect classification label of pronation movement. In this study, the ANN classifier gives a decision every 0.005 seconds (200 Hz).

Although our results cannot be directly compared with results in other studies due the difference in participants, equipment, experiment conditions, type of movement, etc., the results reported in this study has demonstrated some advantages over existing researches. We will compare with some of the works summarized in Table 5.3.

The first advantage is that the number of movements involved in this work is much greater than most studies. The work done by Adewuyi et al. [153] is the only study that involves more movement than this work. They report very high accuracy of up to 96% for classification of 19 classes. In their work, 19 electrodes are placed on the surface of the hand to capture the EMG signals responsible for fine motor control of the fingers. However, this electrode configuration is limited to only amputees who still retain a portion of the hand. At the same time, it is also inconvenient for healthy people to wear many electrodes. Works by Tenore et al. [143] Kanitz et al. [154] show that accurate classification of 12 finger motions is possible but they also face the disadvantage of having very large number of electrodes. In contrast, our work involves a smaller number of electrodes on the forearm which contributes to reducing equipment costs and preparation time, hence increases the usability of the system. Another wonderful advantage of using small number of electrodes is that it is easier to configure the current setup onto existing prosthetic hand. Furthermore, this work also offers the highest ratio of movements to electrodes (N_m/N_{ch}).

On the other hand, the limitation of the proposed system lies in the fact that the accuracy is lower than others studies. One of the reasons for this is that duration of each motion is too long. Many participants have reported experiencing difficulty in sustaining each movement for 5 seconds. Pronation/supination and flexion/extension of the index, middle, and the ring finger movements were especially hard according to the participants. This can be observed by looking at the ANN output signal where the system outputs the correct decisions only for the first 3 seconds. Muscle fatigue is also another reason for low accuracy. Participants also reported that they experienced muscular fatigue after performing 6-7 continuous classification trials (11-12 trials, if including trials from the training stage). The effects of the fatigue can be seen in the gradual decline of correct rates shown in Fig. 5.12. The results of a paired t-test show that decline of accuracy due to fatigue starts on the 8th trial ($p < 0.1$) and drops significantly on the 9th trial ($p < 0.05$, approximately 1 hour of continuous usage). This observation suggests that in practice, a control strategy that will hold the posture of the prosthetic hand without having to sustain muscular contraction may be desirable to help relief the level of fatigue. Also, re-training of the classifier should be performed after 1 hour of continuous usage. Thus, the above results address the research question number 3.

It is also worth mentioning that there is a tradeoff between the number of channels and the accuracy of the system. In practice, depending on the demands of the user or the type of application, the number of electrodes should be configured for each user in order to suit the needs of any individual.

5.5.2.2 Classification of 17 Movements Using Testing Data Obtain on a Different Day

The classification results of 17 motions where training and testing data sets are not from the same day are shown in Fig. 5.11. According to this figure, the accuracy of classification using ANN parameters that are a few days old is around 40%. Depending on user and their condition, the system can yield an accuracy of 56% at best. Although re-training the classifier is highly recommended in order to restore dexterous control, the results suggest that control of the prosthetic hand is possible to a certain degree without having to re-train the classifier. An extension to this study would be to investigate how accuracy changes over time in order to reduce the number of recalibration and optimize the usability.

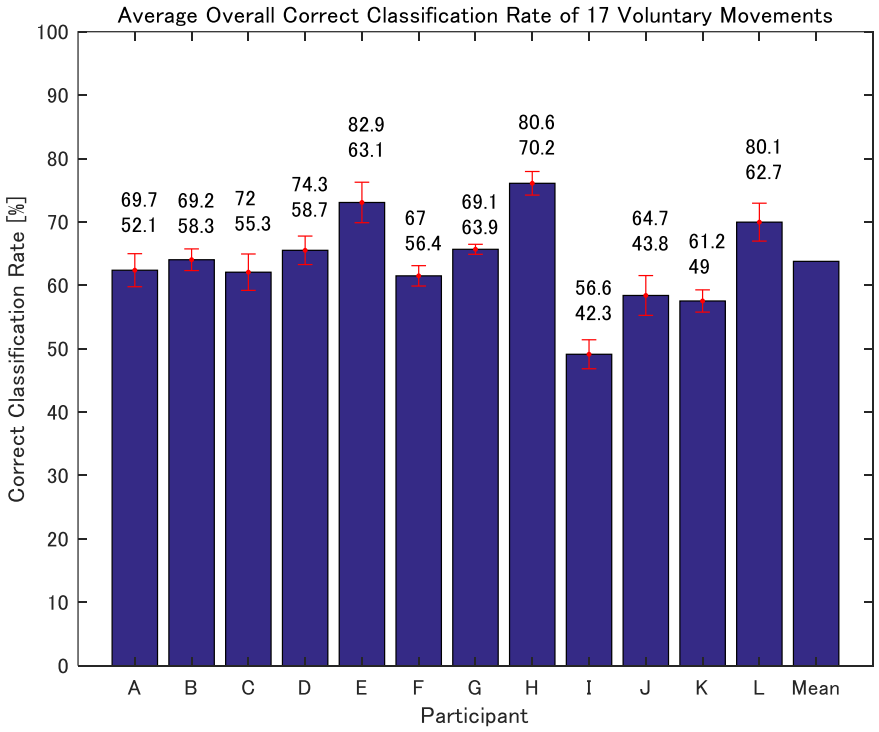

Fig. 5.10 Average overall correct classification rate of 17 voluntary movements of 12 participants. The red error bars indicate standard deviation. The two numbers on top of the bars indicate highest and lowest overall correct rate. Note that the average correct rate of participant A, B, E and H are from the experiment on day 2 (best classification). Also, the mean overall correct rate indicates the overall correct rate across subjects.

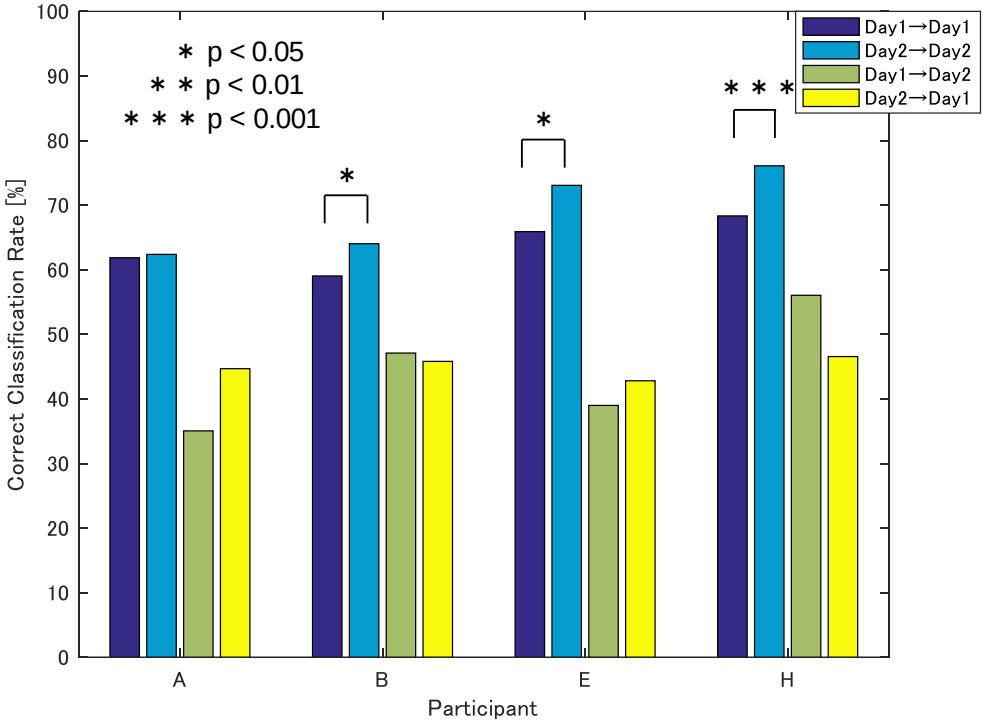

Fig. 5.11 Comparison of mean correct rates of each classification scenario (17 Movements). (*) represents $p < 0.05$ and (***) represents $p < 0.001$.

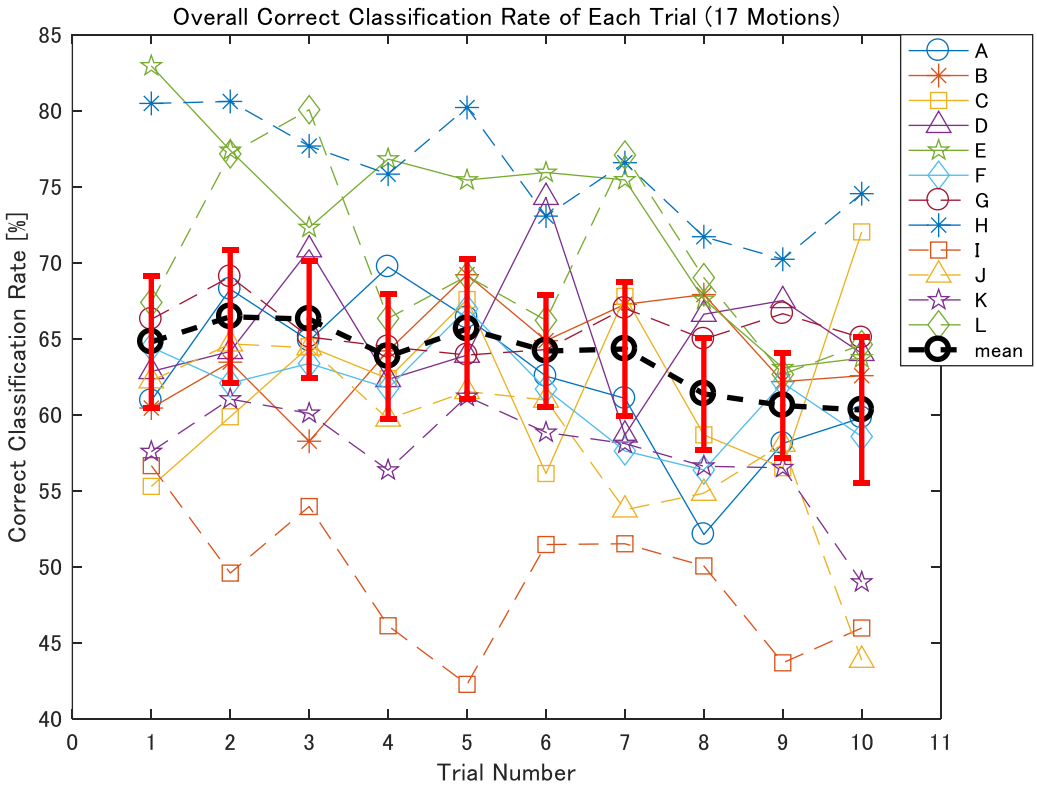

Fig. 5.12 Correct classification rate of 17 voluntary movements of each trial. Note that the correct rates of participant A, B, E and H are from the experiment on day 2 (best classification).

Table 5.3 Summary of existing EMG Based Pattern Recognition Studies

Author/s	**Year**	**No. of Electrodes** N_{ch}	**No. of Movements** N_m	**Sampling Frequency**	N_m / N_{ch}	**Accuracy**	**Number of Subjects**
Fukuda et al. [151]	2004	6	6 W	200 Hz	1	92.1%	3 H and 2 A
Jiang et al. [145]	2005	4	6 IF	2,000 Hz	1.5	80%	10 H
Oskoei & Hu [140]	2008	4	6 (5 W + R)	1,000 Hz	1.5	95 %	11 H
Tenore et al. [143]	2009	32	12 (10 IF & 2 CF)	2,000 Hz	0.38	90%	5 H
		19			0.63	83%	1 A
Ahsan et al. [139]	2011	2	4 W	1,000 Hz	2	88.4%	3 H
Cipriani et al. [133]	2011	8	7 (4 IF + 2CF + HG)	10,000 Hz	0.88	89%	5 H
						79%	
Kanitz et al. [154]	2011	16	13 (12 IF + R)	16,000 Hz	0.81	80%	5 A
Tsujimura et al. [150]	2012	3	3 CF	10,000 Hz	1	97%	5 H and 1 A
Benatti et al. [141]	2015	8	7 (5 W + IF + R)	1,000 Hz	0.88	90%	1 H
Adewuyi et al. [153]	2016	19	19 (12 IF + 7 HG)	1,000 Hz	1	96%	4 H
This work	-	6	17 (10 IF + 6 W + R)	200 Hz	2.83	63.8%	9 H
			9 (4 IF + 4 W + R)		1.5	72.9%	12 H

[1]IF: Individual Finger Movement. W: Wrist Movement. R: Rest State. CF: Combine Finger Movement. HG: Hand Grasp Movement. H: Healthy. A: Amputee

5.5.2.3 Classification of 9 Movements

This scenario is intended to see how much the accuracy improves when the number of classes are reduced to nine. According to Fig. 5.13, under the condition that training and testing are done on the same day, an overall correct rate of 72.9% across subject can be achieved for classification of 9 motions using the proposed method. Also, depending on the participant and the muscle condition, the system can accomplish a correct rate of 92.1% (participant L) or an average accuracy of up to 82.6% (participant F). These results demonstrate that reducing the number of motions helps improve the overall performance. Therefore, if the prosthetic hand is intended for a specific task, limiting the number of motions can significantly increase the performance and usability of the system. Furthermore, the above results also help strengthened the conclusion that a

consumer-grade EMG sensor can serve as a modality in myoelectric prosthetic control.

Compared with the scenario dealing with 17 motions (Fig. 5.11), it is interesting to see that no significant statistical difference can be observed for participant B, E and H in this scenario. On the other hand, statistical difference can now be observed for participant A. This statistical difference was not present in the previous classification scenario with 17 movements. The above results suggest that for participant B, E and H, the accuracies of the selected 9 motions may already be relatively high to begin with and that the trainings done on day 1 may not be sufficient to significantly improve these accuracies. The opposite could be implied for participant A. Since the current skill level and the rate of improvement is different for each individual for each type of motion, a training method/menu specifically tailored for each individual may help improve the accuracy significantly.

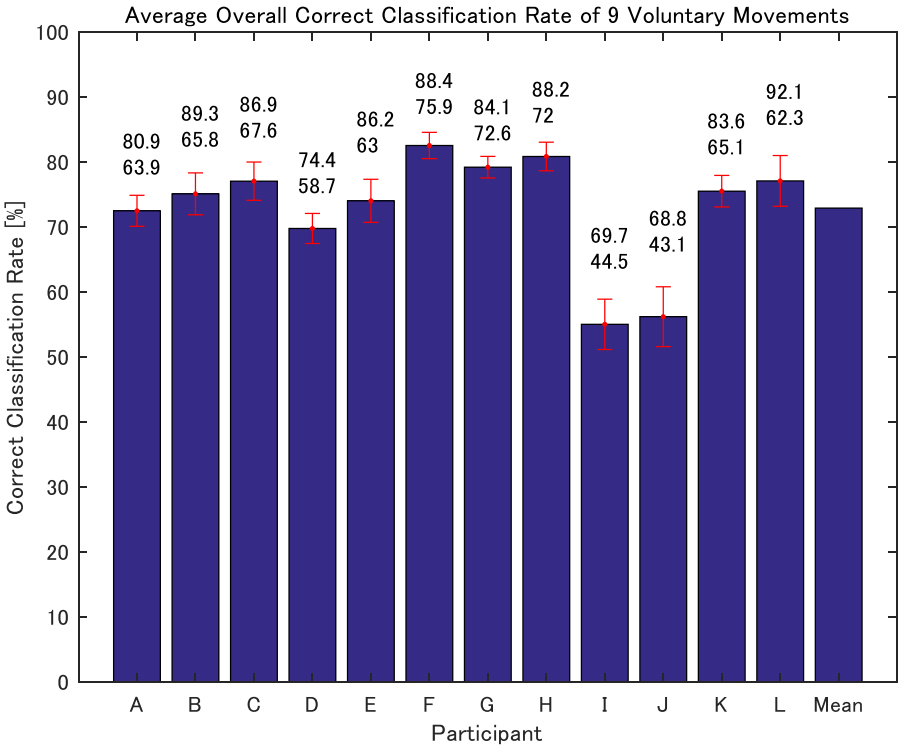

Fig. 5.13 Average overall correct classification rate of 9 voluntary movements of 12 participants. The red error bars indicate standard deviation. The two numbers on top of the bars indicate highest and lowest overall correct rate. Note that the average correct rate of participant A, B, E and H are from the experiment on day 2 (best classification). Also, the mean overall correct rate indicates the overall correct rate across subjects.

5.5.2.4 Classification of 9 Movements Using Testing Data Obtain on a Different Day

The classification results of 9 motions where training and testing data sets are not from the same day are shown in Fig. 5.14. According to this figure, the accuracy of classification using ANN parameters that are a few days old is around 50%. Depending on user and their condition, the system can yield an accuracy of 67.5% at best. Compared to the scenario involving 17 movements, the accuracy has improved greatly. An extension to this study would be to test this scenario in real-time in order to evaluate the feasibility of a system with accuracy of around 50%.

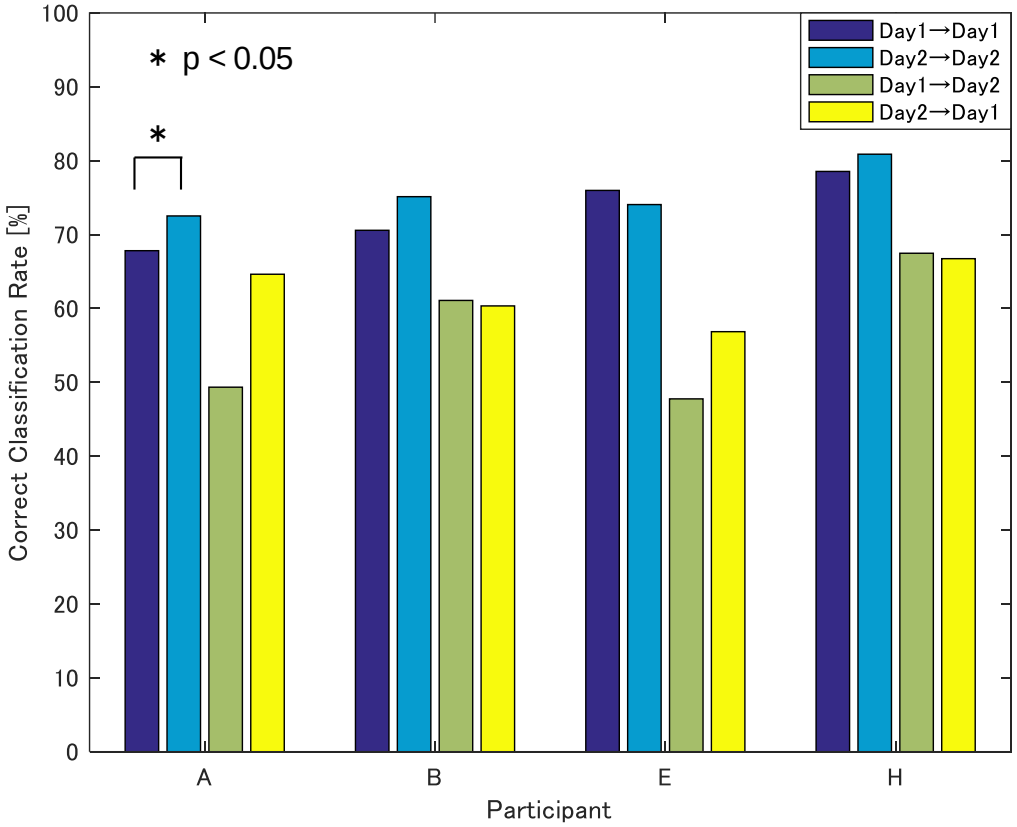

Fig. 5.14 Comparison of mean correct rates of each classification scenario (9 movements). (*) represents $p < 0.05$.

5.5.2.5 Erroneous Classification

Further analysis shows that erroneous classification sometimes occurs for motions associated with fingers. As shown in Fig. 5.15, for example, when the participant flexes his/her ring finger, the ANN sometimes misclassifies the motion as flexion of the middle finger. This happens because as the participant tries to flex the ring finger, the middle finger also flexes as well. Another example is when the participant extends his/her index finger or performs hand opening motion, the ANN misclassifies the intended motion as extension of the ring finger. In this case, misclassification happens because the muscles associated with the movement of these fingers are very close to each other which makes it difficult to obtain distinguishable EMG patterns. Interestingly, the motions that often get misclassified are different depending on who the user is. This may be due to the fact that each participant executes each motion in a different manner. An extension to this study would be to discuss ways to deal with these erroneous classifications in order to improve the accuracy.

Executed Motion \ True Label	Pro	Sup	Flex	Ext	Grasp	Open	TF	TE	IF	IE	MF	ME	RF	RE	LF	LE	Rest
Pro	69.8	4.2	1.9	0.1	1.0	0.0	3.2	1.5	6.2	0.5	0.6	0.3	0.6	1.3	1.2	0.7	6.8
Sup	0.3	66.5	0.1	0.3	0.1	1.7	3.4	5.5	2.2	5.2	2.3	0.6	2.5	0.6	1.4	1.0	6.4
Flex	2.0	0.2	81.3	0.1	1.0	0.0	0.1	0.6	0.4	2.1	1.7	0.8	1.3	0.3	0.5	4.9	2.6
Ext	0.1	1.1	0.0	89.0	0.0	3.2	1.1	0.1	0.6	0.5	0.0	0.3	0.2	2.4	0.4	0.1	0.9
Grasp	3.7	1.8	5.8	0.2	71.0	0.0	1.9	0.9	2.1	1.1	0.9	1.8	2.0	0.7	1.5	0.7	3.7
Open	0.0	2.6	0.0	5.2	0.0	56.4	5.6	1.1	3.6	3.7	0.3	3.2	0.4	10.5	5.6	1.0	0.8
TF	1.6	4.9	0.0	0.9	0.5	3.3	57.9	5.9	5.0	5.4	1.5	0.8	0.9	1.7	5.8	1.5	2.5
TE	1.5	2.9	0.9	0.1	0.2	1.8	1.0	67.0	3.7	6.0	3.9	0.2	1.0	0.5	0.7	5.9	2.6
IF	3.0	5.8	0.4	0.4	3.3	1.6	1.4	2.9	50.1	2.3	7.0	1.6	2.5	4.8	6.6	2.0	4.2
IE	0.5	3.6	0.9	0.2	1.5	3.9	6.2	11.6	3.5	43.3	7.7	0.7	1.3	4.3	3.9	4.1	2.9
MF	2.0	1.6	1.0	0.1	1.3	0.2	1.3	5.1	7.0	4.3	53.9	1.4	3.6	4.7	7.4	2.5	2.6
ME	0.2	2.7	0.1	0.1	1.8	2.7	3.1	0.2	1.0	1.8	0.5	62.0	6.5	7.9	6.1	1.7	1.4
RF	0.3	0.7	2.1	0.0	1.1	0.2	0.3	1.0	3.2	1.6	5.2	3.9	65.6	2.5	3.6	7.0	1.6
RE	0.5	2.2	0.0	2.1	0.5	8.9	2.1	1.8	3.4	1.6	1.9	2.8	1.2	49.8	15.8	4.1	1.2
LF	0.3	1.4	0.1	0.5	0.2	2.3	7.3	2.9	7.1	3.0	1.9	5.9	1.0	6.6	57.1	1.3	1.0
LE	0.6	0.4	1.1	0.0	0.4	1.0	0.3	3.6	4.0	2.8	3.0	0.2	5.1	6.8	2.9	64.9	2.7
Rest	1.2	4.0	0.6	0.4	0.2	0.2	2.2	0.7	1.2	3.6	0.6	0.6	0.6	1.1	3.5	0.6	78.6

Fig. 5.15 Confusion matrix of classification performance across subject. The 17 motions include pronation (pro), supination (sup), flexion (flex), extension (ext), hand grasping (grasp), hand opening (open), thumb flexion (TF) and extension (TE), index finger flexion (IF) and extension (IE), middle finger flexion (MF) and extension (ME), ring finger flexion (RF) and extension (RE), little finger flexion (LF) and extension (LE), and rest state (rest).

5.6 Conclusions

In this chapter, a signal processing technique to classify 17 voluntary movements from EMG signals is proposed. The major novelty of this study is the use of a small set of low-cost EMG sensors (low sampling rate) to classify a reasonably large number of hand movements. Only six electrodes were used for EMG recording. In the proposed method, power spectrum densities are used as features and the motions are classified using artificial neural network. Online classification experiments were conducted on 12 participants to evaluate the validity of the proposed method. The results show that the proposed method is capable of achieving 42-83% overall accuracy (average of 63.8% across subjects). Statistical analysis results suggest that improvement in accuracy may be due to the fact that the user had gained more experience from the training on the previous day. Results also indicate that the accuracy drops significantly after one hour of continuous usage and re-training of the classifier is recommended. Based on the above results combined with the fact that users can promptly modify any incorrect classifications by looking at the actual output of the prosthetic hand, the proposed algorithm demonstrates the potential to classify 17 voluntary movements from 6 consumer grade EMG sensors. Furthermore, classifying 9 motions using this method could achieve 43%-92% accuracy (average of 72.9% across subjects). Based on this result, if the prosthetic hand is intended for a specific task, limiting the number of motions can significantly increase the performance and usability. Overall, the findings reported in this study have given us an idea of the extent of how well the current state-of-the-art classification scheme can perform with limited hardware. The discussions have also revealed the challenges towards developing a practical and multi-functional prosthesis. An extension to this study would be to raise the overall performance by improving the feature extraction algorithm as well as devising a training method in order to improve the accuracy.

6 Development of a Hybrid Brain Machine Interface Based on the Fusion of Electroencephalographic and Electromyographic Activities

Abstract: This chapter proposes a design of hybrid brain machine interface (HBMI) that combines brain and muscle signals intended to improve the controllability of the system. As a possible application of HBMI, we will assume that the proposed system will be used to control a prosthetic hand. The proposed system enables users to control the prosthetic hand using EMG signals. The user intention of ‘action’ and ‘rest’ are detected from EEG signals and the detection results are used to modify the control input for the prosthetic hands as well as reduce misclassification of EMG-based BMI system. Online experiments are conducted to evaluate the effectiveness of the proposed system. Results suggests that using EEG in parallel with EMG helps reduce erroneous classifications. The results also show that EEG can be used to modify the motion trajectories of the prosthetic hand. Based on these results, HBMI is effective for raising the controllability and usability of BMI systems. This work presents a foundation for further research that aims to develop a practical BMI system with consumer-grade acquisition device.

6.1 Introduction

Electroencephalograph (EEG) based brain machine interfaces (BMI) has the potential to provide users with highly intuitive control of external devices. Although there has been immense progress in the BMI technology over the last few years [159], in general, it is still difficult to decode the user's intention using non-invasive brain signals and the task becomes even more challenging when the brain signals are recorded by a consumer-grade device. The studies in chapters 3 and 4 have demonstrated that while it is feasible to use a consumer-grade EEG device for external device control, the number of commands (classes) are limited to 3 or 4 for steady state visual evoked potential (SSVEP) based BMI, and limited to 2 or 3 for motor imagery (MI) based BMI. Unless the system is intended for patients in the later stages of amyotrophic lateral sclerosis (ALS) whose only way of controlling a device is by using brain signals, the small number of functional commands makes it difficult to deploy the current BMI technology into real-life usage scenarios.

In contrast, using electromyographic (EMG) signals as a control input can provide the users with up to 17 types of commands (with rest state included), even with low-cost acquisition device as demonstrated in chapter 5. In addition, EMG offers a relatively faster interaction speed than EEG during real-time control and is therefore a more suitable candidate for external device control. However, as demonstrated in chapter 5, additional improvements could be made to reduce misclassifications in order to improve the usability of the system. It is also shown that accuracy decreases with prolonged usage due to factors like muscle fatigue.

Recently, as an approach to overcome the limitations and improve the usability of BMI systems, the concept of parallel usage of at least one BMI and at least one additional communication channel (e.g. another physiological signal or assistive input devices such as joysticks or switches) called hybrid BMI (HBMI) was suggested and developed [160]-[162]. The idea of an HBMI is very appealing because it can increase the possibility to provide a larger number of commands for control. Other benefits of HBMI include improved accuracy and information transfer rates. These benefits have been verified by previous studies [163]-[171].

For the purpose of developing a low-cost BMI system with a high level of usability and controllability, this is study proposes the concurrent use of EEG and EMG signals for HBMI systems. In our HBMI framework, EMG will be used as the primary control signal while EEG will be will be use as a secondary control signal to modify the trajectory and to reduce the misclassifications.

6.2 The Hybrid Machine Interface (HBMI)

As already mentioned, HBMI combines two or more types of BMI in an attempt to compensate for the shortcomings and utilize the advantages of each BMI system. In general, two systems can be combined sequentially or simultaneously as shown in Fig. 6.1. In a simultaneous HBMI, both systems are process in parallel and may play the same or different role to achieve a certain goal. In the case that two systems play the same role, the feature vectors from each system can be combined into one larger feature vector and fed into one classification algorithm, or the decisions made by each system can be fused together to make one final decision. On the other hand, both systems can play two different roles simultaneously to achieve one larger goal. For example, a 2-dimensional cursor control can be achieved by controlling the horizontal movements with motor imagery paradigm, and controlling the vertical movements with P300 paradigm [172].

Sequential HBMIs can be further categorized into sequential-switch or sequential-selector type HBMI. In sequential-switch HBMIs, the output of one system is used as the input of the other system. This approach is mostly used when the first system task is to indicate that the user does not intend to communicate or as a “brain switch” [160]. On the other hand, in a sequential-selector type HBMI, the first system can decide to choose a certain function as a selector, then the second system can control levels in a specified sequence [173].

In recent years, there has been more attention to HBMI systems. A list of existing HBMI systems and their features are summarized in Table 6.1. In this study, a simultaneous HBMI, combining EEG and EMG signals will be explored. The feasibility of the proposed system will be evaluated and discussed.

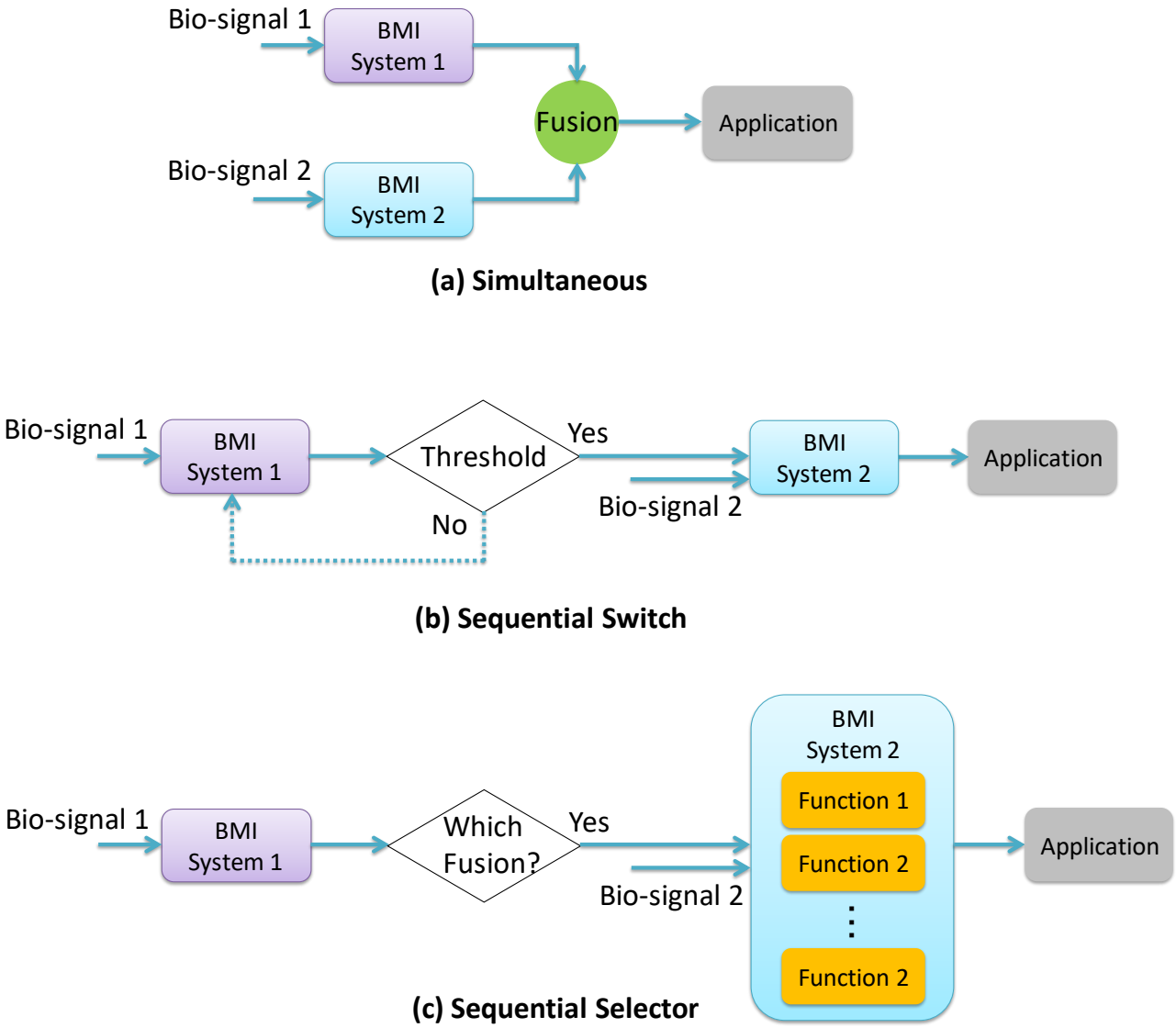

Fig. 6.1 A schematic diagram of sequential and simultaneous hybrid brain machine interface (HBMI) systems.

Table 6.1 A comparison of several different hybrid brain machine interface (HBMI) systems (adapted from [168])

Paper #	Type of Signal	Fusion Approach	Improvement
[169]	ERD, SSVEP	Simultaneous	Improve accuracy
[170]	ERD, SSVEP	Sequential	False positive rate was reduced
[163]	P300, SSVEP	Sequential	Improved information transfer rate
[171]	P300, ERD	Sequential	Expand control functions in virtual environment
[164]	ERD, EOG	Simultaneous	Improvement in classification accuracy, reduction in number of electrodes and training time
[165]	ERD, EOG	Sequential	Improvement in performance
[166]	EEG, EMG	Simultaneous	Improvement in performance
[167]	ERD, NIRS	Simultaneous	Improvement in classification accuracy and performance

6.3 Experimental Methods

6.3.1 EEG/EMG-based HBMI Architecture

The aim of this study is to explore the feasibility of a HBMI system that classifies hand/wrist movements from EMG signal which will be translated into operative commands for control of external devices. At the same time, the control input (control signal) for the external device will be modified and the misclassifications will be reduced using EEG signals. In this study, we will apply the HBMI system to prosthetic hand control as an example. The concept of the proposed HBMI system is shown in Fig. 6.2.

According to Fig. 6.2, the proposed HBMI system consists of two subsystems; the EEG BMI system and the EMG BMI system. The role of the EMG BMI system is to classify hand movements from EMG signal while EEG BMI system is used to classify two mental states, i.e. the intention to perform hand movements and rest state from EEG signals. The classification output of the EEG BMI subsystem is used to modify the classification output of the EMG BMI system before it is translated into operative commands for controlling external devices. More specifically, if the EEG BMI system decides that the user is in a relaxed state, then the classification signal of the EMG BMI system is modified to output a rest (no-motion) command as the final decision. In this way, erroneous classification caused by unintentional movement of the hand, subtle movements of muscles, changes in muscle condition etc. can be reduced to enhance the controllability and the usability of the control system.

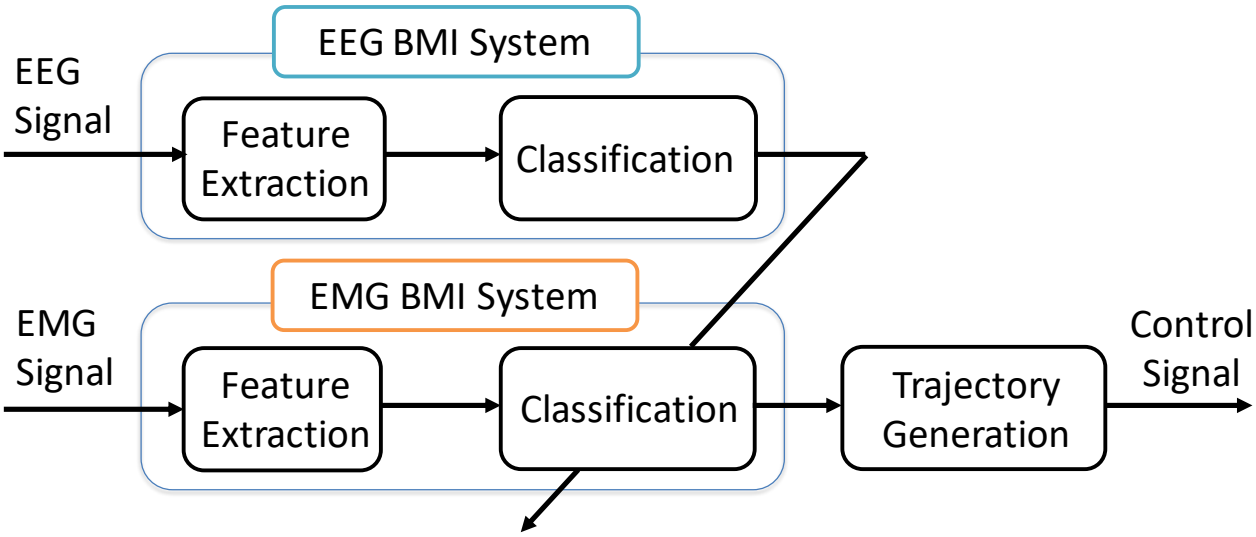

Fig. 6.2 A schematic diagram of the concept of the proposed system.

The design of HBMI system is based on the physiological function of brain wave rhythms. It is well known that the amplitude of alpha rhythms (8-13 Hz) attenuates during mental activities such as thinking and execution of movement [36]. Based on this phenomenon, we hypothesize that alpha activities would increase during rest/unintended hand movements and decrease during intended movements. As such, distinguishing between intended movements and unintended movements should be possible by observing the changes in alpha activities.

In this study, EMG is recorded using the Myo armband (manufactured by Thalmic Labs Inc.). The Myo armband is a consumer-grade EMG acquisition device consisting of a circular array of 8 electrodes (Fig. 6.3). The EMG signals are sampled at 200Hz and transferred to the PC wirelessly which help raise the level of usability. The EEG is measured using Emotiv EPOC+ headset which has a sampling frequency 128 Hz. In this study, only 2 electrodes over the occipital lobe (O1 and O2) are used (Fig. 6.4). The software development environment is MATLAB/Simulink®. The proposed algorithm is executed after being built by Simulink real-time workshop.

Fig. 6.3 Myo armband. 8 electrodes for EMG recording are arranged in a circular array. The sensor is also equipped with a 9-axis IMU. The EMG data is acquired at 200Hz while the IMU data is acquired at 50Hz.

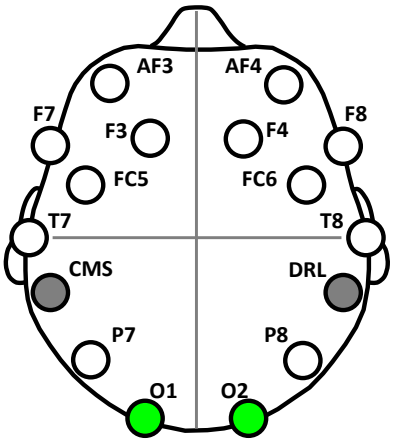

Fig. 6.4 Location of electrodes. Only 2 electrodes located on the occipital lobe are used in this study.

6.3.2 Task Design

In this experiment, the subjects are asked to sit comfortably and perform 5 hand motions (including a rest state) according to the cues. The motions include flexion/extension of the wrist, and grasping/opening of the hand. The experiment protocol is shown in Fig. 6.5. During the execution of the task, EMG signals and EEG signals are recorded simultaneously. To simulate unintended hand movement, the same hand motion is repeated again, but this time, in a relaxed state.

The experiment is divided into two parts: offline training and online testing. In the first part, training data are acquired to train the classifier. The second part involves online classification in order to evaluate the validity of the proposed system.

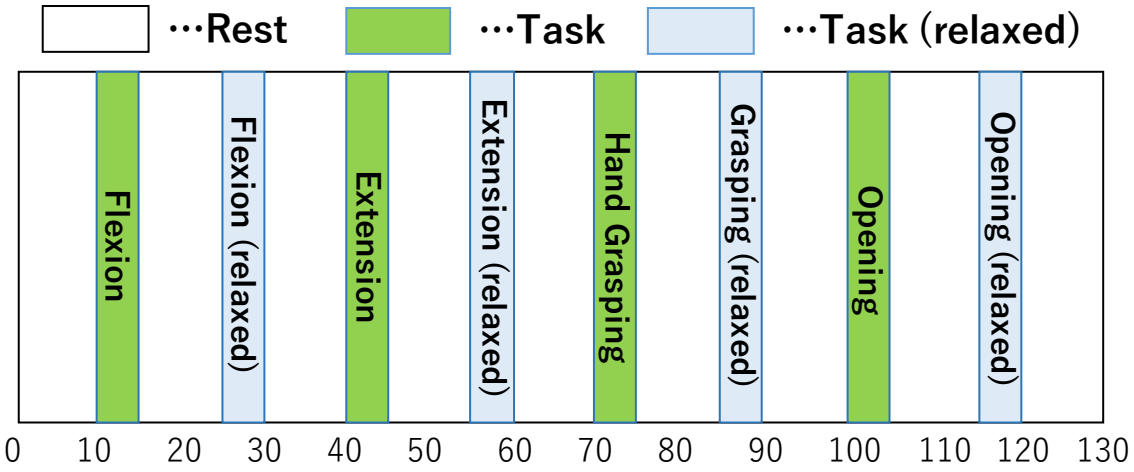

Fig. 6.5 Experimental protocol of a trial. A total of 5 hand motions are executed in this experiment.

6.3.3 Preprocessing of EEG and EMG Signals

Using the same preprocessing procedure as chapter 3, first, the DC offset of the EEG signal is removed by demeaning, i.e. subtracting the average amplitude of the raw EEG signal during the first 5 seconds from the whole signal. Next, a second order bandpass filter is applied to the EEG signal to emphasize the 10Hz frequency component. Next, the bandpass filtered EEG signal is full-wave rectified. Lastly, a second order lowpass filter is applied to the EEG signals.

In the case with EMG signals, first, resampling of the data so that the sampling frequency of the EMG signals is the same as the sampling frequency of EEG signals (128Hz). This is done by interpolating the data by a factor of 16 followed by decimating the data by a factor of 25. After the data has been resampled, demeaning is applied to remove the DC offset.

Fig. 6.6 shows an example of preprocessed EMG and EEG signals (O1 and O2 electrode only). According to this figure, muscle activity can be observed even when hand motions are performed in a relaxed manner. Since less force is used to perform the movements, the amplitude of EMG signals is smaller compared to that of normal hand motion tasks. In addition, it is also observable that alpha activity of both O1 and O2 decreases during intended hand motions. On the other hand, an increase in alpha activity can be seen when the user performs the hand motions in a relaxed. Furthermore, according to Fig. 6.7, statistical differences in alpha activity have been confirmed. Thus, this confirms that our hypothesis is correct and suggests that discrimination between intentional and unintentional movement from alpha activity is possible.

6.4 Classification of Hand Motions

6.4.1 Feature Extraction of EEG signals

In this study, we attempt to classify two mental states, i.e. the intent to move and rest state, from EEG signals. To do so, first, down-sampling of preprocessed EEG signal of both O1 and O2 channels by a factor of 8 is performed. Next, 2-dimensional (2 channels) feature vectors are constructed from the down-sampled signal. Then, the feature vectors are normalized so that the feature values range from -1 to 1. Lastly, the training data are fed into the ANN to be trained. Here, the EEG signals during hand movements belong to the ‘movement’ class and EEG signal during rest belong to the ‘rest’ class.

6.4.2 Feature Extraction of EMG signals

In order to classify hand motions, this study adopts the same algorithm proposed in chapter 5. First, FFT is applied to the preprocessed EMG signals to extract the power spectrum densities. Next, a feature vector is formed based on the extracted points. These feature vectors are then normalized and fed into the ANN to be classified.

6.4.3 Postprocessing of classification results

As depicted in Fig. 6.2, the output results of EEG BMI system are used to modify the classification outputs of the EMG BMI system. The modifications are done in a way such that when the user is in a relaxed state, no motion commands will be sent to the external device (e.g. prosthetic hand). To do so, we focus on the output result of EEG BMI system. If the value of the output neuron belonging to the rest class is higher than the threshold value T, then the classification output of EMG BMI system is labeled as ‘rest state’. More specifically, the output neuron belonging to the rest class

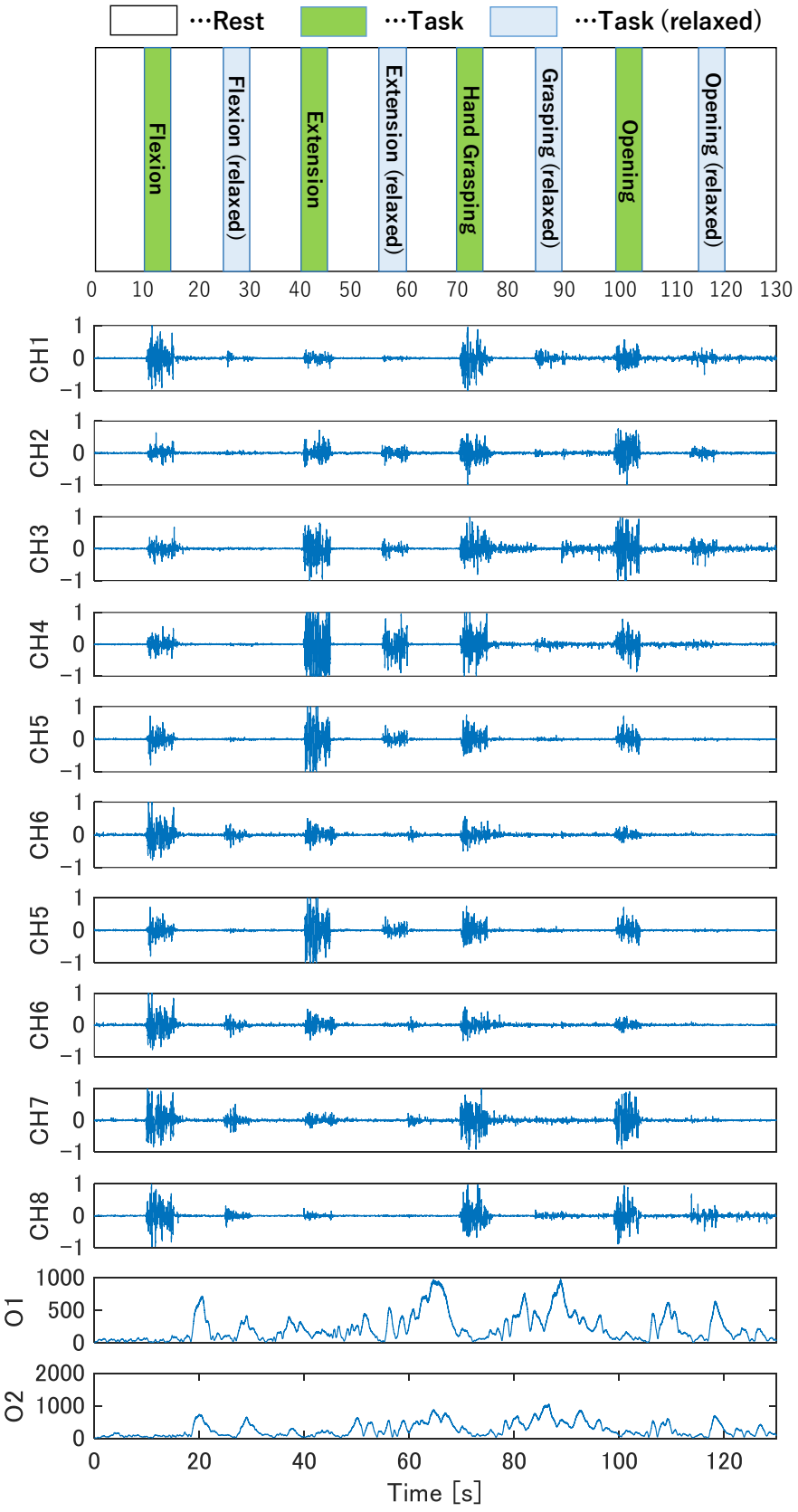

Fig. 6.6 An example of preprocessed EMG and EEG signals. The first 8 rows show the time response of preprocessed EMG signal. The last 2 rows show the time response of preprocessed EEG signal of O1 and O2 electrodes.

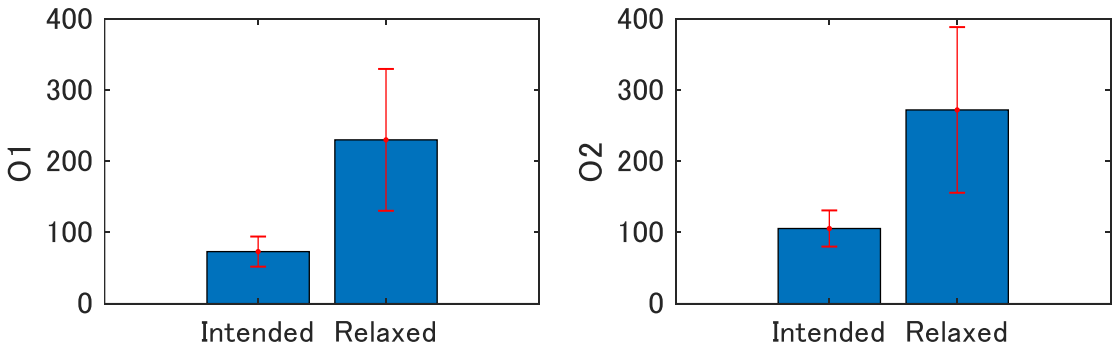

Fig. 6.7 Alpha activity (10Hz) during intended hand motion and relaxed hand motion

will take the value of 1, while the output neuron of all other hand classes will take the value of 0. An example of this procedure is illustrated in Fig. 6.8. The effect of different threshold values on system performance is investigated and discussed in the next section.

6.5 Experiment

6.5.1 Participants

In this study, the experiments were carried out with the cooperation of one able-bodied male participant. The entire protocol and aims of the study are fully explained to him before the experiment, and he signed the written informed consent. All of the experiments are conducted with the approval from Tokyo Denki University Human Bioethics Committee. Previously, this participant has experienced with both EMG and EEG BMI experiments.

6.5.2 Results

Fig. 6.8 shows an example of classification result. As shown in this figure, the misclassifications of EMG BMI system are corrected. Comparing Fig. 6.8 (b) to Fig. 6.8 (c), it is clear that misclassifications has been greatly reduced.

Fig. 6.9 shows the FPR of online classification when only EMG signal are used (EMG only) and when both EMG and EEG are used (EMG+EEG). According to this figure, FPR of hand motion is lower in HBMI for all threshold value except for $T = 1.0$. This shows that the proposed system is functional and effective in reducing FPR. Furthermore, ROC curve in Fig. 6.10 shows that there is a tradeoff relationship between TPR and FPR. By using this tradeoff, the user can adjust the responsiveness and the accuracy to suit the target application.

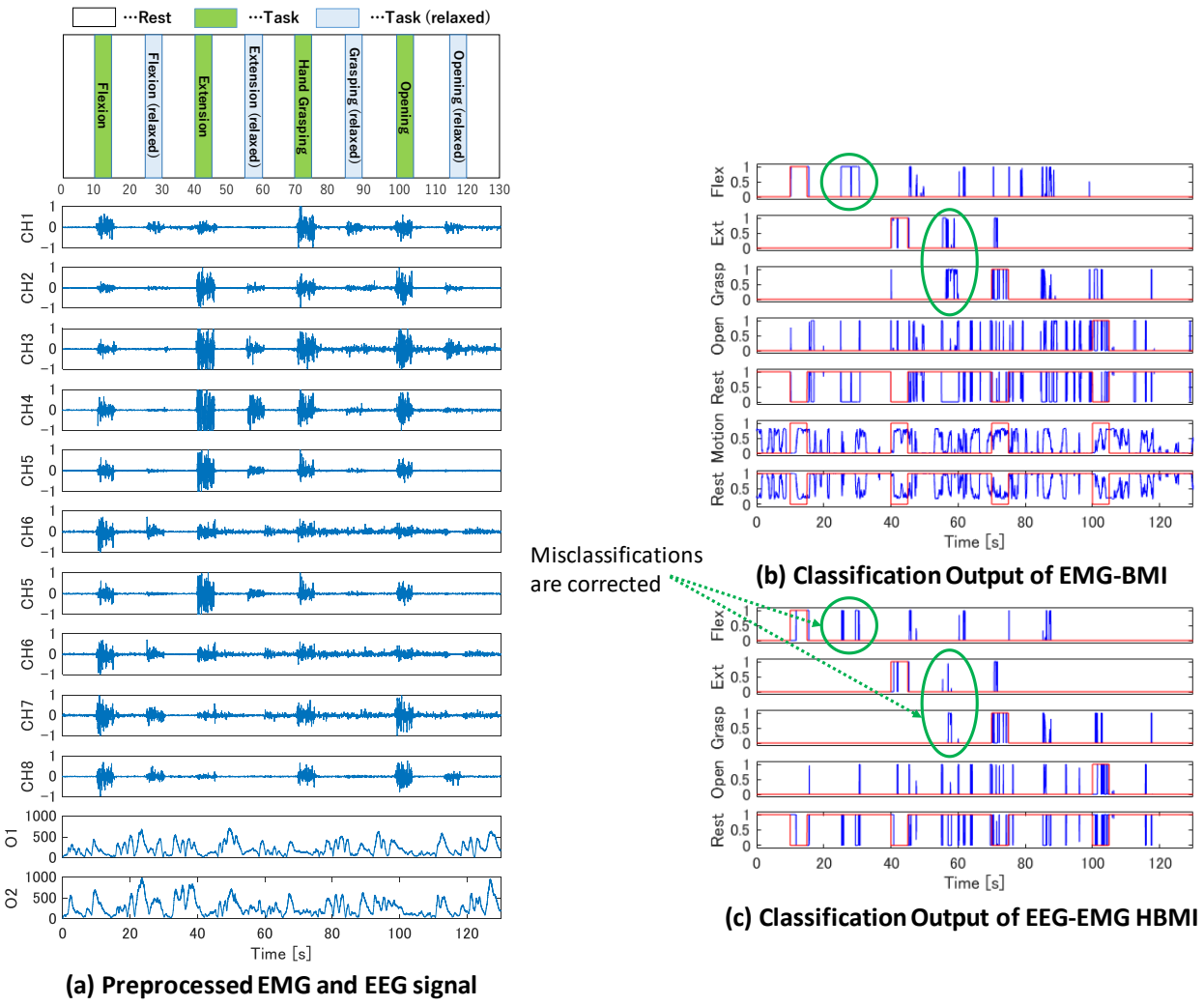

Fig. 6.8 An example of classification result ($T = 0.8$).

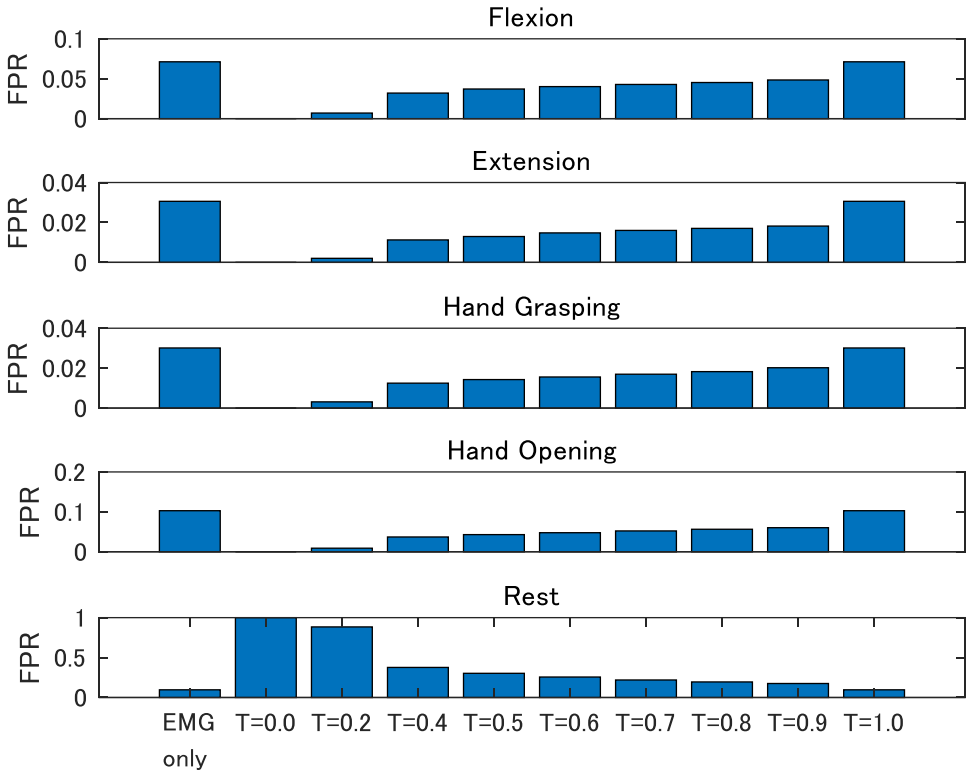

Fig. 6.9　False postive rates of each motion.

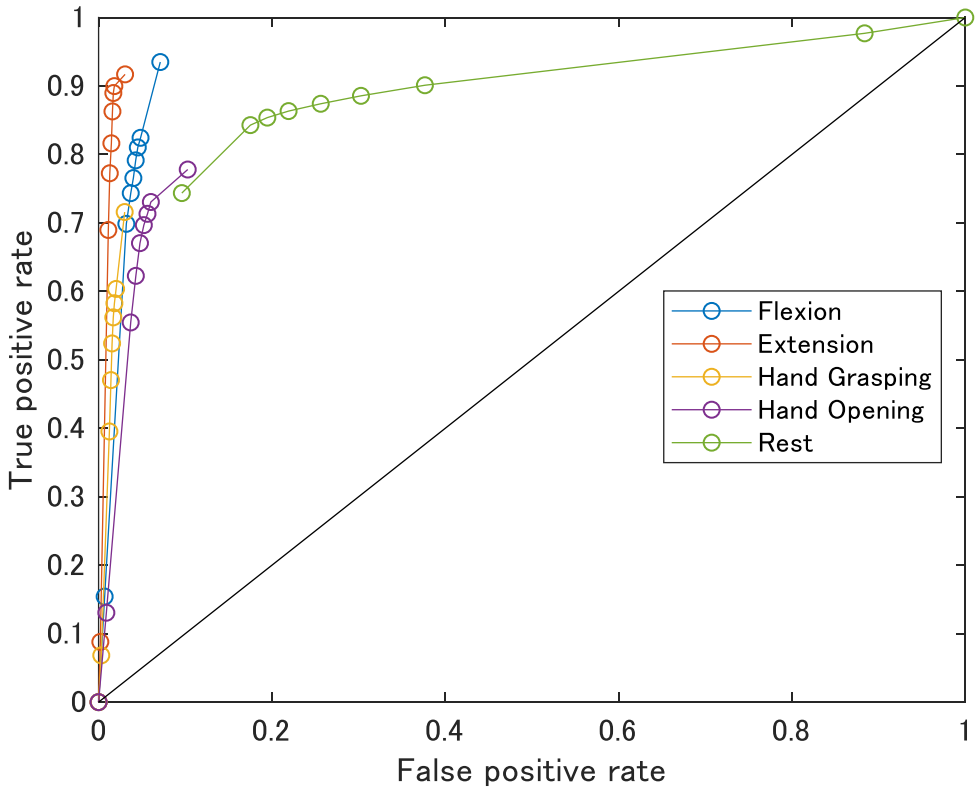

Fig. 6.10　ROC curve of the proposed HBMI system.

6.6 Conclusion

In this chapter, a hybrid brain machine interface based on the fusion of electroencephalographic and electromyographic activities is proposed. In this system, external devices are controlled by the EMG-based BMI system. The EEG-based BMI helps reduce the misclassifications and also modify the control input for the device. Online classifications were conducted to evaluate the validity of the proposed HBMI system. Results show that concurrent use of EMG and EEG system helps reduce the number of misclassifications. Based on the above results, the hybridization of EMG and EEG signals for control of external device can provide better controllability of external devices, thus, enhancing the level of usability of consumer-grade acquisition device. An extension to this study would be explore other fusion techniques.

7 Conclusion

In this dissertation, the designs of 4 types of brain machine interface (BMI) systems has been proposed. They include a design of a self-paced steady state visually evoked potential (SSVEP) based BMI system, a motor imagery based BMI system for classification of three mental states, electromyography (EMG) based BMI system for control of myoelectric prosthetic hand, and a hybrid BMI (HBMI) system that fuses electroencephalography (EEG) with EMG to provide enhanced controllability and usability. Experiments are designed and conducted to evaluate the feasibility of each BMI system. The results of each system are summarized as follows:

In the design of the a 3-class self-paced SSVEP-based BMI, two low-cost EEG sensors are used to capture the SSVEP responses. Multiple second order bandpass filters are employed to extract SSVEP features and the type of response is classified using artificial neural network (ANN). Experimental results showed that the proposed design is capable of achieving an average accuracy of up to 93% and a mean information transfer rate of up to 4.2 bits/min. Furthermore, tradeoff between the number of commands and accuracy is also presented. This tradeoff allows the user to adjust the responsiveness and the accuracy to suit their preference or target application. Overall, the results of this study have demonstrated that a consumer-grade EEG device can serve as a modality in SSVEP-based BMI for device control applications. The limitation of this design is the need to constantly gaze at the stimuli and may cause severe fatigue after prolonged use.

In the design of a 3-class motor imagery based BMI, 8 low-cost EEG sensors are used to capture the EEG signals. Power spectrum densities are extracted from EEG signals during mental tasks and fed to the ANN in order to detect the user intention. Experiment results showed that the proposed method is capable of achieving an overall true positive rate of up to 67% with 15 minutes of training time by a first time BMI user. Furthermore, a tradeoff between true positive rate and false positive rate is also presented. Again, based on this tradeoff, the user can adjust the responsiveness and the accuracy to suit their preference or target application. Lastly, a hamming window size of 64 samples is found to be optimal for achieving real-time control when performing spectral analysis. In this design, although the need to constantly gaze at the stimuli is alleviated, the number of commands are limited to 2-3 for achieving acceptable accuracy with low-cost acquisition device.

In the design of an EMG-based BMI, 6 consumer-grade EMG electrodes are used to capture muscle activity during arm/hand movements. Power spectrum densities are extracted from EMG signals and fed to the ANN in order to detect the hand motions. Experimental results showed that the proposed algorithm achieves an overall correct classification rate of up to 83%; thus, demonstrating the potential to classify 17 movements from 6 EMG sensors. Furthermore; classifying 9 motions using this method could achieve an accuracy of up to 92%. These results show that if the prosthetic hand is intended for a specific task; limiting the number of motions can significantly increase the performance and usability. Compared to EEG, EMG is easier to analyze and more reliable as an input source. Despite these advantages, more improvements in responsiveness and accuracy is still needed to raise the level of usability.

In the design of a hybrid BMI (HBMI) system, EMG and EEG are fused together in an attempt to raise the controllability of the system. EMG is used to control the prosthetic hand while EEG is used to reduce misclassifications. Results showed that using EEG in parallel with EMG helps reduce erroneous classifications. The results also show that EEG can be used to modify the motion trajectories of the prosthetic hand. Based on these results, HBMI is effective for raising the controllability and usability of BMI systems.

As a future work, more efforts can be put in to improve the efficiency of feature extraction and classification algorithms. Investigations on the performance of ensemble classifier such as AdaBoost or random forest could also be conducted. Also, design and implementation of a control strategy that allows dynamic control of the prosthetic hand could help realize a more natural hand movement, similar to that of the human hand. Finally, additional experiments using the prosthetic hand to execute everyday tasks could be performed to evaluate the total performance of the whole system.

Overall, this work has provided a foundation for further research that aims to develop a practical BMI system with consumer-grade acquisition device. Our results are supportive that consumer-grade acquisition device can serve as a modality in device control, and their usability can be further enhanced by combining multiple BMI systems together.

References

[1] J. R. Wolpaw, N. Birbaumer, D. J. McFarland, G. Pfurtscheller, T. M. Vaughan, "Brain–computer interfaces for communication and control," *Clinical Neurophysiology*, vol. 113, issue 6, pp. 767-791, June 2002.

[2] J. J. Daly and J. R. Wolpaw, "Brain–computer interfaces in neurological rehabilitation," *The Lancet Neurology*, vol. 7, issue 11, pp. 1032-1043, November 2008.

[3] A. B. Schwartz, X. T. Cui, D. J. Weber, "Brain-Controlled Interfaces: Movement Restoration with Neural Prosthetics," *Neuron*, vol. 52, issue 1, pp. 205-220, 5 October 2006.

[4] L. R. Hochberg, D. Bacher, B. Jarosiewicz, N. Y. Masse, J. D. Simeral, J. Vogel, S. Haddadin, J. Liu, S. S. Cash, P. van der Smagt and J. P. Donoghue, "Reach and grasp by people with tetraplegia using a neurally controlled robotic arm," *Nature*, vol. 485, pp.372-375, 17 May 2012.

[5] J. D. Simeral1, S-P Kim, M. J. Black, J. P. Donoghue and L. R. Hochberg, "Neural control of cursor trajectory and click by a human with tetraplegia 1000 days after implant of an intracortical microelectrode array," *Journal of Neural Engineering*, vol. 8, no. 2, 24 March 2011.

[6] A. B. Ajiboye, J. D. Simeral, J. P. Donoghue, L. R. Hochberg and R. F. Kirsch, "Prediction of Imagined Single-Joint Movements in a Person With High-Level Tetraplegia," *IEEE Transactions on Biomedical Engineering*, vol.59, no.10, pp. 2755-2765, October 2012.

[7] J. L. Collinger, B. Wodlinger, J. E. Downey, W. Wang, E. C. Tyler-Kabara, D. J. Weber, A. JC McMorland, M. Velliste, M. L. Boninger and A. B. Schwartz, "High-performance neuroprosthetic control by an individual with tetraplegia," *The Lancet*, vol. 381, issue 9866, pp. 557-564, 16 February 2013

[8] Y. Chae, J. Jeong and S. Jo, "Toward Brain-Actuated Humanoid Robots: Asynchronous Direct Control using an EEG-Based BCI," *IEEE Transactions on Robotics*, vol. 28, no. 5, October 2012.

[9] K. Tanaka, K. Matsunaga and H. O. Wang, "Electroencephalogram-Based Control of an Electric Wheelchair," *IEEE Transactions on Robotics*, vol. 21, no. 4, pp. 762-766, August 2005.

[10] F. Galan, M. Nuttin, E. Lew, P. W. Ferrez, G. Vanacker and J. del R. Millan, "A brain-actuated wheelchair: Asynchronous and non-invasive Brain-computer interfaces for continuous control of robots," *Clinical Neurophysiology*, vol. 119, issue 9, pp. 2159-2169, September 2008.

[11] J. Long, Y. Li, H. Wang, T. Yu, J. Pan and F. Li, "A Hybrid Brain Computer Interface to Control the Direction and Speed of a Simulated or Real Wheelchair," *IEEE Transactions on Neural Systems and Rehabilitation Engineering*, vol. 20, no. 5, pp. 720-729, September 2012.

[12] K. Choi and A. Cichocki, "Control of a Wheelchair by Motor Imagery in Real Time," *Proc. of the 9th International Conference on Intelligent Data Engineering and Automated Learning*, pp. 330-337, Springer, 2008.

[13] K. LaFleur, K. Cassady, A. Doud, K. Shades, E. Rogin and B. He, "Quadcopter control in three-dimensional space using a noninvasive motor imagery-based brain–computer interface," *Journal of Neural Engineering*, vol.10, no. 4, 4 June 2013.

[14] F. Karmali, M. Polak and A. Kostov, "Environmental Control by a Brain-Computer Interface," *Proc. of the 22nd Annual EMBS International Conference*, vol.4, pp. 2990-2996, 2000.

[15] G. Edlinger, C. Holzner, C. Guger, C. Groenegress and M. Slater, "Brain-Computer Interfaces for Goal orientated Control of a Virtual Smart Home Environment," *Proceedings of the 4th International IEEE EMBS Conference on Neural Engineering*, pp. 463-465, 2009.

[16] C. Holzner, C. Guger, G. Edlinger, C. Grönegress and M. Slater, "Virtual Smart Home Controlled By Thoughts," *2009 18th IEEE International Workshops on Enabling Technologies: Infrastructures for Collaborative Enterprises*, pp. 236-239, 2009.

[17] W. T. Lee, H. Nisar, A. S. Malik and K. H. Yeap, "A Brain Computer Interface for Smart Home Control," *2013 IEEE 17th International Symposium on Consumer Electronics (ISCE)*, pp. 35-36, 2013.

[18] K. Oum, H. Ayaz, P. A. Shewokis, P. Diefenbach, "MindTactics: A Brain Computer Interface Gaming Platform," *2010 2nd International IEEE Consumer Electronics Society's Games Innovations Conference*, pp. 1-5, 2010.

[19] N. Chumerin, N. V. Manyakov, M. van Vliet, A. Robben, A. Combaz and M. M. Van Hulle, "Steady-State Visual Evoked Potential-Based Computer Gaming on a Consumer-Grade EEG Device," *IEEE Transactions on Computational Intelligence and AI in Games*, vol. 5, no. 2, pp. 100-110, June 2013.

[20] B. van de Laar, H. Gürkök, D. Plass-Oude Bos, M. Poel and A. Nijholt, "Experiencing BCI Control in a Popular Computer Game," *IEEE Transactions on Computational Intelligence and AI in Games*, vol. 5, no. 2, pp. 176-184, June 2013.

[21] D. Marshall, D. Coyle, S. Wilson and M. Callaghan, "Games, Gameplay, and BCI: The State of the Art," *IEEE Transactions on Computational Intelligence and AI in Games*, vol. 5, no. 2, pp. 82-99, June 2013.

[22] M. M. Moore, "Real-World Applications for Brain–Computer Interface Technology", *IEEE Transactions on Neural Systems and Rehabilitation Engineering*, vol.11, no. 2, June 2003.

[23] R. Maskeliunas, R. Damasevicius, I. Martisius and M. Vasiljevas, “Consumer-grade EEG devices: are they usable for control tasks?,” *PeerJ*, 4, e1746, 2016.

[24] A. Nijholt, D. Tan, G. Pfurtscheller, C. Brunner, J. del R. Millán, B. Allison, B. Graimann, F. Popescu, B. Blankertz and K.R. Müller, “Brain-Computer Interfacing for Intelligent Systems,” *IEEE Intelligent Systems*, vol. 23, no. 3, May-June 2008.

[25] S. Fazli, M. Danóczy, F. Popescu, B. Blankertz, K.R. Müller, “Using Rest Class and Control Paradigms for Brain Computer Interfacing”, In: Cabestany J., Sandoval F., Prieto A., Corchado J.M. (eds) Bio-Inspired Systems: Computational and Ambient Intelligence. IWANN 2009. *Lecture Notes in Computer Science*, vol 5517. Springer, Berlin, Heidelberg.

[26] B. Blankertz, K.R. Müller, D. Krusienski, G. Schalk, J. R. Wolpaw, A. Schlögl, G. Pfurtscheller, J. del R. Millán, M. Schröder, N. Birbaumer, “The BCI Competition III: Validating Alternative Approaches to Actual BCI Problems,” *IEEE Transactions on Neural Systems and Rehabilitation Engineering*, vol. 14, no. 2, June 2006

[27] G. Townsend, B. Graimann, and G. Pfurtscheller, “Continuous EEG classification during motor imagery-simulation of an asynchronous BCI,” *IEEE Transactions on Neural Systems and Rehabilitation Engineering*, vol. 12, no. 2, pp. 258-265, June 2004.

[28] P. Batres-Mendoza, C. R. Montoro-Sanjose, E. I. Guerra-Hernandez, D. L. Almanza-Ojeda, H. Rostro-Gonzalez, R. J. Romero-Troncoso and M. A. Ibarra-Manzano, “Quaternion-Based Signal Analysis for Motor Imagery Classification from Electroencephalographic Signals,” *Sensors*, vol.16, no. 3, 2016.

[29] H. Mo, Y. Zhao, “Motor Imagery Electroencephalograph Classification Based on Optimized Support Vector Machine by Magnetic Bacteria Optimization Algorithm,” In: Tan Y., Shi Y., Buarque F., Gelbukh A., Das S., Engelbrecht A. (eds) *Advances in Swarm and Computational Intelligence*. ICSI 2015. Lecture Notes in Computer Science, vol. 9140, pp 415-424, Springer, Cham, 2015

[30] A. Buttfield, P. W. Ferrez, J. del R. Millan, “Towards a robust BCI: error potentials and online learning,” *IEEE Transactions on Neural Systems and Rehabilitation Engineering*, vol. 14, no. 2, pp. 164-168, June 2006

[31] G. Santhanam, S. I. Ryu, B. M. Yu, A. Afshar and K. V. Shenoy, “A high-performance brain-computer interface,” *Nature*, vol. 442, pp. 195-198, 2006.

[32] M. A. L. Nicolelis, “Actions from thoughts,” *Nature*, vol. 409, pp. 403-407, 2001.

[33] D. M. Taylor, S. I. Tillery, A. B. Schwartz, “Direct cortical control of 3D neuroprosthetic devices,” *Science*, vol. 296, no. 5574, pp. 1829-1832, 2002.

[34] M. van Gerven, J. Farquhar, R. Schaefer, R. Vlek, J. Geuze, A. Nijholt, N. Ramsey, P. Haselager, L. Vuurpijl, S. Gielen and P. Desain, “The brain-computer interface cycle,” *Journal of Neural*

Engineering, vol. 6, no. 4, 2009.

[35] R. P. N. Rao and R. Scherer, "Brain-Computer Interfacing [In the Spotlight]," *IEEE Signal Processing Magazine*, vol. 27, issue 4, pp. 152-150, July 2010.

[36] L. F. Nicolas-Alonso and J. Gomez-Gil, "Brain Computer Interfaces, a Review," *Sensors*, vol. 12(2), pp. 1211-1279, July 2012.

[37] B. Kleber and N. Birbaumer, "Direct brain communication: neuroelectric and metabolic approaches at Tübingen," *Cognitive Processing*, vol. 6, issue 1, pp. 65-74, 2005.

[38] D. J. Krusienski, G. Schalk, D. J. McFarland and J. R. Wolpaw, "A μ-Rhythm Matched Filter for Continuous Control of a Brain-Computer Interface," *IEEE Transactions on Biomedical Engineering*, vol. 54, issue 2, pp. 273-280, 2007.

[39] T. Hinterberger, S. Schmidt, N. Neumann, J. Mellinger, B. Blankertz, G. Curio and N. Birbaumer, "Brain-computer communication and slow cortical potentials," *IEEE Transactions on Biomedical Engineering*, vol. 51, issue 6, pp. 1011-1018, 2004.

[40] G. Pfurtscheller, C. Neuper, G. R. Müller, B. Obermaier, G. Krausz, A. Schlögl, R. Scherer, B. Graimann, C. Keinrath, D. Skliris, M. Wörtz, G. Supp and C. Schrank, "Graz-BCI: state of the art and clinical applications," *IEEE Transactions on Neural Systems and Rehabilitation Engineering*, vol. 11, issue 2, pp. 1-4, 2003.

[41] S. Baillet, J. C. Mosher and R. M. Leahy, "Electromagnetic brain mapping," *IEEE Signal Processing Magazine*, vol. 18, issue 6, pp. 14-30, November 2001.

[42] S. Laureys, M. Boly and G. Tononi, "Functional Neuroimaging," in *The Neurology of Consciousness: Cognitive Neuroscience and Neuropathology*, S. Laureys and G. Tononi, Eds. New York, NY, USA: Academic Press, 2009, pp. 31-42.

[43] D. Regan, *Human Brain Electrophysiology: Evoked Potentials and Evoked Magnetic Fields in Science and Medicine*, New York, NY, USA: Elsevier, 1989.

[44] Y. Wang, R. Wang, X. Gao, B. Hong and S. Gao, "A practical VEP-based brain-computer interface," *IEEE Transactions on Neural Systems and Rehabilitation Engineering*, vol. 14, issue 2, pp. 234-240, June 2006.

[45] C. S. Herrmann, "Human EEG responses to 1-100 Hz flicker: resonance phenomena in visual cortex and their potential correlation to cognitive phenomena," *Experimental Brain Research.*, 137(3-4), pp. 346-353, 2001.

[46] J. Yin, D. Jiang and J. Hu, "Design and application of brain-computer interface web browser based on VEP," *2009 International Conference on Future BioMedical Information Engineering*, pp. 77-80, 2009.

[47] D. Zhu, J. Bieger, G. G. Molina and R. M. Aarts, "A Survey of Stimulation Methods Used in SSVEP-Based BCIs," *Computational Intelligence and Neuroscience*, vol. 2010, 2010.

[48] P. L. Lee, J. C. Hsiehc, C. H. Wua, K. K. Shyua and Y. T. Wu, "Brain computer interface using flash onset and offset visual evoked potentials," *Clinical Neurophysiology*, vol. 119, issue 3, pp. 605-616, March 2008.

[49] I. Volosyak, "SSVEP-based Bremen-BCI interface--boosting information transfer rates," *Journal of Neural Engineering*, vol. 8, no. 3, 2011.

[50] B. Z. Allison, D. J. McFarland, G. Schalk, S. D. Zheng, M. M. Jackson and J. R. Wolpaw, "Towards an independent brain–computer interface using steady state visual evoked potentials," *Clinical Neurophysiology*, vol. 119, issue. 2, pp. 399-408, February 2008.

[51] D. Zhang, A. Maye, X. Gao, B. Hong, A. K Engel and S. Gao, "An independent brain–computer interface using covert non-spatial visual selective attention," *Journal of Neural Engineering*, vol. 7, no. 1, 2010.

[52] N. Birbaumer, T. Elbert, A. G. Canavan and B. Rockstroh, "Slow potentials of the cerebral cortex and behavior," *Physiological Reviews*, vol. 70, no. 1, pp. 1-41, 1990.

[53] A. Kübler, B. Kotchoubey, T. Hinterberger, N. Ghanayim, J. Perelmouter, M. Schauer, C. Fritsch, E. Taub and N. Birbaumer, "The thought translation device: a neurophysiological approach to communication in total motor paralysis," *Exp Brain Res.*, 124(2), pp. 223-232, 1999.

[54] N. Birbaumer, T. Hinterberger, A. Kübler and N. Neumann, "The thought-translation device (TTD): Neurobehavioral mechanisms and clinical outcome," *IEEE Transactions on Neural Systems and Rehabilitation Engineering*, vol. 11, issue 2, pp. 120-123, June 2003.

[55] I. H. Iversen, N. Ghanayim, A. Kübler, N. Neumann, N. Birbaumer, J. Kaiser, "A brain-computer interface tool to assess cognitive functions in completely paralyzed patients with amyotrophic lateral sclerosis," *Clinical Neurophysiology*, vol. 119, issue 10, pp. 2214-2223, October 2008.

[56] L. A. Farwell, E. Donchin, "Talking off the top of your head: toward a mental prosthesis utilizing event-related brain potentials," *Electroencephalography and Clinical Neurophysiology*, 70(6), pp. 510-523, December 1988.

[57] E. Donchin and D. B. Smith, "The contingent negative variation and the late positive wave of the average evoked potential," *Electroencephalography and Clinical Neurophysiology*, 29(2), pp. 201-203, August 1970.

[58] J. Polich, P. C. Ellerson and J. Cohen, "P300, stimulus intensity, modality, and probability," *International Journal of Psychophysiology*, 23(1-2), pp. 55-62, 1996.

[59] D. Ravden and J. Polich, "On P300 measurement stability: habituation, intra-trial block variation, and ultradian rhythms," *Biological Psychology*, vol. 51, issue 1, pp. 59-76, October 1999.

[60] N. Birbaumer, N. Ghanayim, T. Hinterberger, I. Iversen, B. Kotchoubey, A. Kubler, J. Perelmouter, E. Taub and H. Flor, "A spelling device for the paralysed," *Nature*, vol. 398, pp. 297-298, March 1999.

[61] E. M. Mugler, C. A. Ruf, S. Halder, M. Bensch and A. Kubler, "Design and Implementation of a P300-Based Brain-Computer Interface for Controlling an Internet Browser," *IEEE Transactions on Neural Systems and Rehabilitation Engineering*, vol. 18, issue 6, pp. 599-609, December 2010.

[62] A. Furdea, S. Halder, D. J. Krusienski, D. Bross, F. Nijboer, N. Birbaumer and A. Kübler, "An auditory oddball (P300) spelling system for brain-computer interfaces," *Psychophysiology*, vol. 46, issue 3, pp. 617-625, May 2009.

[63] B. Rivet, A. Souloumiac, V. Attina and G. Gibert, "xDAWN Algorithm to Enhance Evoked Potentials: Application to Brain–Computer Interface," *IEEE Transactions on Biomedical Engineering*, vol. 56, issue 8, pp. 2035-2043, August 2009.

[64] A. Rakotomamonjy and V. Guigue, "BCI Competition III: Dataset II- Ensemble of SVMs for BCI P300 Speller," *IEEE Transactions on Biomedical Engineering*, vol. 55, issue 3, pp. 1147-1154, March 2008.

[65] G. Pfurtschellera and F. H. Lopes da Silva, "Event-related EEG/MEG synchronization and desynchronization: basic principles," *Clinical Neurophysiology*, vol. 110, issue 11, pp. 1842-1857, November 1999.

[66] M. Jeannerod, "Mental imagery in the motor context," *Neuropsychologia*, vol. 33, issue 11, pp. 1419-1432, November 1995.

[67] G. Pfurtscheller, C. Neuper, D. Flotzinger and M. Pregenzer, "EEG-based discrimination between imagination of right and left hand movement," *Electroencephalography and Clinical Neurophysiology*, 103(6), pp. 642-651, December 1997.

[68] G. Pfurtscheller and C. Neuper, "Motor imagery and direct brain-computer communication," *Proceedings of the IEEE*, vol. 89, issue 7, pp. 1123-1134, July 2001.

[69] B. Blankertz, C. Sannelli, S. Halder, E. M. Hammer, A. Kübler, K.-R. Müller, G. Curio and T. Dickhaus, "Neurophysiological predictor of SMR-based BCI performance," *NeuroImage*, vol. 51, issue 4, pp. 1303-1309, July 2010.

[70] J. R. Wolpaw, D. J. McFarland and T. M. Vaughan, "Brain–Computer Interface Research at the Wadsworth Center," *IEEE Transactions on Rehabilitation Engineering*, vol. 8, issue 2, pp. 222-226, June 2000.

[71] B. Blankertz, F. Losch, M. Krauledat, G. Dornhege, G. Curio and K.R. Müller, "The Berlin Brain--Computer Interface: Accurate Performance From First-Session in BCI-Naïve Subjects," *IEEE Transactions on Biomedical Engineering*, vol. 55, issue 10, pp. 2452-2462, October 2008.

[72] O. Bai, V. Rathi, P. Lin, D. Huang, H. Battapady, D.-Y. Fei, L. Schneider, E. Houdayer, X. Chen and M. Hallett, "Prediction of human voluntary movement before it occurs," *Clinical Neurophysiology*, vol. 122, issue 2, pp. 364-372, February 2011.

[73] Hand and Brain: The Neurophysiology and Psychology of Hand Movements, by Patrick Haggard and J. Randall Flanagan, Academic Press, Jun 24, 1996

[74] Functional Anatomy for Sport and Exercise: Quick Reference, by Clare Milner, Routledge, 2008

[75] TeachMeAnatomy, http://teachmeanatomy.info/upper-limb/muscles/hand/ (Accessed on: 2017/11/13)

[76] Anatomy of the human body, by Henry Gray. 20th ed., thoroughly rev. and re-edited by Warren H. Lewis.

[77] Konrad, P. The ABC of EMG, A Practical Introduction to Kinesiological Electromyography; Noraxon Inc.: Scottsdale, AZ, USA, 2005.

[78] Wan Daud, W.M.B.; Yahya, A.B.; Horng, C.S.; Sulaima, M.F.; Sudirman, R. Features Extraction of Electromyography Signals in Time Domain on Biceps Brachii Muscle; International Journal of Modeling and Optimization: Bucharest, Romania, 2013, Volume 3.

[79] M. B. I Reaz, M. S. Hussain and F. Mohd-Yasin, "Techniques of EMG Signal Analysis: Detection, Processing, Classification and Applications," *Biological Procedures Online*, vol. 8, pp 11-35, 2006.

[80] Chowdhury, R.H.; Reaz, M.B.I.; Ali, M.A.M. Surface Electromyography Signal Processing and Classification Techniques. Sensors 2013, 13, 12431–12466.

[81] Nadzri, A.A.A.; Ahmad, S.A.; Marhaban, M.H.; Haslina, J. Characterization of surface electromyography using time domain features for determining hand motion and stages of contraction. Australas. Phys. Eng. Sci. Med. 2014, 37, 133–137.

[82] Nardo, F.D.; Mengarelli, A.; Maranesi, E.; Burattini, L.; Fioretti, S. Assessment of the ankle muscle co-contraction during normal gait: A surface electromyography study. J. Electromyogr. Kinesiol. 2015, 25, 347–354.

[83] Ahmad, S.A.; Chappel, P.H. Surface EMG pattern analysis of the wrist muscles at different speeds of contraction. J. Med. Eng. Technol. 2009, 33, 376–385.

[84] Nazmi, N.; Rahman, M. A. A.; Yamamoto, S.; Ahmad, S. A.; Zamzuri, H.; Mazlan, S. A. A Review of Classification Techniques of EMG Signals during Isotonic and Isometric Contractions. Sensors 2016, 16, 1304, doi:10.3390/s16081304.

[85] Japan Intractable Diseases Information Center | Number of Recipient Certificates Issued for Specific Disease Treatment: http://www.nanbyou.or.jp/entry/1356 (accessed on 2016/7/22).

[86] The International Alliance of ALS/MND Associations: https://www.alsmndalliance.org (accessed on 2017/6/18).

[87] M. Velliste, S. Perel, M. C. Spalding, A. S. Whitford, A. B. Schwartz: Cortical control of a prosthetic arm for self-feeding, *Nature*, 453:7198 (2008), 1098-1101.

[88] T. Jiralerspong, F. Sato, C. Liu, J. Ishikawa: Spectral analysis and artificial neural network based

classification of three mental states for brain machine interface applications, in *Proc. 2016 International Joint Conference on Neural Networks (IJCNN)*, Vancouver, 2016.

[89] J. Meng, S. Zhang, A. Bekyo, J. Olsoe, B. Baxter, B. He: Noninvasive Electroencephalogram Based Control of a Robotic Arm for Reach and Grasp Tasks, *Scientific Reports*, 6:38565 (2016).

[90] Müller-Putz G, Scherer R, Brauneis C and Pfurtscheller G 2005 Steady-state visual evoked potential (SSVEP)-based communication: impact of harmonic frequency components, *Neural Eng*., December 2005.

[91] Birbaumer N, Kübler A, Ghanayim N, Hinterberger T, Perelmouter J,. Kaiser J, Iversen I, Kotchoubey B, Neumann N, Flor H. The thought translation device (TTD) for completely paralyzed patients. *IEEE Trans on Rehabilitation Engineering*, vol. 8, Issue 2, Jun 2000.

[92] P. Martinez, H. Bakardjian, A. Cichocki: Fully Online Multicommand Brain-Computer Interface with Visual Neurofeedback Using SSVEP Paradigm, *Computational Intelligence and Neuroscience*, 2007, Article ID: 94561.

[93] B. Allison, T. Lüth, D. Valbuena, A. Teymourian, I. Volosyak, A. Gräser: BCI Demographics: How Many (and What Kinds of) People Can Use an SSVEP BCI?, *IEEE Transactions on Neural Systems and Rehabilitation Engineering*, 18:2 (2010), 107-116.

[94] R. Ortner, B. Z. Allison, G. Korisek, H. Gaggl, G. Pfurtscheller: An SSVEP BCI to Control a Hand Orthosis for Persons With Tetraplegia, *IEEE Transactions on Neural Systems and Rehabilitation Engineering*, 19:1 (2011), 1-5.

[95] X. Chen, Y. Wang, M. Nakanishi, X. Gao, T. P. Jung, S. Gao: High-speed spelling with a noninvasive brain–computer interface, *Proceedings of the National Academy of Sciences*, 112:44 (2015), E6058–E6067.

[96] T. Cao, X. Wang, B. Y. Wang, C. M. Wong, F. Wan, P. U. Mak, P. I. Mak, M. I. Vai: A high rate online SSVEP based brain-computer interface speller, in *Proc. of 5th International IEEE/EMBS Conference on Neural Engineering (NER)*, Cancun, 2011.

[97] L. D. Liao, C. Y. Chen, I J. Wang, S. F. Chen, S. Y. Li, B. W. Chen, J. Y. Chang, C. T. Lin: Gaming control using a wearable and wireless EEG-based brain-computer interface device with novel dry foam-based sensors, *Journal of NeuroEngineering and Rehabilitation*, 9:2 (2012).

[98] A. Güneysu, H. L. Akin: An SSVEP based BCI to control a humanoid robot by using portable EEG device, in *Proc. of 35th Annual International Conference of the IEEE Engineering in Medicine and Biology Society (EMBC)*, Osaka, 2013

[99] K. Holewa, A. Nawrocka: Emotiv EPOC neuroheadset in brain - computer interface, in *Proc. of 15th International Carpathian Control Conference (ICCC)*, Velke Karlovice, 2014.

[100] I. Martišius, R. Damaševičius: A Prototype SSVEP Based Real Time BCI Gaming System, *Computational Intelligence and Neuroscience*, 2016 (2016), Article ID: 3861425.

[101] P. Białas, P. Milanowski: A High Frequency Steady-State Visually Evoked Potential Based

Brain Computer Interface Using Consumer-grade EEG Headset, in *Proc. of 36th Annual International Conference of the IEEE Engineering in Medicine and Biology Society (EMBC)*, Chicago, 2014

[102] D. Aminaka, S. Makino, and T. M. Rutkowski, "Chromatic SSVEP BCI paradigm targeting the higher frequency EEG responses," in *Asia-Pacific Signal and Information Processing Association, 2014 Annual Summit and Conference (APSIPA)*, Dec 2014, pp. 1–7.

[103] X. Mao, M. Li, W. Li, L. Niu, B. Xian, M. Zeng, G. Chen: Progress in EEG-Based Brain Robot Interaction Systems, *Computational Intelligence and Neuroscience*, 2017 (2017), Article ID: 1742862.

[104] Z. Wu, Y. Lai, Y. Xia, D. Wu, D. Yao: Stimulator selection in SSVEP-based BCI, *Medical Engineering and Physics*, 30:8 (2008), 1079-1088.

[105] Homepage – Emotiv: https://www.emotiv.com (accessed 2017/11/8)

[106] F. Stahl, I. Jordanov, "An overview of the use of neural networks for data mining tasks", *Journal of the Brazilian Neural Network Society*, vol. 9, no. 3, pp. 202-212, 2011.

[107] A. Ubeda, E. Ianez, J. Badesa, R. Morales, J. M. Azorin, and N. Garcia, "Control Strategies of an Assistive Robot Using a Brain-Machine Interface," *IEEE Transactions on Neural Systems and Rehabilitation Engineering*, vol. 20, no. 5, pp. 720-729, September 2012

[108] J. Pardey, S. Roberts and L. Tarassenko, "A review of parametric modeling techniques for EEG analysis," *Medical Engineering & Physics*, vol. 18, issue 1, pp. 2-11, 1996.

[109] W. D. Penny, S. J. Roberts, E. A. Curran and M. J. Stokes, "EEG-based communication: A pattern recognition approach," *IEEE Transactions on Rehabilitation Engineering*, vol. 8, issue 2, pp. 214-215, June 2000.

[110] C. Guger, A. Schlögl, C. Neuper, D. Walterspacher, T. Strein, and G. Pfurtscheller, "Rapid prototyping of an EEG-based brain–computer interface (BCI)," *IEEE Transactions on Rehabilitation Engineering*, vol. 9, issue 1, pp. 49–58, March 2001.

[111] S. Cerutti, G. Chiarenza, D. Liberati, P. Mascellani and G. Pavesi, "A parametric method of identification of single-trial event-related potentials in the brain," *IEEE Transactions on Biomedical Engineering*, vol. 35, no. 9, pp. 701-711, September 1988.

[112] D. P. Burke, S. P. Kelly, P. de Chazal, R. B. Reilly and C. Finucane, "A Parametric Feature Extraction and Classification Strategy for Brain–Computer Interfacing," *IEEE Transcations on Neural Systems and Rehabilitation Engineering*, vol. 13, no. 1, pp. 12-17, March 2005.

[113] I. E. Gareis, R. C. Acevedo, Y. V. Atum, G. G. Gentiletti, V. M. Bañuelos and H. L. Rufiner, "Determination of an optimal training strategy for a BCI classification task with LDA," *Proc. of the 5th International IEEE EMBS Conference on Neural Engineering*, pp. 286-289, 27 April-1 May 2011.

[114] S. Bhattacharyya, A. Khasnobish, S. Chatterjee, A. Konar and D.N Tibarewala, “Performance Analysis of LDA, QDA and KNN Algorithms in Left-Right Limb Movement Classification from EEG Data,” *Proc. of 2010 International Conference on Systems in Medicine and Biology*, pp. 126-131, 16-18 December 2010.

[115] F. Lotte, M. Congedo, A. Lecuyer, F. Lamarche and B. Arnaldi, “A review of classification algorithms for EEG-based brain-computer interfaces,” *Journal of Neural Engineering*, vol. 4 no. 2, pp. R1-R13, 31 January 2007.

[116] G. Pfurtscheller, J. Kalcher, C. Neuper, D. Flotzinger, and M. Pregenzer, “On-line EEG classification during externally-paced hand movements using a neural network-based classifier,” *Electroencephalography and Clinical Neurophysiology*, vol. 99, pp. 416–425, 1996.

[117] N. F. F. Ebecken, “An Overview on the Use of Neural Networks for Data Mining Tasks,” *Journal of the Brazilian Neural Network Society*, vol. 9, issue 3, pp. 202-212, 2011.

[118] 小高知宏：はじめての機械学習，オーム社，2011.

[119] Y. Wang, B. Hong, X. Gao, and Shangkai Gao, “Implementation of a Brain-Computer Interface Based on Three States of Motor Imagery,” *Proc. of the 29th Annual International Conference of the IEEE Engineering in Medicine and Biology Society*, pp. 5059-5062, 2007.

[120] W. G. Baxt, “Improving the Accuracy of an Artificial Neural Network Using Multiple Differently Trained Networks,” Neural Computation, vol. 4, issue 5, pp. 772-780, 1992

[121] G. N. Bebis, M. Georgiopoulos, G. M. Papadourakis, and G. L. Heileman, “Increasing classification accuracy using multiple-neural-network schemes,” *Proceedings of SPIE 1709, Applications of Artificial Neural Networks III*, pp. 221-231, September 1992

[122] H. L. Tran, V. N. Pham, and H. N. Vuong, “Multiple neural network integration using a binary decision tree to improve the ECG signal recognition accuracy,” *International Journal of Applied Mathematics and Computer Science*, vol. 24, issue 3, pp. 647-655, September 2014

[123] Chao, E. Y. S.; An, K-N; Cooney, W. P.; and Linscheid, R. Biomechanics of the Hand: A Basic Research Study; World Scientific Publishing: Teaneck, NJ, USA, 1989; pp. 5-75; ISBN: 978-9971-5-0103-7

[124] Pillet, J.; Didierjean-Pillet, A. Aesthetic hand prosthesis: gadget or therapy? Presentation of a new classification. Journal of Hand Surgery: British & European Volume 2001, 6, 523-528, doi:10.1054/jhsb.2001.0658.

[125] Ministry of Health, Labour and Welfare, Social Welfare and War Victims’ Relief Bureau, Department of Health and Welfare for Persons with Disabilities Policy Planning Division. Report on Survey on persons with physical disability 2006; Ministry of Health, Labour and Welfare, 2006; pp. 3-4 (in Japanese)

[126] Pezzin, L. E.; Dillingham, T. R.; Mackenzie, E. J.; Ephraim, P.; Rossbach, P. Use and satisfaction with prosthetic limb devices and related services. Archives of Physical Medicine and Rehabilitation 2004, 85, 723-729, doi:10.1016/j.apmr.2003.06.002.

[127] Biddiss, E. A.; Chau, T. T. Upper limb prosthesis use and abandonment: A survey of the last 25 years. Prosthetics and Orthotics International 2007, 31, 236-257, doi:10.1080/03093640600994581.

[128] Bionic hand with 14 grip patterns that makes common tasks easy. – bebionic. Available online: http://bebionic. com/the_hand/grip_patterns (accessed on 18 July 2016)

[129] i-limb ultra | Touch Bionics. Available online: http://www.touchbionics.com/products/active-prostheses/i-limb-ultra (accessed on 18 July 2016)

[130] Wiste, T. E.; Dalley, S. A.; Withrow, T. J.; Goldfarb, M. Design of a multifunctional anthropomorphic prosthetic hand with extrinsic actuation. IEEE/ASME Transactions on Mechatronics 2009, 14, 699-706, doi:10.1109/ICORR.2009.5209496.

[131] Losier, Y.; Clawson, A.; Wilson, A.; Scheme, E.; Englehart, K.; Kyberd, P.; Hudgins B. An overview of the UNB hand system. Proc. 2011 MyoElectric Controls/Powered Prosthetics Symposium Fredericton 2011.

[132] Belter, J. T.; Dollar, A. M. Novel differential mechanism enabling two DOF from a single actuator: Application to a prosthetic hand. Proc. IEEE International Conference on Rehabilitation Robotics (ICORR) 2013, 1-6, doi:10.1109/ICORR.2013.6650441.

[133] Cipriani, C.; Controzzi, M.; Carrozza, M. C. The SmartHand transradial prosthesis. Journal of NeuroEngineering and Rehabilitation 2011, 8, 1-13, doi:10.1186/1743-0003-8-29.

[134] Liu, H.; Wu, K.; Meusel, P.; Seitz, N.; Hirzinger, G.; Jin, M. H.; Liu, Y. W.; Fan, S. W.; Lan, T.; Chen, Z. P. Multisensory five-fingered dexterous hand: The DLR/HIT Hand II. Proc. IEEE/RSJ International Conference on Intelligent Robots Systems (IROS) 2008, 3692-3697, doi:10.1109/IROS.2008.4650624.

[135] Kamikawa Y.; Maeno, T. Underactuated five-finger prosthetic hand inspired by grasping force distribution of humans. Proc. IEEE/RSJ International Conference on Intelligent Robots Systems (IROS) 2008, 717-722, doi:10.1109/IROS.2008.4650628.

[136] Krausz, N. E.; Rorrer, R. A. L.; Weir, R. F. ff. Design and Fabrication of a Six Degree-of-Freedom Open Source Hand. IEEE Transactions on Neural Systems and Rehabilitation Engineering 2016, 24, 562-572, doi:10.1109/TNSRE.2015.2440177.

[137] Jahan M.; Manas, M.; Sharma, B. B.; Gogoi, B. B. Feature extraction and pattern recognition of EMG-based signal for hand movements. Proc. 2015 International Symposium on Advanced Computing and Communication (ISACC) 2015, doi:10.1109/ISACC.2015.7377314.

[138] Zhang, H.; Zhao, Y.; Yao, F.; Xu, L.; Shang, P.; Li, G. An adaptation strategy of using LDA

classifier for EMG pattern recognition. Proc. 35th Annual International Conference of the IEEE Engineering in Medicine and Biology Society (EMBC) 2013, 4267-4270, doi:10.1109/EMBC.2013.6610488.

[139] Ahsan, Md. R.; Ibrahimy, M. I.; Khalifa, O. O. Electromygraphy (EMG) signal based hand gesture recognition using artificial neural network (ANN). Proc. 2011 4th International Conference on Mechatronics (ICOM) 2011, doi:10.1109/ICOM.2011.5937135.

[140] Oskoei, M. A.; Hu, H. Support Vector Machine-Based Classification Scheme for Myoelectric Control Applied to Upper Limb. IEEE Transactions on Biomedical Engineering 2008, 55, 1956-1965, doi:10.1109/TBME.2008.919734.

[141] Benatti, S.; Casamassima, F.; Milosevic, B.; Farella, E.; Schönle, P.; Fateh, S.; Burger, T.; Huang, Q.; Benini, L. A Versatile Embedded Platform for EMG Acquisition and Gesture Recognition. IEEE Transactions on Biomedical Circuits and Systems 2015, 9, 620-630, doi:10.1109/TBCAS.2015.2476555.

[142] Riillo, F.; Quitadamo, L.R.; Cavrini, F.; Gruppioni, E.; Pinto, C.A.; Cosimo Pastò, N.; Sbernini, L.; Albero, L.; Saggio, G. Optimization of EMG-based hand gesture recognition: Supervised vs. unsupervised data preprocessing on healthy subjects and transradial amputees. Biomedical Signal Processing and Control 2014, 14, 117-125, doi:10.1016/j.bspc.2014.07.007.

[143] Tenore, F. V. G.; Ramos, A.; Fahmy, A.; Acharya, S.; Etienne-Cummings, R.; Thakor, N. V. Decoding of Individuated Finger Movements Using Surface Electromyography. IEEE Transactions on Biomedical Engineering 2009, 56, 1427-1434, doi:10.1109/TBME.2008.2005485.

[144] Huang, H.; Zhou, P.; Li, G.; Kuiken, T. Spatial Filtering Improves EMG Classification Accuracy Following Targeted Muscle Reinnervation. Ann Biomed Eng. 2009, 37, 1849-1857, doi:10.1007/s10439-009-9737-7.

[145] Jiang, M. W.; Wang, R. C.; Wang, J. Z.; Jin, D. W. A Method of Recognizing Finger Motion Using Wavelet Transform of Surface EMG Signal. Proc. of the 27th Annual International Conference of the Engineering in Medicine and Biology Society 2005, 2672-2674, doi:10.1109/IEMBS.2005.1617020.

[146] Englehart, K.; Hudgins, B.; Parker, P. A.; Stevenson, M. Classification of the myoelectric signal using time-frequency based representations. Medical Engineering and Physics 1999, 21, 431–438, doi:10.1016/S1350-4533(99)00066-1.

[147] Huang, Y.; Englehart, K. B.; Hudgins, B.; Chan, A. D. C. A Gaussian mixture model based classification scheme for myoelectric control of powered upper limb prostheses. IEEE Transactions on Biomedical Engineering 2005, 52, 1801-1811, doi:10.1109/TBME.2005.856295.

[148] Pylatiuk, C.; Schulz, S.; Doderlein, L. Results of an Internet survey of myoelectric prosthetic hand users. Prosthetics Orthotics International 2007, 31, 362–370, doi:10.1080/03093640601061265.

[149] Drake, R.; Vogl, A. W.; Mitchell, A. Gray's Anatomy for Students, 2nd ed., Churchill Livingstone, Amsterdam, The Netherlands, 2004, ISBN: 9781455755417.

[150] Tsujimura, T.; Yamamoto, S.; Izumi, K. Hand Sign Classification Employing Myoelectric Signals of Forearm. In Computational Intelligence in Electromyography Analysis - A Perspective on Current Applications and Future Challenges, Naik, G. R., InTech, 2012, doi:10.5772/51080.

[151] Fukuda, O.; Bu, N.; Tsuji, T. Control of an Externally Powered Prosthetic Forearm Using Raw-EMG Signals. Transactions of the Society of Instrument and Control Engineers 2004, 40, 1124-1131 (in Japanese).

[152] Liu, L.; Liu, P.; Clancy, E. A.; Scheme, E.; Englehart, K. B. Electromyogram Whitening for Improved Classification Accuracy in Upper Limb Prosthesis Control. IEEE Transactions on Neural Systems and Rehabilitation Engineering 2013, 21, 767-774, doi:10.1109/TNSRE.2013.2243470.

[153] Adewuyi, A. A.; Hargrove, L. J.; Kuiken, T. A. An Analysis of Intrinsic and Extrinsic Hand Muscle EMG for Improved Pattern Recognition Control. IEEE Transactions on Neural Systems and Rehabilitation Engineering 2016, 24, 485-494, doi:10.1109/TNSRE.2015.2424371.

[154] Kanitz, G. R.; Antfolk, C.; Cipriani, C.; Sebelius F.; Carrozza, M. C. Decoding of Individuated Finger Movements Using Surface EMG and Input Optimization Applying a Genetic Algorithm. Proc. of the 2011 Annual International Conference of the IEEE Engineering in Medicine and Biology Society 2011, 1608-1611, doi:10.1109/IEMBS.2011.6090465.

[155] Hargrove, L. J.; Englehart, K.; Hudgins, B. A comparison of surface and intramuscular myoelectric signal classification. IEEE Transactions on Biomedical Engineering 2007, 54, 847–853, doi:10.1109/TBME.2006.889192.

[156] Kambayashi, A.; Kuniyasu, K.; Jiralerspong, T.; Ishikawa J. Identification of voluntary movements of five fingers for myoelectric prosthetic hand. Proc. of the 32nd Annual Conference of the Robotics Society of Japan 2014, 32. (in Japanese).

[157] Merletti, R. Standards for Reporting EMG Data. Journal of Electromyography and Kinesiology 2017, 35, 1-2, doi: 10.1016/S1050-6411(17)30219-5

[158] Shim, H.; An, H.; Lee, S.; Lee, E. H.; Min, H.; Lee, S. EMG Pattern Classification by Split and Merge Deep Belief Network. Symmetry 2016, 8, 148, doi:10.3390/sym8120148.

[159] Allison B Z, Wolpaw E W and Wolpaw J R 2007 Brain–computer interface systems: progress and prospects Expert Rev. Med. Devices 4 463–74

[160] Pfurtscheller G, Allison BZ, Brunner C, Bauernfeind G, Solis-Escalante T, et al.(2010) The

hybrid BCI. *Frontiers in Neuroscience*, vol.4(30): 1–11.

[161] Milla´n JD, Rupp R, Mu¨ller-Putz GR, Murray-Smith R, Giugliemma C, et al.(2010) Combining brain-computer interfaces and assistive technologies: state-of-the-art and challenges. Front Neurosci 4: 161.

[162] Allison BZ, Leeb R, Brunner C, Mu¨ller-Putz GR, Bauernfeind G, et al. (2012) Toward smarter BCIs: extending BCIs through hybridization and intelligent control. J Neural Eng 9(1): 1–7.

[163] R. C. Panicker, S. Puthusserypady, and Y. Sun, "An asynchronous P300 BCI with SSVEP-based control state detection," *IEEE Transactions on Biomedical Engineering*, Vol. 58, No. 6, pp.1781–1788, 2011

[164] Y. Punsawad, Y. Wongsawat, and M. Parnichkun, "Hybrid EEG-EOG brain-computer interface system for practical machine control," Proc. of the *IEEE Engineering in Medicine and Biology Society Conference*, pp. 1360–1363, 2010

[165] X. Yong, M. Fatourechi, R. K. Ward, and G. E. Birch, "The design of a point-and-click system by integrating a self-paced brain-computer interface with an eye-tracker," *IEEE Journal on Emerging and Selected Topics in Circuits and Systems*, Vol. 1, No.4, pp. 590–602, 2011.

[166] R. Leeb, H. Sagha, R. Chavarriaga, and J. del R. Millan, "A hybrid brain-computer interface based on the fusion of electroencephalographic and electromyographic activities," *Journal of Neural Engineering*, Vol. 8, No. 2, 2011

[167] S. Fazli, J. Mehnert, J. Steinbrink G. Curio, A. Villringer, K.R. Müller, B. Blankertz, "Enhanced performance by a hybrid NIRS-EEG brain computer interface," Neuroimage, Vol. 59, pp. 519–529, 2011

[168] S. Amiri, R. Fazel-Rezai, and V. Asadpour, "A Review of Hybrid Brain-Computer Interface Systems," *Advances in Human-Computer Interaction*, Vol. 2013, 2013

[169] B. Z. Allison, C. Brunner, V. Kaiser, G. R. Muller-Putz, C. Neuper, and G. Pfurtscheller, "Toward a hybrid brain-computer interface based on imagined movement and visual attention," *Journal of Neural Engineering*, Vol. 7, No. 2,2010

[170] G. Pfurtscheller, T. Solis-Escalante, R. Ortner, P. Linortner, and G. R. Muller-Putz, "Self-paced operation of an SSVEP-based orthosis with and without an imagery-based "brain switch": a feasibility study towards a hybrid BCI," *IEEE Trans.on Neural Systems and Rehabilitation Engineering*, Vol. 18, No. 4, pp.409–414, 2010

[171] Y. Su, Y. Qi, J. X. Luo, B. Wu, F. Yang, Y. Li, Y. T. Zhuang, X. X. Zheng, W. D. Chen, "A hybrid brain-computer interface control strategy in a virtual environment," J*ournal of Zhejiang University*, Vol. 12, No. 5, pp. 351–361, 2011

[172] Y. Li, J. Long, T. Yu, Z. Yu, C. Wang, H. Zhang, C. Guan, "An EEG-Based BCI System for

2-D Cursor Control by Combining Mu/Beta Rhythm and P300 Potential," *IEEE Transactions on Biomedical Engineering*, vol. 57, no. 10, pp.2495-2505, 2010

[173] B. Choi, S. Jo, "A Low-Cost EEG System-Based Hybrid Brain-Computer Interface for Humanoid Robot Navigation and Recognition," *PLoS One*, vol. 8, no. 9, e74583, 2013

List of Publications

Journal Papers

[1] **Trongmun Jiralerspong**, Emi Nakanishi, Chao Liu, Jun Ishikawa, “Experimental Study of Real-Time Classification of 17 Voluntary Movements for Multi-Degree Myoelectric Prosthetic Hand,” *Applied Sciences*, Vol. 7, No. 11, 1163, 2017

Book Chapters

[1] Hitomi Honoki, **Trongmun Jiralerspong**, Fumiya Sato, Jun Ishikawa, “Experimental Evaluation of Steady State Visual Evoked Potentials for Brain Machine Interface,” in AETA 2017 - *Recent Advances in Electrical Engineering and Related Sciences: Theory and Application*, Lecture Notes in Electrical Engineering, Vol. 465, Springer, 2017.

International Conference Papers (refereed)

[1] **Trongmun Jiralerspong**, Chao Liu, and Jun Ishikawa, “Identification of Three Mental States Using a Motor Imagery Based Brain Machine Interface,” in *Proc. of 2014 IEEE Symposium on Computational Intelligence in Brain Computer Interfaces (CIBCI)*, 2014

[2] **Trongmun Jiralerspong**, Fumiya Sato, Chao Liu, and Jun Ishikawa, “Spectral Analysis and Artificial Neural Network Based Classification of Three Mental States for Brain Machine Interface Applications," in *Proc. of 2016 International Joint Conference on Neural Networks (IJCNN)*, 2016

[3] Emi Nakanishi, **Trongmun Jiralerspong**, Asuka Kambayashi, and Jun Ishikawa, “Classification of 17 Voluntary Movements Using Principal Component Analysis for Myoelectric Prosthetic Hand,” in *Proc. of 2016 IEEE International Conference on Systems, Man, and Cybernetics (SMC)*, 2016

Domestic Conference Proceedings

[1] **銭智定**，石川潤，“ブレイン・マシン・インタフェースに関する研究―脳波を用いた上下運動の識別―”，日本ロボット学会学術講演会予稿集，３１巻，２０１３年

[2] **銭智定**，劉超，石川潤，“脳波信号を用いた上下動作意思のオンライン識別”，日本ロボット学会学術講演会予稿集，３２巻，２０１４年

[3] 神林明日香, 國安夏奈, **銭智定**, 石川潤，“筋電義手の５指随意動作識別に関する研究”，日本ロボット学会学術講演会予稿集，３２巻，２０１４年

[4] 中西絵美，**銭智定**，神林明日香，石川潤，“主成分分析に基づく筋電義手の５指随意動作の識別”，日本ロボット学会学術講演会予稿集，３３巻，２０１５年

[5] 銭智定，中西絵美，劉超，石川潤，“筋電義手の前腕 17 動作識別のための周波数領域における特徴量解析”，LIFE2016，２０１６年

[6] 佐藤史也，銭智定，吉川真実，石川潤，“運動想起 BMI における電極位置とチャネル数による識別率への影響”，LIFE2016，２０１６年

Newspaper Article

[1] 腕の動き, AI で分析 細かく動く電動義手へ, 日経産業新聞，２０１６年６月１４日　掲載

Acknowledgements

First, I’d like to express my deepest appreciation to my advisor Professor Jun Ishikawa, for the time he spent consulting and helping me on my ideas. His constant unconditional support, guidance, incredible patience, enthusiasm and encouragement were invaluable throughout my doctoral studies without which this dissertation would have not been possible.

Beside my advisor, I would also like to express my sincere thanks to my co-advisor associate Professor Norihiro Kamamichi, for his insightful comments, questions and especially for carefully evaluating my work. Again, without all of those lengthy discussions and comments, this doctoral dissertation would not have been feasible.

I thank my lab members of the robotics laboratory (Ishikawa Laboratory) at Tokyo Denki University for all their encouragement and support throughout my studies. Special thanks to all participants who participated in the BMI experiments. Their help was indispensable in the achievements of my research.

I would also like to express my gratitude to Ms. Chao Liu for her support and encouragement throughout my academic pursuits here in Japan. Also, her valuable advice and constructive criticism on my research were essential for the completion this dissertation.

Last but not least, I would like to express my deepest gratitude to my family: my parents and my sister for supporting my choices throughout my life, for their dedication, encouragement, advice, and the many years of support. Their unconditional love has been a very strong motivation during all my life and was what made everything possible. Without their continuous support and comprehension, I would not have been able to find the drive and willingness to finish my doctoral studies.